Environmental Investigations in the West Tahta Region, Upper Egypt: A Hydrogeochemical, Geophysical and Remote Sensing Study

Esam Abu El-Sebaa Osman Ismail

Dissertation submitted to:
Department Angewandte Geowissenschaften Geophysik
Lehrstuhl für Angewandte Geophysik
Montanuniversität Leoben, Austria

Januar, 2013

Declaration

I declare in lieu of oath, that I wrote this thesis and performed associated research myself, using only literature cited in this volume.

Esam Ismail

Leoben, 05-01-13

CONTENTES

CHAPTER THREE

Geophysical Studies

CHAPTER FOUR

Hydrogeology and Hydrogeochemistery Studies

LIST OF FIGURES

LIST OF Tables

Table **page**

Acknowledgements

First and foremost thanks to ALLAH, the most kind and the most merciful and who gives me everything and allows accomplishment of this work.

I offer my sincerest gratitude to my two supervisors, Prof. Dr. Erich Niesner and Prof. Dr Hermann Mauritsch, they are supported me throughout my thesis with his patience and knowledge. If it were not for his invaluable assistance, this thesis would not have been completed or written. One simply could not aspire for a friendlier and more-supporting supervisor.

With great pleasure, I'm honored to express my deepest gratitude and thanks to my Prof. Dr. Abdullah Fayed, Ass. Prof. of water resources Department, National Authority of Remote Sensing and Space Sciences, for his great help and honest assistance and cooperation he offered throughout the study.

I would like to express my thanks to Prof. Dr. Esam El-Sayed, head of Geology Department, Faculty of Science, Minia University, for his guidance into my life after my bachelor education. Special thanks are due to Ass. Prof. Mohamed Abu-Heleika, Geology Department, Faculty of Science, Minia University, for helping offered during field work and continuous discussions.

I want to thank in general all fellows, members of the Geophysical institute Montan University and the steering committee for creating such a friendly and stimulating context that widened my scientific understanding of life sciences in many aspects. Special thanks go to Mrs. Pretzenbacher, will always be remembered for her energy to help and also moral support.

I deliver my sincere gratitude to many friends and colleagues for scientific discussion, advice and continuous support that have always been so greatly appreciated

I like to take this opportunity to thank the Egyptian governorate providing financial support to make this work possible

Last but by no means least, I like to thank my family and close relatives for helping me with general education and giving me the opportunity to start and pursue a career in science as well as their never-ending encouragement and ongoing support.

I would never have been able to finish my dissertation without support of my Egyptian friends in Leoben and the Egyptian cultural office in Vienna.

Above all, I would like to thank my wife Radwa Mohamed for her personal support and great patience at all times cheering me up and stood by me through thick and thin. Likewise, my parents, brother and sister as well as my children (Hams and Abd Elrahman) have given me their unequivocal support, for which mere expressions of thankfulness would have never been sufficient.

Esam Ismail

ZUSAMMENFASSUNG

Das Untersuchungsgebiet West Tahta liegt in Ober Ägypten und ist charakterisiert durch ein überwiegend trockenes Klima mit sehr geringen Niederschlägen. Das Gebiet wurde in den letzten Jahren im Rahmen eines großen Projektes, intensiv untersucht. Das Ziel war die Abklärung der im Untergrund vorhandenen Grundwasserreserven, sowie deren Eignung für die Versorgung wachsender Siedlungen und geplanter Erweiterungen der landwirtschaftlich nutzbaren Flächen. Letzteres betrifft vor allem die westlichen Anteile. Das Grundwasser ist in Anbetracht der geringen Niederschläge einerseits und der großen Entfernung für die Zuleitung von Nilwasser andererseits, von entscheidender Bedeutung für jedwede Entwicklung dieser Region.

In der vorliegenden Studie wurden vorerst Methoden der Fernerkundung eingesetzt, um Veränderungen in der Entwicklung sowohl der Städte und Siedlungen sowie der landwirtschaftlichen Nutzflächen zwischen 1987 und 2009 zu quantifizieren.

Zur Abschätzung der Geometrie des Grundwasserkörpers wurden 29 geoelektrische Tiefensondierungen durchgeführt, die in drei Quer- und einem Längsprofil, bezogen auf die Talachse, angeordnet wurden. Durch diese Anordnung konnte einerseits an den Profilkreuzungspunkten die Genauigkeit der berechneten Teufenlagen der Schichtgrenzen sowie andererseits deren Dreidimensionalität dargestellt werden.

Zur Abklärung der Eignung des Grundwassers für verschiedene Verwendungszwecke wurden 34 Wasserproben genommen, davon 6 Proben aus den Oberflächenwässern und 28 aus dem Grundwasser. Durch die chemische Charakterisierung der Wässer wurde versucht die Quelle für die Einspeisung in das Grundwasser sowie deren Verwendbarkeit zu klären. Abschließend wurden Analysen der Untersuchungen von 1989 und 2011 gegenüber gestellt und einer Interpretation der eingetretenen Veränderungen zugeführt.

Der Vergleich der landwirtschaftlichen Nutzflächen ergab eine Zunahme zwischen 1987 und 2009 von 1785.9 ha. Dies entspricht einem jährlichen Zuwachs von 81.2 ha. Die Zunahme der Siedlungsflächen betrug im gleichen Zeitraum 223.1ha, somit einem jährlichen Zuwachs von 10.14 ha.

Die geoelektrischen Untersuchungen im Arbeitsgebiet ergaben einen geoelektrischen Vier – Schichten – Fall, das heißt, dass der sedimentäre Untergrund durch vier, über den charakteristischen elektrischen Widerstand unterscheidbaren

Schichten, aufgebaut wird.

Die erste Schicht wird von Wadi Ablagerungen im Westen und überwiegend Ton und Nilschlamm im Osten dominiert. Der zweite Horizont entspricht nach den gemessenen Widerständen einem trockenen bis feuchten Sand. Darunter folgt der dritte Horizont, der dem Grundwasserträger entspricht und von Sand,- sandigem Ton und Schottereinlagerungen aufgebaut wird. Der elektrische Widerstand variiert zwischen 28 und 100 Ohmm, die Mächtigkeit zwischen 18 und 144 m. Der vierte Horizont entspricht dem tonigen Grundwasserstauhorizont mit extrem niederen Widerständen.

Die Speisung des Grundwasserkörpers erfolgt im Wesentlichen durch das Kanalsystem, das Nilwasser zur Bewässerung der Nutzflächen , heranführt und teilweise bereits am Transportweg versickert. Der Wasserverbrauch wird durch die Verdunstung signifikant beeinträchtigt.

Nach den chemischen Analysen wies ein erheblicher Teil des Oberflächenwassers 1989 Trinkwasser Qualität auf. Im Jahre 2011 hat sich die Qualität wesentlich verschlechtert; das heißt die Eignung als Trinkwasser ist nicht mehr gegeben. Sowohl die Salinität als auch die Ionen Konzentration liegen über den zulässigen Grenzwerten. War 1989 das Grundwasser unbedenklich für die Bewässerung, trifft dies 2011 nur noch auf die Hälfte zu.

Aus diesen Ergebnissen und den daraus resultierenden Schlüssen kann die hohe Priorität dieser Untersuchungen für alle künftigen Entwicklungen im Niltal abgeleitet werden.

ABSTRACT

The west Tahta area lies in Upper Egypt and is characterized by a dry climate and a scarcity of surface water. This area has been subjected to an extensive reclamation project over the past few years. The reclamation project has lead to changes in both the agricultural and urban areas, as well as to changes in the quantity and quality of the groundwater. Groundwater is the main source of water in the region due to infrequent rain and no near by sources of surface water.

In this study we used remote sensing techniques to detect the changes in the agricultural area, the urban area, and the River Nile between 1987 and 2009. 29 vertical electrical sounding was done to evaluate the geometry of the aquifer. We collected and analyzed 34 water samples (6 of surface water and 28 of groundwater) to determine the source and the type of groundwater and evaluate these water samples for different purposes. In the last part we compare the groundwater samples collected and analyzed by RIGW in 1989 and groundwater samples collected and analyzed in 2011.

The total increase in the agricultural area from 1987 to 2009 is about 1785.9 hectare with an average annual growth rate of 81.2 ha/year. The total increase in urban area from 1987 to 2009 is about 223.1ha with an average annual growth rate 101.45 ha/year.

From the geophysical study, we found that the area under investigation represented a geophysical four-layer case. The first layer (surface layer) is represented by wadi deposits in the west and clay in the east. The second layer is represented by wet sand. The third layer acts as the main aquifer in the study area and is composed of sand and gravel. This layer has resistivity ranging from 28 to 99 ohm, and its thickness ranges from 18 to 144m. The fourth layer acts as the base of the aquifer and is composed of clay with low resistivity.

The recharge of the aquifer is mainly from surface water, especially from the irrigation canals, which play a major role in the configuration of the water table. The discharge of this aquifer takes place through evaporation. The majority of the

studied surface water appears to be suitable for drinking. Most of the groundwater collected in 1989 is also suitable for drinking. However, the majority of the 2011 groundwater has impermissible levels and major ions. Most of the 1989 groundwater samples are suitable for irrigation purposes, while only about half of the 2011 groundwater samples are. The other half is (bad or) unsuitable due to its high salinity.

CHAPTER ONE

Introduction

1.1. General outline

Egypt is located in the arid zone of North Africa, which is characterized by limited fresh water supplies and by a rapidly growing population. The agricultural area is more or less restricted to the Nile valley. To handle this major problem in Egypt desert reclamation projects were started. The heavy demands on water resources, especially in arid and semiarid regions where surface water resources are limited, become clear immediately. The groundwater is one of the most valuable natural resources, supporting human health, economic development, and ecological diversity. Because of its inherent qualities (e.g. consistent temperature, widespread and continuous availability, excellent natural quality, limited vulnerability, low development costs, drought reliability, etc.), it has become an immensely important and dependable source of water in all climatic regions, including both urban and agricultural areas of developed and developing countries (Todd and Mays, 2005). Furthermore, groundwater is emerging as a formidable poverty-alleviation tool, which can be delivered directly to poor communities more cheaply, quickly, and easily than canal water (IWMI, 2001). Of the 37 MKm^3 of freshwater estimated to be present on earth, about 22% is groundwater, which constitutes about 97% of all liquid freshwater, available for humans potential use (Foster, 1998).

The study area lies in Upper Egypt and has been subjected to an extensive reclamation project over the past few years. The agricultural area increased from 1989 to 2009 by 1785.96 Hectare with an average annual growth rate of 81.18 Hectare/year. This agricultural development depends largely on groundwater, as well as a limited supply of surface water from the River Nile and nearby canals.

In this study we used remote sensing techniques to detect the changes in the urban area, agricultural area, and River Nile from 1989 to 2011. Additionally, we made 29 vertical electric soundings (VES) to evaluate the geometry of the aquifer in the study area. We also collected 34 water samples (6 from surface water and 28 from groundwater) for a complete chemical analysis, we calculated the salinity and ion dominance, determined the water types, and evaluated the quality of the water for different purposes (see chapter four). In the last part

of this study, we used 36 groundwater samples collected and analyzed chemically in 1989 (RIGW, 1989) to detect the changes in the quality of the groundwater from 1989 to 2011.

1.2. Location and climate

The area under investigation (West Tahta) lies in Sohage Governorate in Upper Egypt (Fig.1.1), which belongs to the arid belt of Egypt characterized by long, hot summers, warm winters, and scarce rainfall, except for the occasional storms. Rain is rare and randomly distributed throughout the area. The average air temperature is about 36.5ºC in summer and 15.5ºC in winter. The relative humidity in winter is higher than in summer and varies between 35 and 61% (Ayman, A., 2009).The monthly evapotranspiration ranges from 3.5mm day^{-1}in January to 9.9 mm day^{-1} in June. The evaporation loss from the water distribution system varies from 2.1 mm day^{-1} in January to 8.3 mm day^{-1} in June. Between 1960 and 1998, the average value of precipitation in Sohage Governorate was recorded as 2.25 mm/year (MAE, 2000).

1.3. Aim of the present work

The main aim of the present study is to present: the changes in the River Nile, the agricultural areas and the urban areas between 1987 and 2011; the identification of the groundwater aquifers; the delineation of the subsurface conditions based on interpretations of available geophysical data; hydrochemical characteristics of the aquifers; the evaluation of the water quality for different purposes; and the changes in the groundwater quality between 1989 and 201.

1.4. Field, sampling, and analytical techniques

Before beginning the field work, Landsat TM images from 1987 and Egypt sat images from 2009 (Figures 1.2, 1.3), were used to detect the changes in agricultural areas, urban areas, and the River Nile in the study area between these years. To complete the change detection analysis we applied a post classification, which includes image classification, change detection and accuracy assessment. For visual interpretation, the most usual band combinations, 2, 1, 3 and 7, 4, 2 are represented with red, green, and blue, respectively (Scepan, et al., 1999; Bakr et al. 2010).

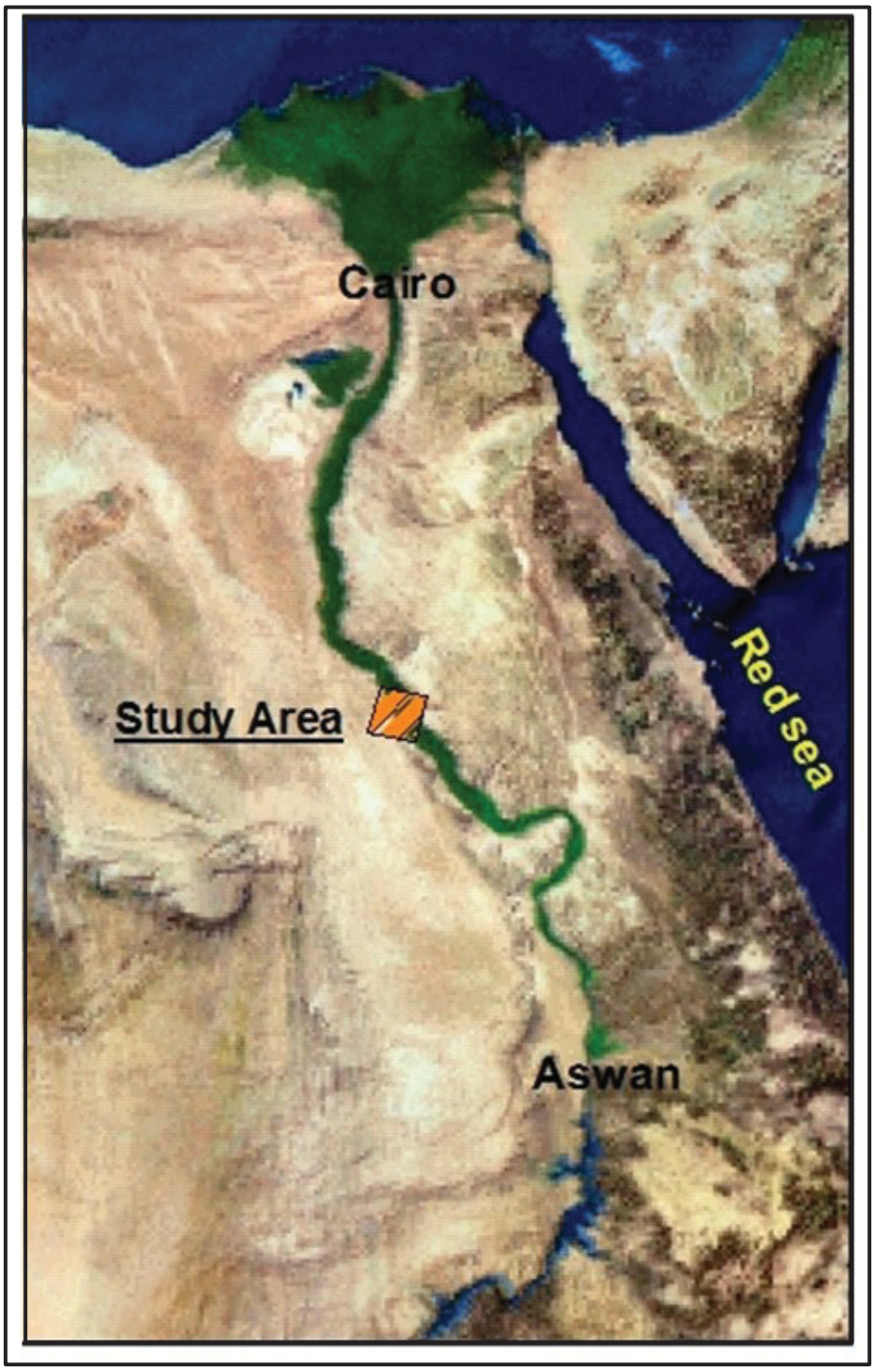

Fig. (1.1): Location of the study area

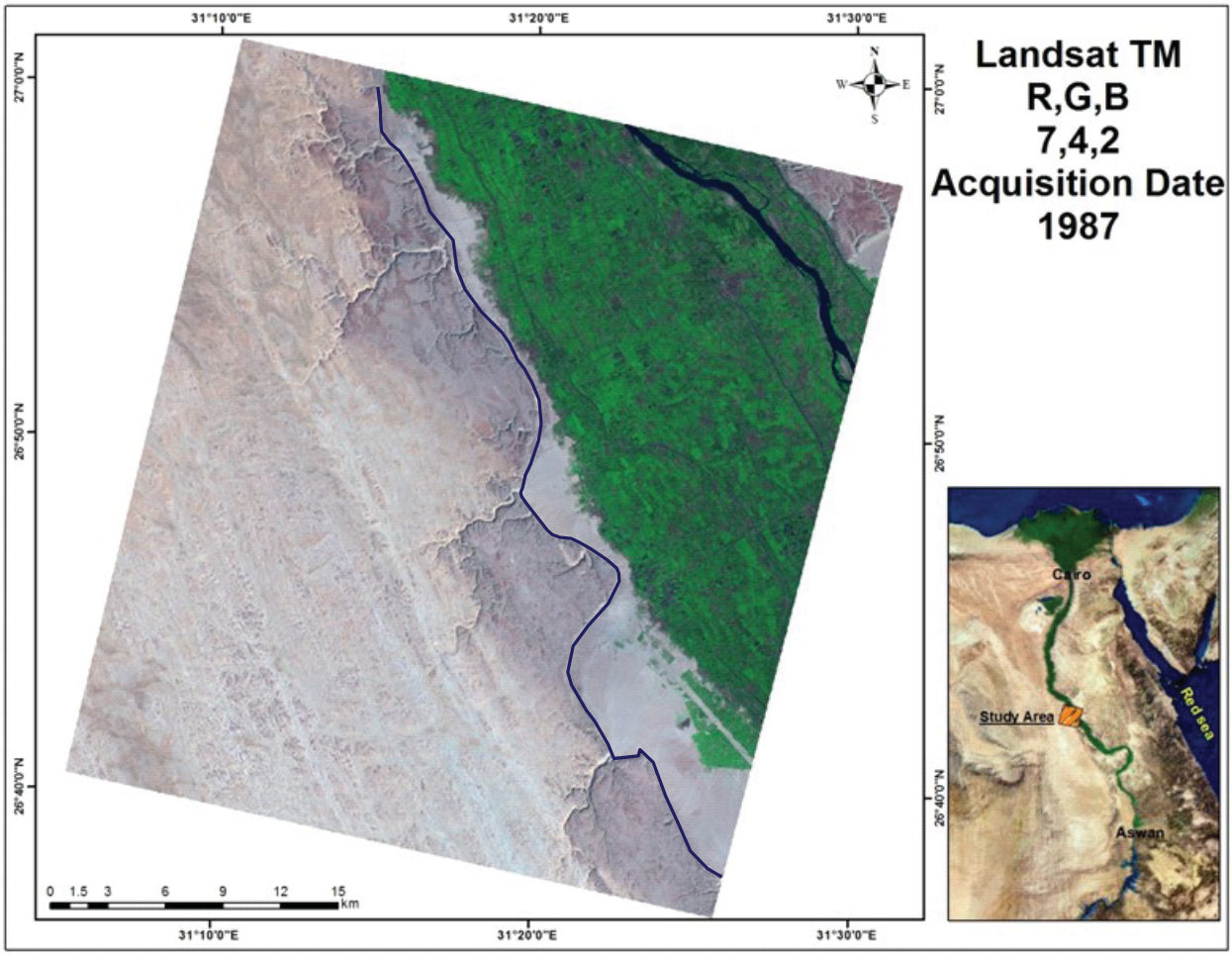

Fig. (1.2): Land sat TM acquired in 1987 (Blue Line is Scarp border)

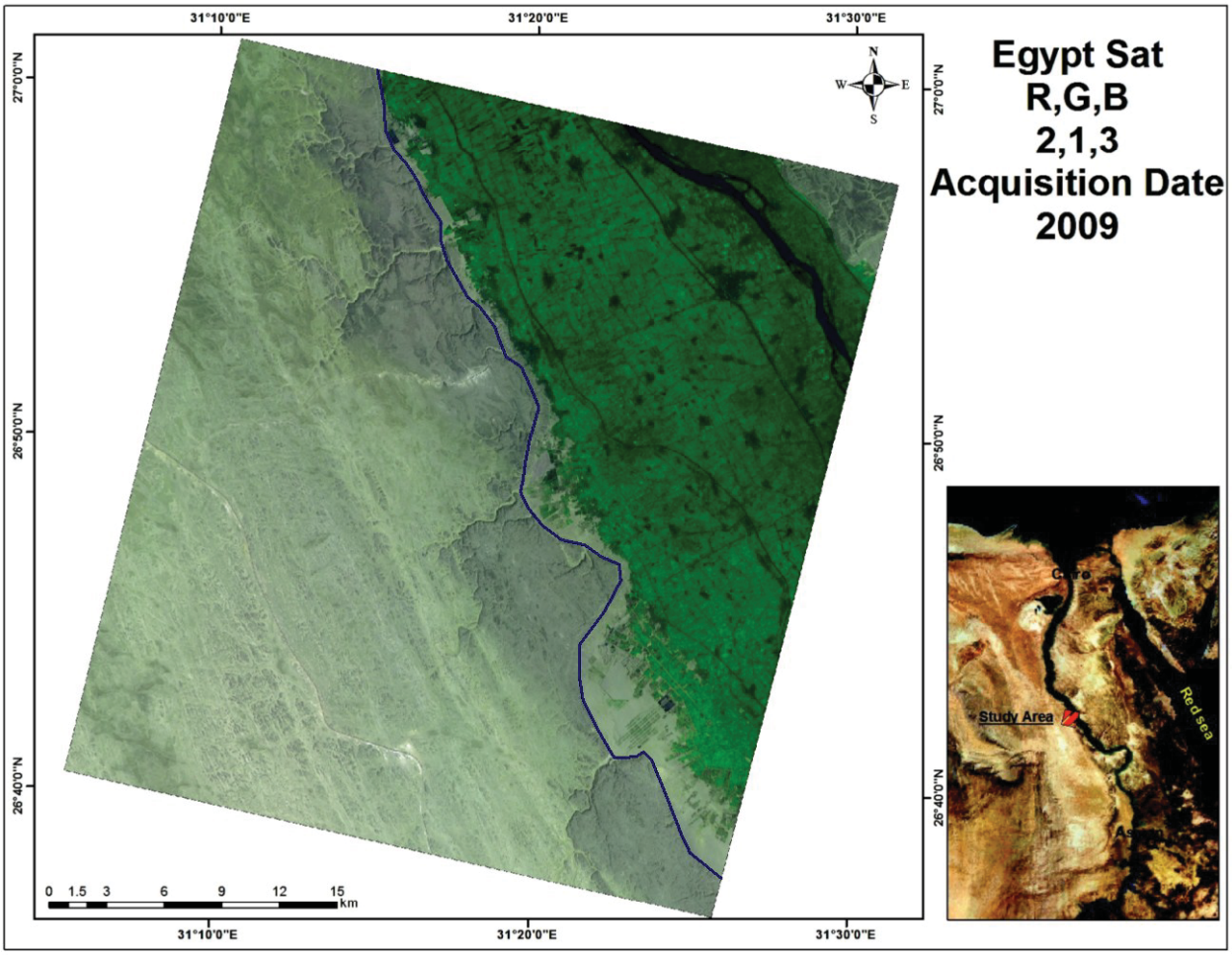

Fig. (1.3): Egypt Sat 2009 (Blue line is the Scarp border)

The digital data were processed for geometric and radiometric corrections using ERDAS Imagine processing software. ERDAS imagine – version 9.2 (Leica Geosystems, 2008) software was used (in this study) to analyze satellite images and to produce classified images of the area under investigation, as well as landuse maps and their changes. The TM data and Egypt sat data were classified using unsupervised and supervised classification techniques. The landuse maps of 1987 and 2009 were prepared by computing overall change patterns in each category.

The field work included a survey and a study of the physical features and rock formations in the area, as well as a recording the water level in the wells. 34 water samples were collected from the study area, representing both the surface water (six samples) and the groundwater (28 samples across the area of study). The electrical conductivity, total dissolved salts, and hydrogen ion concentration were measured in the field and in the laboratory. 29 vertical

electrical soundings were carried out in the field to determine the specific resistivity and the thickness of the distinct layers within the subsoil.

After finishing the field and laboratory work, the construction of the water level and water flow maps for the study area, as well as complete chemical analysis of the collected water samples, was carried out. The major cations and major anions were measured in the laboratory, and the results are presented in part per million, equivalent parts per million, and percent part per million, along with the ion dominance, sodium adsorption ratio, and water types.

1.5. Previous work

The area under investigation lies in the Sohag Governorate, Upper Egypt. Many studies were carried out in Sohag governorate on the geology, geomorphology, geophysical studies, hydrogeology, and hydrochemistry. Geology and geomorphology of the area has been studied by many authors (Ball, 1909; Said 1960, 1962, 1975, 1981 and 1990; Chumakove, 1967; Ahmed, 1980; Abdel Moneim, 1992; Abdel Moneim et al., 1999 a, b; Mahran and El Haddad, 1992; Omer, 1996; Omer and Abdal Moneim, 2001; Hassan, 2005; and Gomaa 2006), for example:

Ball, 1909 pointed out that the terraces of Post-Eocene times formed as a result of aggradations and degradation of the Nile Valley relative to the eustatic changes of the ultimate base of the Mediterranean Sea. Said (1960, 1962, 1975 and 1981) studied the geomorphological units and geologic formations, as well as the geologic structural features along the Nile River, giving us a good sense of the lithostratigraphic succession during Lower Eocene, Upper Pliocene and Lower and Upper Pleistocene. Ahmed, 1980 Mahran and El Haddad, 1992 studied the surface and subsurface structure features in Sohag area. El-Haddad et al., 2003 studied the hydrographical patterns and pointed out some wadis in the study area that were being cultivated by using the groundwater, especially in the areas facing old channels. The shallow aquifers result in promising sites for more productive and better quality wells.

The hydrogeologic conditions of Sohag Governorate were studied by many Scientists. Abdel Moneim, A. A. (1988, 1992, and 1999 a, b) studied the hydrogeology of the Nile Basin in the Sohag province and carried out numerical simulation and groundwater management of Sohag

aquifer. He described the geoelectrical and hydrogeological investigations of the groundwater resources in the area west of the cultivated land at Sohag. Attia, F. R., 1985 and Barber, W. and Carr, D.P., 1981 studied the management of water systems in Upper Egypt. Diab et al., 2002 evaluated the water resources and land suitability for the development of the southern part of Sohag. Korany, E. A., Omran, A. A., and Abdel-Aal, A. A., 2006 established a hydrochemical approach for the assessment of the recharge routes of groundwater in the Quaternary aquifer in the Nile Valley of the Sohag area. Mousa, S., Attia, F. A. and Abuel Fetouh, A. M., 1994 carried out the hydrogeological study of the Quaternary aquifer in the Nile Valley between Asyut and Sohag Governorate by applying geoelectrical methods. Youssef, A. M., Abdel Moneim, A. A., and Abu El-Maged, S. A., 2005 used a geographic information system to study the flood hazard assessment and its associated problems in the Sohag area. Zaki, S. R., 2001 applied the geographical information system and hydrogeological study to evaluate the water resources and landuse projects in the southern part of Sohag Governorate. Omran, A. A., 2008 established an integration of remote sensing, geophysics, and geographic information systems to evaluate the groundwater potential in the Sohag region. Gomaa, A. A., 2006 presented the hydrogeological and geophysical assessment of the reclaimed areas in Sohag. Awad M. A., Nada A. A., Hamza M. S., and Froehlich K., 1995 carried out chemical and isotopic investigation in the groundwater of the Tahta region. RIGW and IWACO, 1989 established an internal report about the development of groundwater for irrigation and drainage in the Nile Valley (West Tahta).

Ahmed A. A., 2007 used the lithologic modeling techniques and groundwater flow modeling to define the characteristics of the aquifer of the Sohag area. Ayman A. A., 2009 used generic and pesticide DRASTIC GIS based models for a vulnerability assessment of the Quaternary aquifer of Sohag. Aymen A. A. and Mohamed H. A., 2009 studied the hydrochemical evaluation and the variation of groundwater and its environmental impact of Sohag region. El-Sayed, S. A., and El-Shater, A.A., 2010 studied the flood plain problems in Sohag Governorate.

1.6. Geology of the study area

The West Tahta area lies in Sohag Governorate and is bordered by the Eocene plateau in the west and the Nile River in the east. This governorate represents a part of the Nile Valley and has been studied by many geologists. According to Said (1981 and 1990) the rock units in the

study area and its surroundings originate from sediment of various ages from Holocene down to Eocene.

Holocene deposits; these deposits are accumulated under different environmental conditions and contain all types of unconsolidated sediments. These deposits are represented by Nile silt, wadi deposits, and fanglomerates.

-Nile silts; cover the majority of the old cultivated land and lie in the eastern part of the study area. They are composed of silts and fine sands dominated by quartz grains and some heavy minerals (Attia, 1954) and result from the seasonal floods of the Nile over the entire Nile basin.

-Wadi deposits; they are build up by poorly bedded gravels and thin coarse sand alternating with pebble beds with thicknesses often exceeding 10 m (El-Hinnawi et al., 1978). These deposits derived from the adjacent limestone plateau during recent times.

-Fanglomerates; these sediments consist of mainly conglomerates and unconsolidated sands with thicknesses varying from a few centimeters along the edges to a few meters near the centers (Hassan et al. 1978).

Pleistocene deposits; these deposits lie directly under the Holocene deposits and on top of Pliocene clay and Eocene limestone. They are composed of sand and gravel. Pleistocene deposits represent the main water bearing formation in the Nile Valley. Said (1981, 1990) classified the Pleistocene deposits in to the following:

-Neonile deposits (Late Pleistocene) are made up of silt and clay and lie over the eroded, uneven surface of the flood plains of the Prenile deposits. These deposits are also found outside the plain as benches fringing the valley.

-Prenile deposits (Middle Pleistocene) are coarse, massive, and thick, and consist of graded sand - gravel unit. They constitute the main aquifer in the study area. They are represented by the Qena Formation and are overlaid by the Abbassia gravel in a limited extension (Said, 1981).

-Protonile deposits (Early Pleistocene) are of fluvial origin and are widely distributed along the western bank of the Nile. They are represented by the Idfu Formation and are composed of gravel and sand embraced in a red brown material. Said (1981) mentioned that there is no record of the Protonile deposits in the subsurface of the Nile Valley, but the graded sand-gravel unit of the succeeding Prenile rests unconformably on the Pliocene sediments.

Pliocene Deposits; Pliocene deposits consist of a lower marine sequence and an upper fluvial sequence. They are represented by dark colored clays inter-bedded with sandstone lenses. The Pliocene cover small parts of the older rocks along the Nile Valley and also represent some Nile terraces. These deposits crop out along the foot slopes of the bounding cliffs of the wadis. The Pliocene deposits lie below the Pleistocene deposits and act as a thick, impermeable one beneath them.

Eocene Deposits; these deposits are bounded the Nile Valley in the east and west as scarps and are made up of carbonates intercalated into clays, shals, and sands. Said, 1960 used Thebes Formation name to the Eocene limestone, and he described this formation as massiv, laminated limestone with flint bands or nodules and marl rich with Nummulites and planktonic foraminifera.

Amer et al., 1970 and Said, 1971 subdivided the Eocene rock exposed between Luxor and Assuit into two formations, namely the Thebes Formation at the base and the Manfalut Formation at the top. The Thebes Formation includes the massive to laminated limestone with flint bands and concretions. The exposed part of the formation decreases gradually toward the north due to the region gentle sloping northward. Figure (1. 4) shows the geological setting of the study area.

1.7. Geological history of the study area

The geological history of the Nile Valley near Tahta, according to Said, 1981extends from the Miocene to the Holocene age as follows:

-In the Miocene age the Mediterranean Sea was largely desiccated, resulting in a lowering fall of the base level. Due to this, the River Nile excavated a deep canyon into the Eocene limestone (Eonile river system).

- In the early Pliocene age the Miocene desiccation of the Mediterranean Sea was followed by a rise of the sea level, causing a marine ingression into the canyon. This transformed the Nile Valley into a narrow sea gulf extending up to Aswan. Interbedded red-brown clays with thin laminae of fine grained sands and silts were deposited this peri-marine to marine environment. In the fringes of the Nile Valley, near the wadis that drain into the River Nile, conglomeratic beds containing coarse sand and marl have been deposited (Armant

Formation). These sediments originate from the late Pliocene age and were principally derived from the adjacent Eocene limestone.

-In the late Pliocene age, the marine environment was gradually transformed into a fluvial environment. The Nile Valley sea gulf changed into a fluvial channel, depositing mainly carbonaceous clays (Paleonile River).

- During the Pleistocene age the River Nile was a competent river system that transported and deposited large amounts of coarse-grained material. In the early Pleistocene age (prenile river System), the River Nile eroded enormous amounts of the fine-grained Pliocene sediments. These fine-grained sediments were probably removed laterally up to the Eocene limestone slopes of the valley. During the prenile river system, many phases of erosion and deposition occurred. The deposits consist of coarsely grained quartz sands cross -bedded with layers of fine gravel and clay (Qena Formation).

Qena Formation is covered by Neonile fine-grained sands and silty sands (Dandara Formation). The prenile sediments in many locations (Qena Formation and Dandara Formation) are coverd by gravel from the late Pleistocene age (Abbassia Formation).

-In the Holocene age the Pleistocene sand and gravel were covered by a regionally extending sacrificial layer of silts and clays from the Holocene age. These silts and clays were floodplain deposits from the River Nile. They become gradually thinner due to the valley's slope.

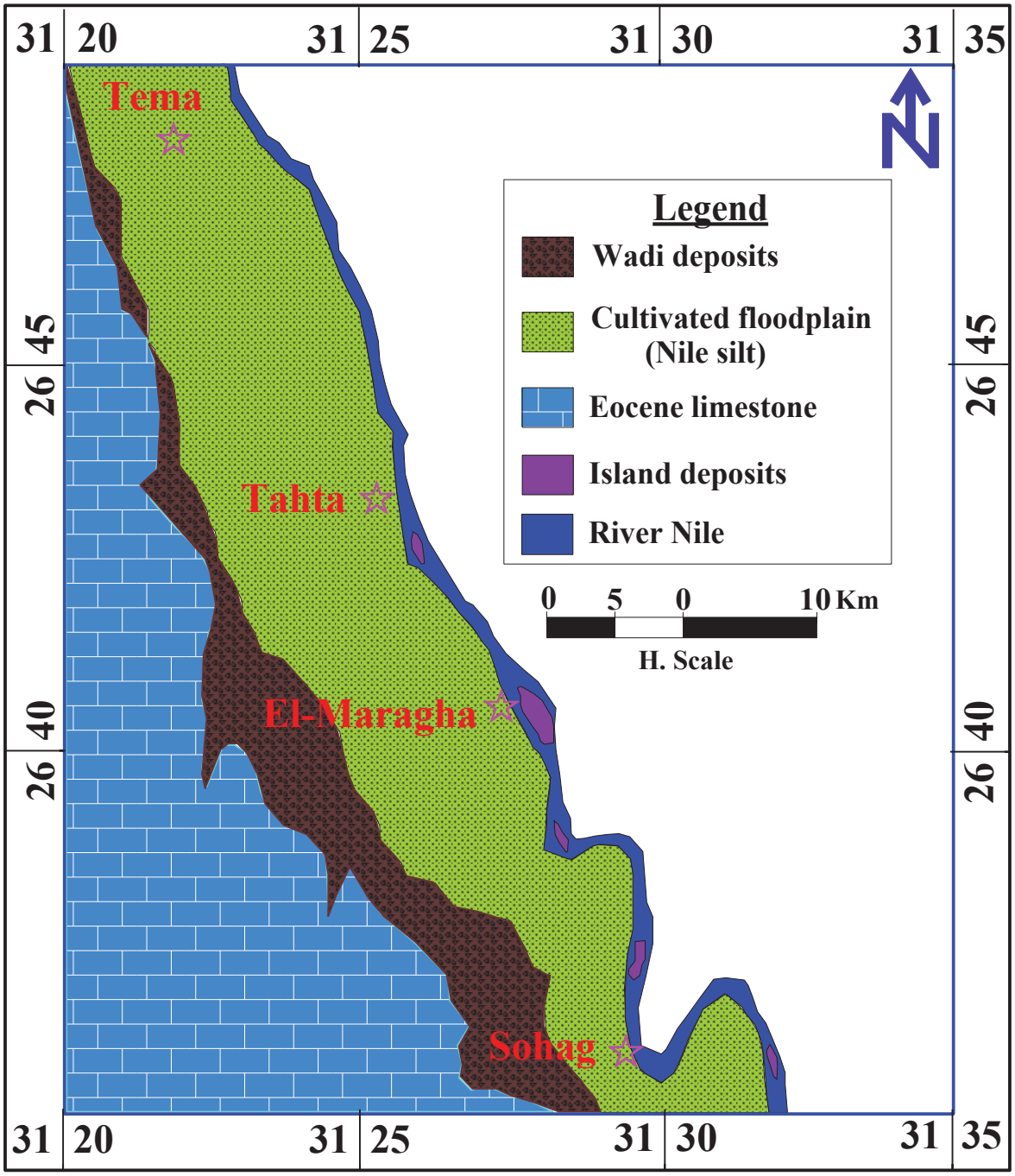

Fig. (1.4): Geologic map of the study area (after El-Sayed Sedek Abu Seif, 2010)

CHAPTER TWO

Remote Sensing Study

2.1. General outline

Egypt is suffering from a rapidly growing of population; the total population increased from 11 million in 1907 to 79.88 million in 2011 (Central Agency for Population Mobilization and Statistics, 2011). This increase forced the people living beside the River Nile to search for a new area to live. Brikowski and Faid, 2006 noticed that the River Nile sediments take up only 5% of Egypt's area but support 90% of Egypt's agricultural production. During the last three decades, the development of the Egyptian desert was characterized by an overpopulation pressure in the narrow Nile Valley and Delta by an average annual growth rate of up to 1.75% (FAOSTAT 2006). The successive governments of Egypt adopted policies seeking self-sufficiency in food production through the extension of cultivated land (1.2% per year) and the maximization of production of the existing agricultural land (Abdulaziz et al., 2009). The national plan aims to exploit 25% of Egypt's territory by the end of the first half of the 21st century. Reclamations for agriculture purposes and human settlements have targeted different areas throughout Egypt and the southern part of the western desert, including where the study area is located.

The study area is located at the western bank of the River Nile at Tahta in the Sohage Governorate in Upper Egypt. Upper Egypt has become important and attractive after the national project of agriculture (Tushka) created. The present study is particularly important as it focuses on the impact of human activities on the overall ecological conditions of the urban environment (Yeh, and Li, 1999). Remote Sensing and GIS techniques are powerful and cost-effective tools for assessing the spatial and temporal dynamics and changes in land-cover and land-use (Hathout, 2002, Herold, Goldstein, and Clarke, 2003 and Serra and Sauri, 2008). Remote sensing data provide an important source to trace land-use changes in areas where ground-based knowledge is sparse (Townshend, 1992; DeFries and Townshend, 1994). Remote sensing data provide valuable multi temporal data on the processes and patterns of land cover and land use change, and GIS is a useful technique for mapping and analyzing these patterns (Zhang, et al., 2002).

2.2. Remote sensing technique

2.2.1. Basic theory

Remote sensing is acquiring information about an object or certain phenomena by using a detector that never makes physical contact with it (Levin, 1999). The remote sensing term is commonly used in electromagnetic techniques of information acquisition. According to Elachi and Van Zyl, 2006 remote sensing is defined as the sensing and recording of energy emitted or reflected by an object or certain phenomena, and processing, analyzing, and applying that information. The electromagnetic radiation (EMR) is energy transmitted through space in the form of electromagnetic waves recorded by ground sensors or remote sensing platforms (satellites).

A satellite system is composed of a scanner with sensors (which are made of detectors) and a satellite platform. The scanner comprises the entire data acquisition system, like the landsat thematic scanner or the Spot panchromatic scanner (Lillesand and Kiefer, 1994). It includes both the sensors and the detectors. There are two types of remote sensing sensors: passive and active. If the sensors detect naturally available electromagnetic radiation, like that from the sun, they are passive sensors. Sensors detecting radiations from artificial sources (transmitter) such as a laser flour sensor or synthetic radar are active remote sensing sensors.

The remote sensing technology has greatly facilitated investigation and monitoring of land use/cover changes. Several factors, such as image quality, data analysis methodology, interpretation techniques, and numerous temporal and phonological considerations, significantly influence the quality of the resulting geospatial information (Vogelmann et al. 2001). Land sat Thematic Mapper (TM) and Enhanced Thematic Mapper Plus (ETM+) data have been widely used for these purposes (Green et al. 1994, Wolter et al. 1995, Kaufman and Seto 2001).

2.2.2. Remote sensing materials

In this study, images from Landsat Thematic Mapper (TM) acquired in 1987 (Fig. 1.2) and Egypt sat acquired in 2009 (Fig. 1.3) have been used to detect the changes in agricultural and urban areas as well as the River Nile, from 1987 to 2009. The topographic maps prepared by the Egyptian Military Survey at a scale of 1:50,000 were also used, in addition to field investigations. Numerous change detection methods have been developed to assess variations

in the land-cover using satellite data, including image differencing, the principal component method, and post-classification comparisons. Of these techniques, the post-classification comparison is preferred. Its accuracy in detecting the dynamic changes depends mainly on the accuracy of the individual classification of each land-cover unit.

2.2.3. Methodology

2.2.3.1. Radiometric calibration

Pixel values in satellite imagery represent the radius of the surface in the form of Digital Numbers (DNs), which are calibrated to fit a certain range of values. The conversion of DN to the absolute radiance value is an important procedure for a comparative analysis of several images taken by different sensors. Each sensor has special calibration parameters used in recording the DN values. The same DN values in two images detected by two different sensors may represent two different radius values (Levin, 1999). Remote sensing systems are designed to measure the radiometric characteristics of the targets of primary interest in the linear region, where the output signal is linearly proportional to the input signal. In this study, radiometric calibration was performed using ERDAS imagine – 9.2 (Leica Geosystems, 2008).

2.2.3.2. Geometric correction

Geometric correction is applied to raw sensors data to correct errors of perspective due to the Earth's curvature and sensor motion. Some of these errors are commonly removed at the sensor's data processing center (NASA). Georeferencing refers to the process of assigning map coordinates to image data.

2.2.3.3. Subset and mask

Image subset reduces the storage capacity of the image file, so analysis processes will be faster. A masked image is a binary image that consists of values of 0 and 1. When a mask is used in a processing function, the areas with values of 1 are processed and the masked 0 values are not. The image mask process is used to reduce the time needed for processing and the storage capacity of processed images (El-Sayed, 2010).

2.2.3.4. Classification

The reflection values in an image depend on the local characteristics of the earth surface, so there is a relationship between land cover and measured reflection values. Multispectral image classification is used to extract thematic information from satellite images in a semi-automatic way (Levin, 1999). Digital image classification uses the spectral information represented by the digital numbers in one or more spectral bands and attempts to classify each individual pixel based on the spectral information (Fig. 2.1).This type of classification is termed spectral pattern recognition. The result of the classified image is a mosaic of pixels, each of which belongs to a particular theme and essentially a thematic "map" of the original image.

There are two types of classes, information classes and spectral classes. Information classes are the categories of interest that the analyst is actually trying to identify in the images, such as different kinds of crops, different forest types or tree species, different geologic units or rock types, etc (Lillesand and Kiefer, 1994). Spectral classes are groups of pixels that are uniform with respect to their brightness values in the different spectral channels of the data. It is the analyst's job to decide on the utility of the different spectral classes and their correspondence to useful information classes. There are two types of classification, unsupervised and supervised.

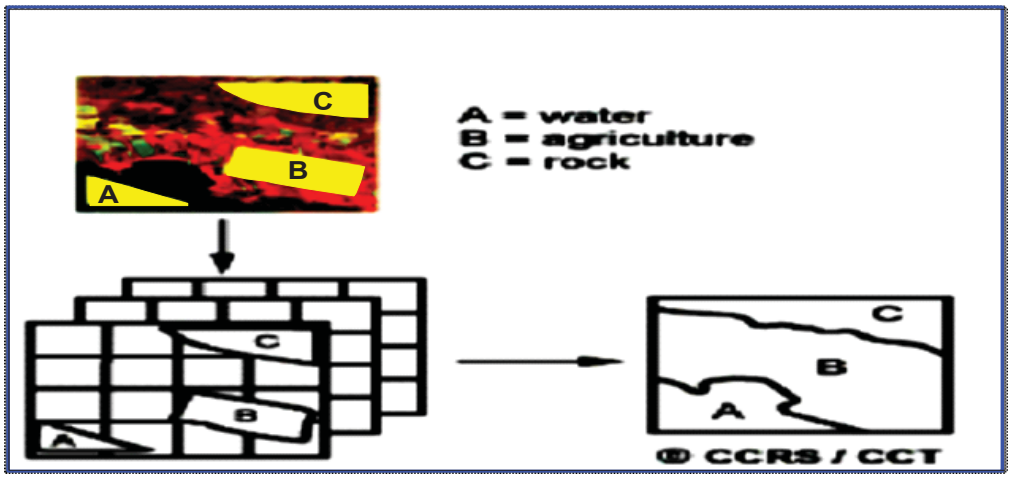

Fig. (2.1): Remote sensing image classification

I. Supervised classification; the analyst identifies in the images homogeneous representative samples of the different surface cover types that are of interest. Thus the analyst is "supervising" the categorization of a set of specific classes. The numerical information given in spectral bands for the pixels comprising these areas was used to train the computer to recognize spectrally similar areas for each class. The computers use a special program or

algorithm, of which there are several variations, to determine the numerical "signatures" for each training class (Fig. 2.2). Once the computer has determined the signatures for each class, each pixel in the image is compared to these signatures and labeled according to their classification. First we identify the information classes, which we then use to determine the spectral classes they are represented by.

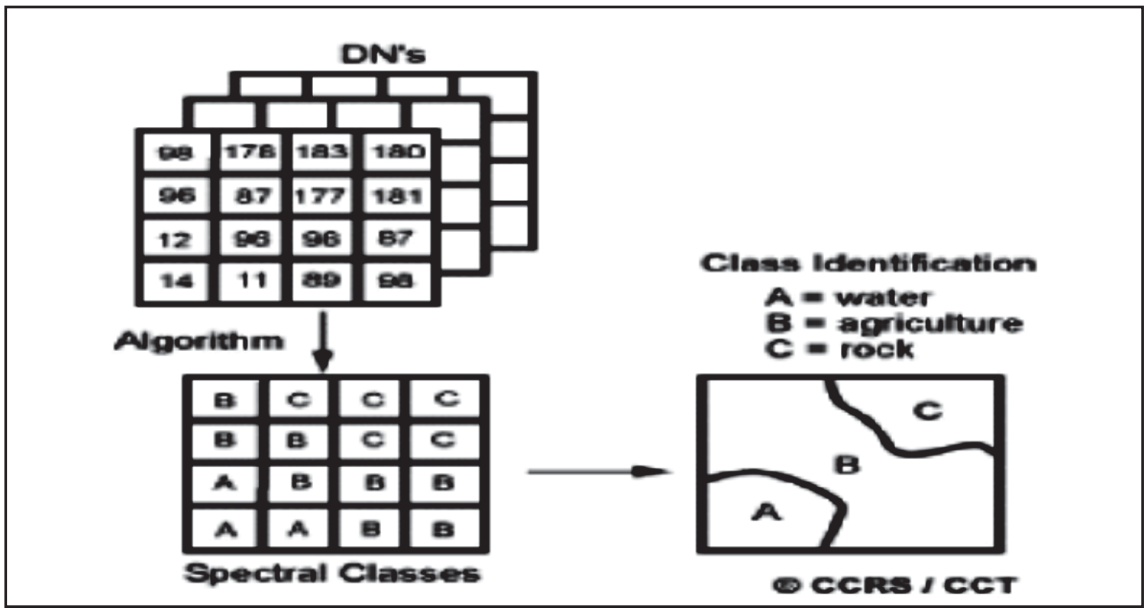

Fig. (2.2): Remote sensing image classification

II. Unsupervised classification; in this classification method, the spectral classes are grouped together first, based on the numerical information in the data, and then matched by the analyst to his information collected from field observation or other sources. Programs, called clustering algorithms, are used to determine the natural (statistical) groupings or structures in the data. Unsupervised classification is therefore not done without any human intervention; however, it does not start with a pre-determined set of classes, as in a supervised classification. One of the first steps before classifying an image is to enhance the image in a way so as to provide rough information of land use differentiation. The simplest way is to combine different bands like infrared, red, and green for false color composite. For accurate results the two major types of image classification were applied in this study, and then the two resulting land-cover maps were evaluated to select the best manner.

In this study the TM data and Egypt sat data were classified by using both supervised and unsupervised classification techniques. The landuse maps from 1987 and 2009 were examined to compute the overall change patterns in each category. For visual interpretation,

the combinations of bands 2, 1, 3 and 7, 4, 2 were assigned the color codes red, green, and blue, respectively (Scepan, et al., 1999; Bakr et al. 2010).

1. Supervised classification (Maximum Likelihood)

Supervised classification was developed for satellite image processing, where it can be applied to the classification of spectral layers. However, it can also be applied to other forms of remote sensing and has been used for the classification of interpolated acoustic reflectance data. Supervised classification depends mainly on the experience and accuracy of the user in detecting the signature differences between various units in the satellite image with the naked eye.

Maximum Likelihood classification is a popular hard classification process where remotely sensed data are based on information from a set of signature files. It is dependent on the probability density function associated with a particular training area. In this classification process, pixels are assigned to the most likely classes based on the comparison of the priority and probability belonging to each of the signatures being considered as a data file. It can be as precise as a single value and can count of the applicable to all pixels, or as broad as an entire image representing different prior probabilities for each pixel. Using ERDAS Imagine Version 9.1, new supervised classification analyses were carried out on the TM (1987) and Egypt sat (2009) images to identify the land use/cover changes in the study area. The supervised classification wasn't able to differentiate between various landcover units, so the unsupervised classification technique, which gave more valuable and accurate results, was utilized.

2. Unsupervised classification

In unsupervised classification, the computer separates the pixels into classes without any direction from the analyst (Sabins, 1997). This means that unsupervised classification techniques do not require the user to specify any information about the features contained in the images. In the study area, the unsupervised classification of the six visible and reflected IR bands of the sub-scene resulted in 20 classes. At this point, the image is difficult to interpret. Decisions need to be made concerning land cover types corresponding to each category.

To make these decisions, additional materials and knowledge of the area are useful. Checking in the field, the various areas discriminated in the digital image should be performed at the time of correction of the image to obtain more accurate results. If this knowledge is not available, scientific reasoning may be used to group the various categories together into related land cover units. In the case of the present study, the latter was the only possibility. The unsupervised classification analyses (Fig. 2.3 and 2.4) were carried out on the TM (1987) and Egypt sat (2009) images to identify the land-use/cover changes in the study area. Three different land-use classes were identified:

1. Agricultural and cultivated lands (green).
2. Urban and man-made structures (black).
3. River Nile (blue).

Post-classification refinement a simple and effective method was used to improve the accuracy of the classification (Harris and Ventura, 1995), since the urban surface is heterogeneous and composed of a complex combination of features (e.g., buildings, roads, grass, trees, soil, and water) (Jensen, 2007). After the post-classification refinement, the misclassifications were mostly corrected. The post-classification transformation of the classified raster into shape three vectors was done using ENVI version 4.5 and ARC GIS tool. The obtained shape three was converted into a geo data base in order to complete a change detection analysis. Before this step, it was necessary to make sure that the classification used for the change detection procedure matches facts in the field obtained using the accuracy assessment technique.

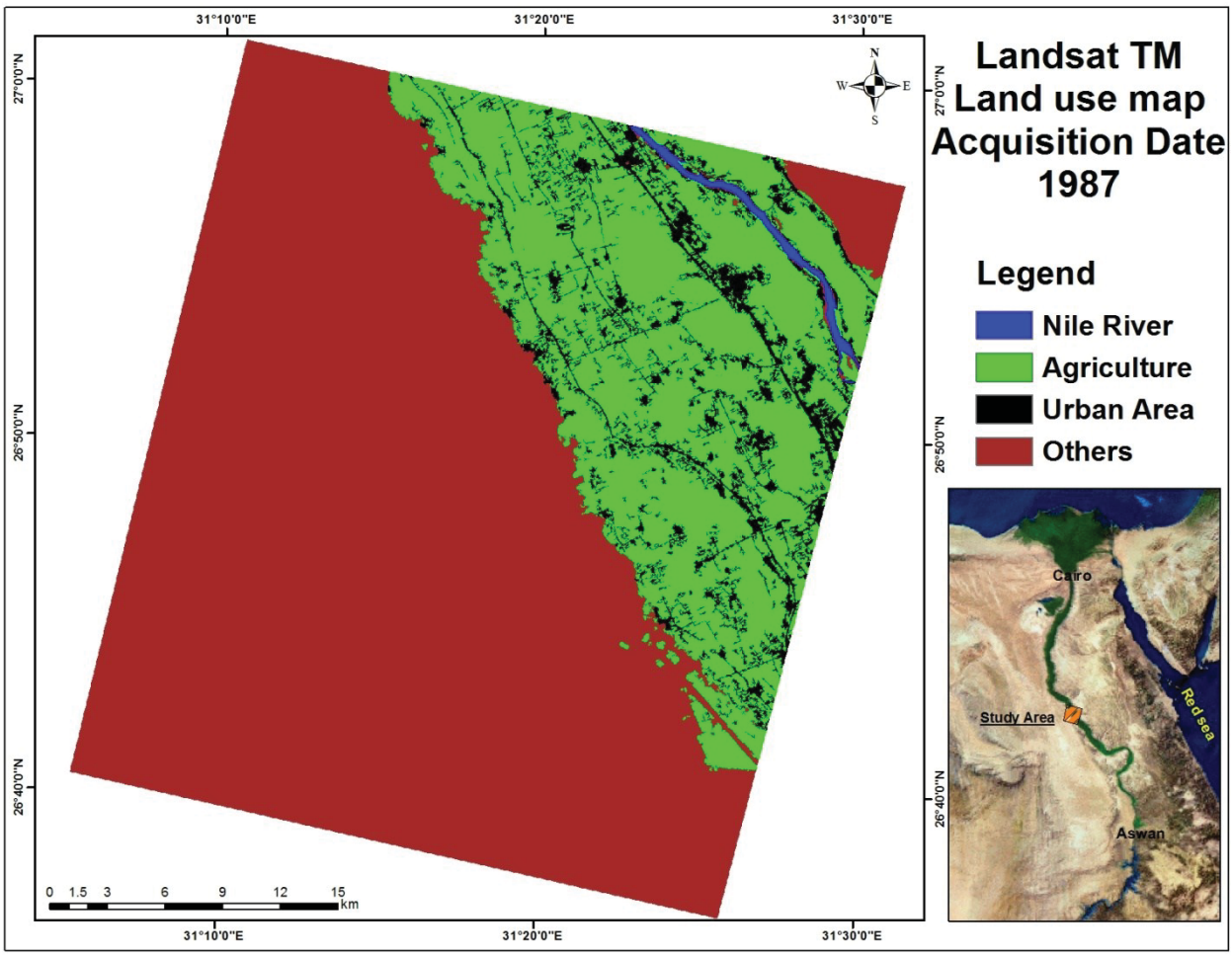

Fig. (2.3): Land-use map 1987

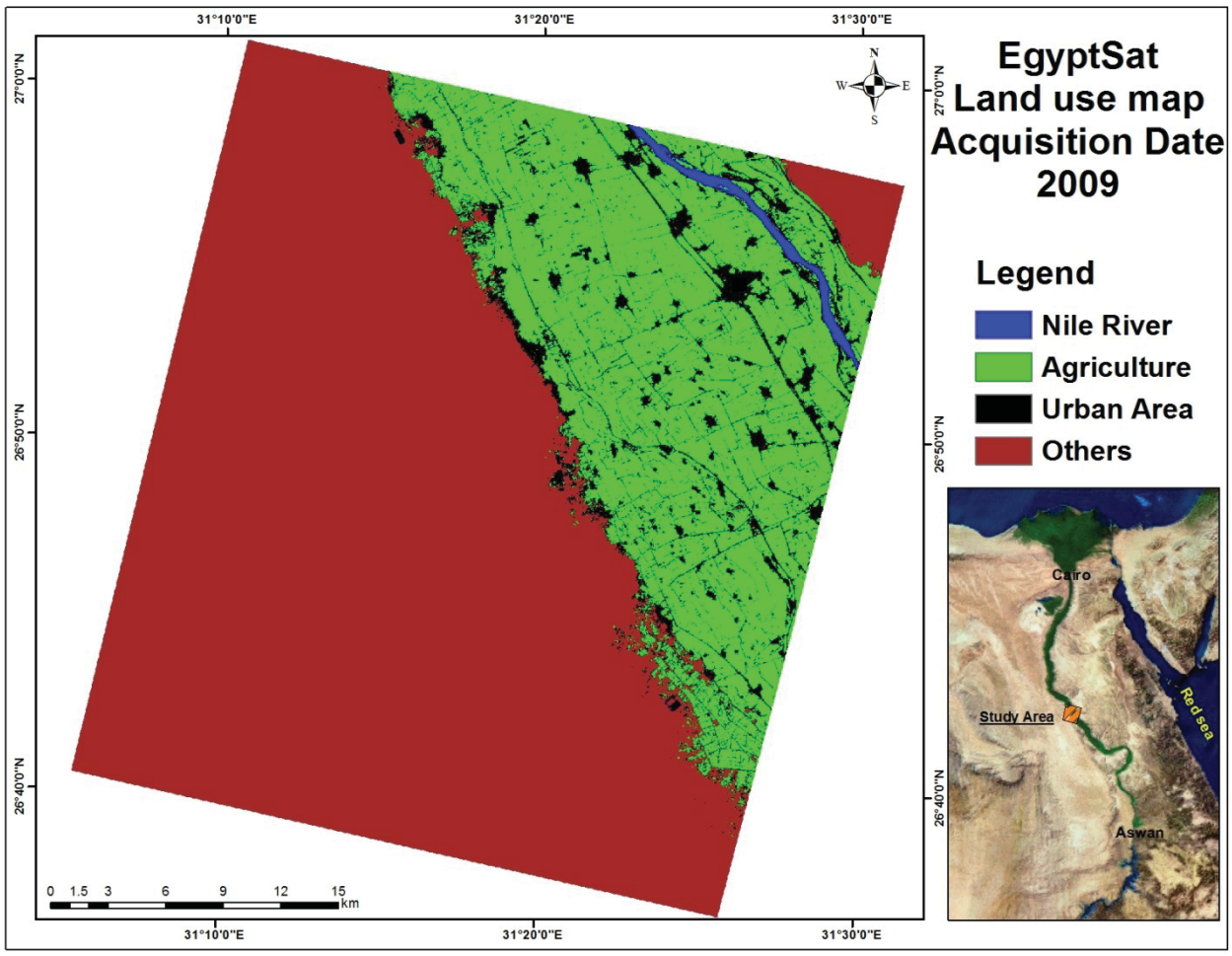

Fig. (2.4): Land-use map 2009

2.2.3.5. Accuracy assessment

Accuracy is the degree of closeness of results to the accepted values. The expected accuracy and the levels of confidence obtained from a particular accuracy assessment depend primarily on the number of samples of each class and the quality of the reference data set involved in the analysis. The classified thematic maps are produced for a wide variety of resources: soil types or properties, land cover, land use, and many more. These maps are not particularly useful without quantitative statements about their accuracy. Generally, classification accuracy refers to the extent of correspondence between the remotely sensed data and the reference information (Jensen, 2007).

The accuracy of digital land cover classifications can be expressed quantitatively by building and interpreting a classification error matrix. An error matrix compares information from a classified image or land cover map to known reference ("truth") sites for a number of sample points. The matrix is a square array of numbers that express the labels of the sample points assigned to a particular category in one classification relative to the labels of samples

assigned to a particular category in another classification. One of the classifications, usually the columns, is assumed to be correct and is considered the reference data. The rows then display the map labels or classification categories generated from remotely sensed data. Two labels from each sample are thus compared to one another:

-Reference data labels: the class label of the "truth" sample point derived from data collected that is assumed to be correct.

-Map labels: the category label of the same sample point derived from the satellite image classification.

The accuracy assessment of the land cover maps extracted from Landsat data includes the generation of 100 random references ("truth points") for each land cover map. Accuracy assessment of the land cover maps after the post-classification refinement and merging of the 20 classes into 3 classes covering the major land cover units was then performed using field data and topographic maps, and the results were recorded in a confusion matrix.

A confusion matrix, a standard method for accuracy assessment (Rosenfield and Fitzpatrick-Lins, 1986; Congalton 1991; Congalton and Green 1999), is applied to detect the accuracy of both the classification and change detection outputs. Two important pieces of information can be derived from the error matrix: errors of omission, or producer's accuracy, and errors of commission, or user's accuracy (Story & Congalton, 1986; Lillesand and Kiefer 1994; Campbell, 2002). The user's accuracy of a specific class is the ratio of the correctly classified samples to the total number of samples selected in that class. A Kappa coefficient is commonly used as a measure of the map accuracy (Hudson and Ramm, 1987; Congalton and Green, 1999). Typically, the overall accuracy target of 85% with no class less than 70% accuracy is acceptable for land-use/land-cover mapping with Land sat data (Thomlinson et al., 1999; Anderson et al., 1976). The accuracy of the land-use/land-cover maps was evaluated at several stages in the processing. Shalaby and Tateishi (2007) found that integrating visual interpretation with supervised classification increases the overall accuracy by about 10 percent in areas that have undergone a severe land-cover change. The expected accuracy and the level of confidence obtained from a particular accuracy assessment approach depend primarily on the number of samples from each class and the quality of the reference data set involved in the analysis. The accuracy of both classification and change detection outputs in terms of agreement between our derived map and references datasets is evaluated empirically using confusion matrices, the standard method for accuracy assessment

(Rosenfield and Fitzpatrick-lins, 1986; Congelton and Green 1999). Important information can be derived from the errors of omission, or producer's accuracy. Commotion can be derived from the error matrix: error of omission and commission are derived from the ratio of the correctly classified samples to the total number of samples selected in the class. Likewise, the producer's accuracy of one class is derived by taking the ratio of correctly defined pixels to the total number of pixels selected for that class in the reference data.

For classification purposes, 75 or 100 samples per land-use is considered acceptable in evaluating large areas (~4000 Km^2) or if there are more than twelve land-use classes in the analysis (Congalton and Green, 1999). After eliminating reference data close to the boundaries, 95 samples, completely included within 10-15 pixels, were randomly selected from reference stations of each land-use class and given a unique identification number. In a random fashion, 35% of these identification numbers were selected randomly for use in an accuracy assessment, and the remainder was used as training sites. Before carrying out the change detection, the accuracy of the land-use/land-cover maps was evaluated at several stages in its processing. Table (2.1) shows the overall accuracy of the land- use/land cover maps, along with the user and producer accuracy and Kappa coefficients of Egypt sat 2009.

Table (2.1): User's and producer's accuracies and Kappa coefficients for the change detection data analysis

Accuracy Total Egypt sat 2009					
Class name	**Reference totals**	**Classified totals**	**Number correct**	**Producers accuracy %**	**Users accuracy %**
Nile River	52	50	49	94.23	98
Agricultural	50	50	47	94	94
Urban	41	50	40	97.56	80
Desert	57	50	48	84.21	96
Total	200	200	184	-	-
Overall classification accuracy = 92%					

Class name	**Kappa statistics**
Nile River	0.97
Agricultural	092
Urban	0.7
Desert	0.94
Total Kappa statistics	**0.89**

In Egypt, the presence of water and vegetation leads to great difficulties to distinguish between urban areas and agriculture fields because of similar visible-near infrared spectra (Pax-Lenney et al., 1996; Abdulaziz et al., 2009). In my study, the calculated overall accuracies represent the maximum obtainable accuracies, but not the optimum. This is due to the errors of omission, which are calculated from the producer accuracy data, not accounting for any possible bias introduced by the details of the sampling process (e.g. the sampling technique itself or the number of samples per class) (Hay 1979). Table (2.1) shows that the agricultural classification accuracy is 94%, while urban classification is 97.56 %, and the River Nile classification accuracy is 94.23%.

2.2.3.6. Change detection

Change detection is a general remote sensing technique that compares images collected in the same area at different times and highlights the features that have changed. Many remote sensing change detection techniques have been developed, and the advantages and

disadvantages of each have been reviewed by a number of authors (Anderson, et al., 1976). New digital change detection techniques are continuing to be developed, primarily in response to the range of social and environmental challenges posed by human transformation of the Earth's surface (Goudie, 1993 and Turner, 1990) and the potential for remote sensing in monitoring related processes (Gutman, 2004, Rasool, 1987 and Ustin, 2004).

All change detection techniques rely on the basic idea that changes in the spectral and/or textural characteristics of geometrically, atmospherically, and topographically corrected remotely sensed images represent changes in the Earth's surface. However, available techniques vary greatly in terms of their input requirements (e.g., classified or non-classified images), difficulty of implementation, and output (e.g., binary change/no change; type of change; magnitude and direction of change). Which change detection technique is most suitable for any given study therefore, largely depends on the objectives of the study and the multi-temporal remote sensing dataset (Jensen, 2004). Lu et al., (2004) identified seven major groups of change detection techniques, including algebra, transformation, and classification, advanced models, (GIS) approaches, and visual analysis, among others. However, the most frequently used change detection algorithms are image differencing, principal components analysis, and post-classification comparison, in that order.

I. Image differencing

This approach involves the subtraction of two images, on a pixel-to-pixel basis, of the same sensor, spatial, spectral, and radiometric resolutions. Recent studies show that image differencing is the most accurate change detection technique (Singh, 1989) but only under the previously discussed conditions. For example weather changes, such as cloud cover and atmospheric temperature, between the two acquisition dates of the images may cause a great change in the pixel value of a specific area, when, in reality, no change actually occurred. Image differencing is most suitable for qualitative change detection analysis.

2. Principal component analysis (PCA)

Principal component analysis is a common data transformation technique for the compression of the information content of a number of bands into just two or three principal components (Jensen, 1995). PCA is a linear transformation which defines a new orthogonal coordinate system in which the data are correlated (Wiemker et al., 1997). PCA highlights the areas of temporal change but does not provide information about the type of change.

3. Post-classification comparison

This type is necessary for the quantitative analysis of the change detection products. In this technique, the change of each class on each date is addressed. This analysis is advantageous as it can be applied to data from different sensors and different spatial resolution, is easy to understand and implement, and is often the most reliable approach (Weismiller et al., 1977 and Jensen and Narumalani, 1992). It also provides a complete change matrix. The accuracy of the change, however, is based on the classification accuracy (Jensen, 1995).

In this study, the post-classification comparison method is the most preferable. The magnitude and location of change ('from-to' change detection matrix) were determined for all the studied years (1987- 2009). The major land-cover changes were color-coded. Table (2.2) shows the observed major land-cover changes, and the area of each land cover class is given in m² with the yearly average change for each type (class).

Table (2.2): The lands-cover changes in (Hectare) in 1987 and 2009 and the average of change per year

Class	1987	2009	Total change	Change/Year
Agricultural	34573.90 ha	36359.80 ha	1785.9 ha	81.2 ha
Urban	6034.37 ha	8265.58 ha	2231.21 ha	101.45 ha
River Nile	686.79 ha	825.11 ha	138.32 ha	6.29 ha

2.3. Discussion and conclusion

Understanding the potentiality of natural resources and natural hazards is very important in the development and also in the creation of new societies (Bakr et al., 2010). This information is not only useful for improving the natural resources, but it also plays a vital role in keeping the land development free from water logging, soil salinity, desertification, and probable natural hazards, such as flash floods (Abdalla M. Faid and Abdulaziz M. Abdulaziz, 2011). The statistics and maps from the analyses are useful for monitoring socioeconomic potential and trends (Abdulaziz et al., 2009).

The agriculture in the study area covered about 34573.90 ha in 1987, and it reached about 36359.80 ha in 2009 (Fig.2.5), which means a total increase in the agricultural area of about

1785.9 ha, with an average annual growth rate of 81.2 ha/year. This increase in the agricultural area is due to the extensive reclamation project in the study area. The presence of underground water, represented by the Quaternary aquifer, plays an important role in the development. This aquifer mainly recharges from the surface water (River Nile and irrigation canal), which leads to the groundwater being suitable for irrigation, due to the low level of salinity and the low sodium adsorption ratio.

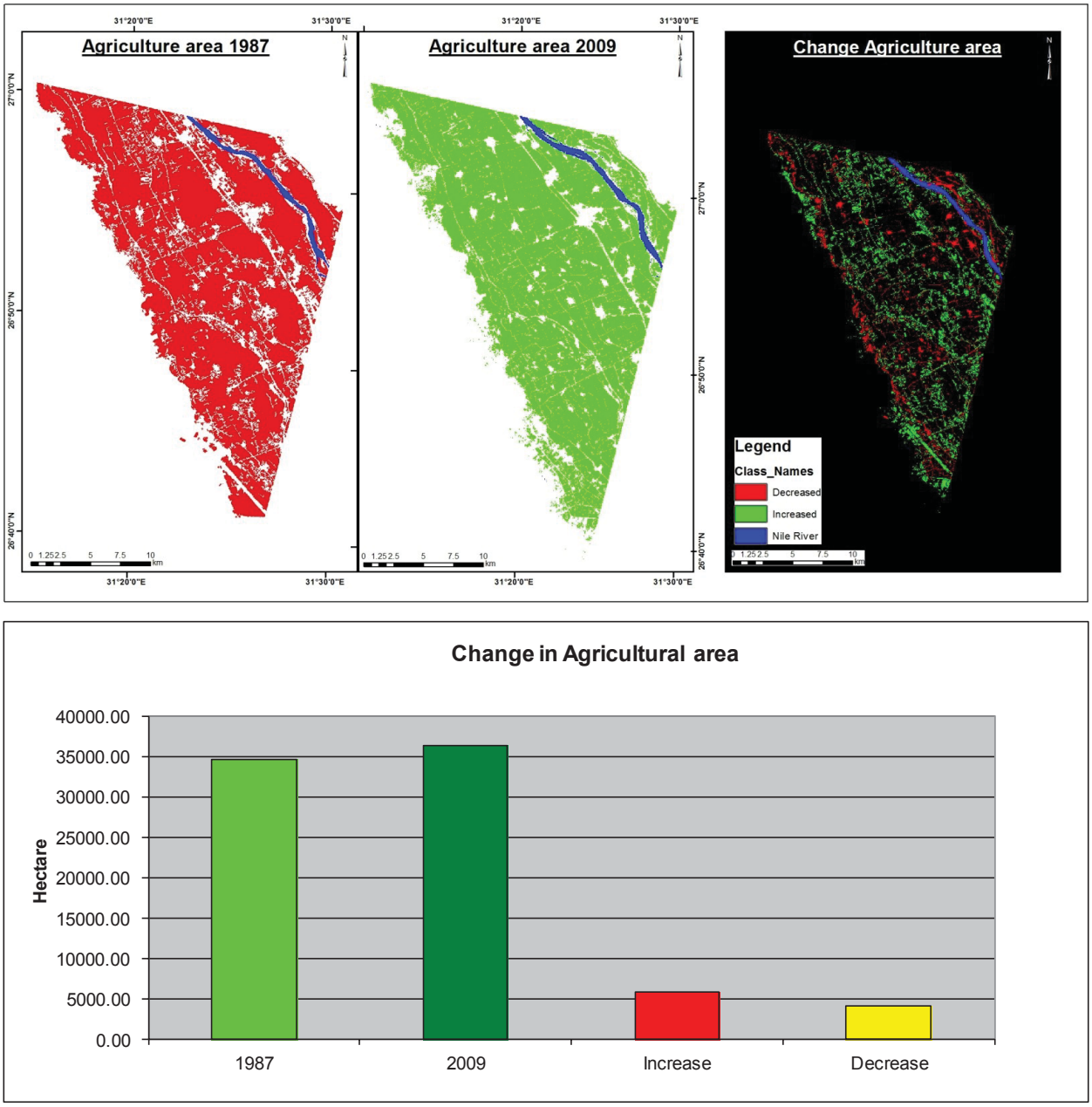

Fig. (2.5): Change detection map in agricultural area

The presence of water suitable for life acts as the main role in the development, which lead to an extensive urban project to resolve the increasing population. Figure (2.6) shows total urban area in 1987 as 6034.37 ha, and in 2009 it reached 8265.58 ha with a total increase of about 2231.21 ha with an average annual growth rate of 101.45 ha/year.

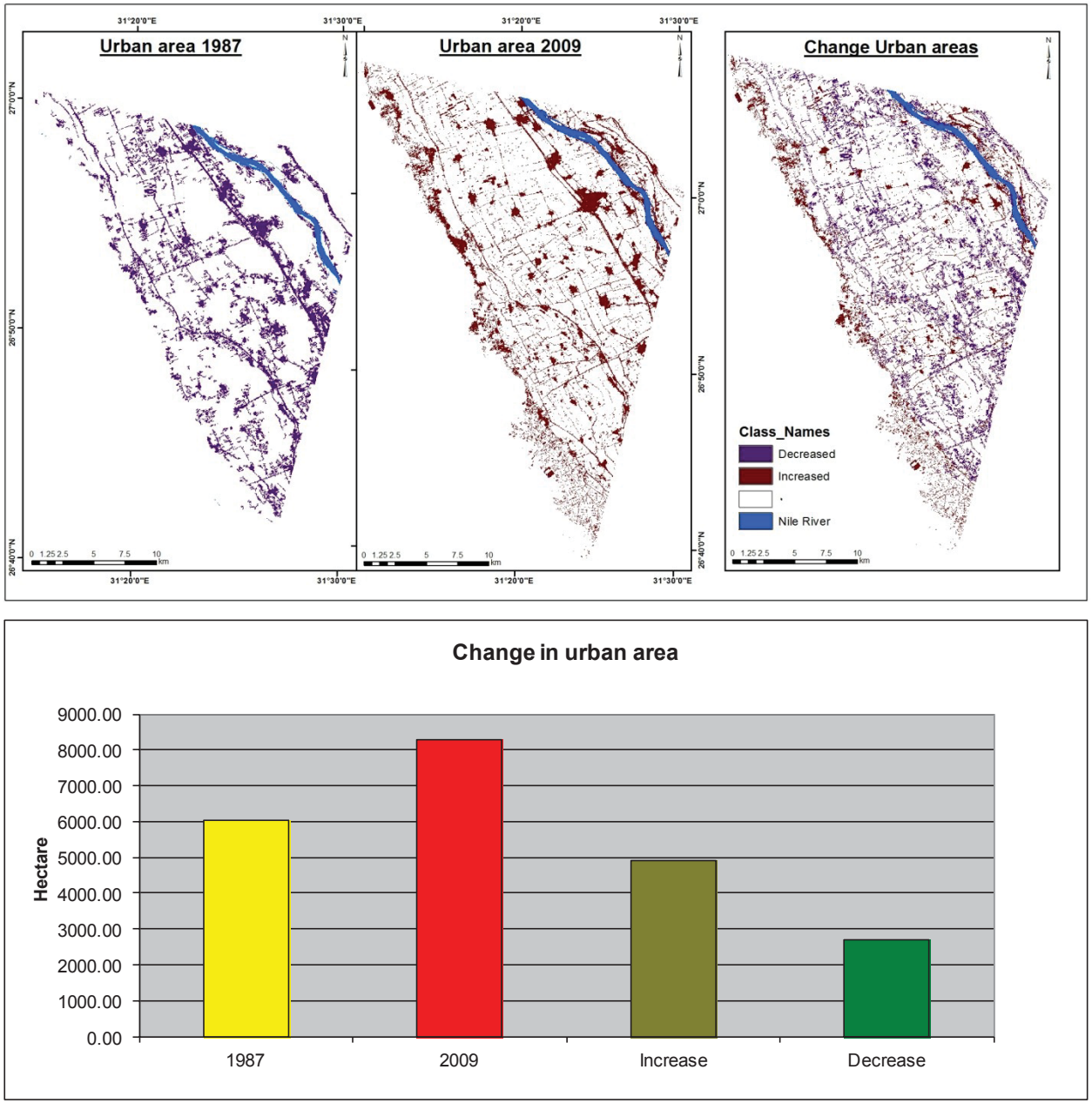

Fig. (2.6): Change detection map in urban area

The River Nile is the main source of surface water in the study area and acts as the source of the recharge of the quaternary aquifer, which acts as the main source of groundwater in the

area under investigation. The River Nile (Fig. 2.7), covered 686.79 ha in 1987 and 825.11 ha in 2009 with a total change of 138.32 ha and an average annual growth rate 6.29 ha/year.

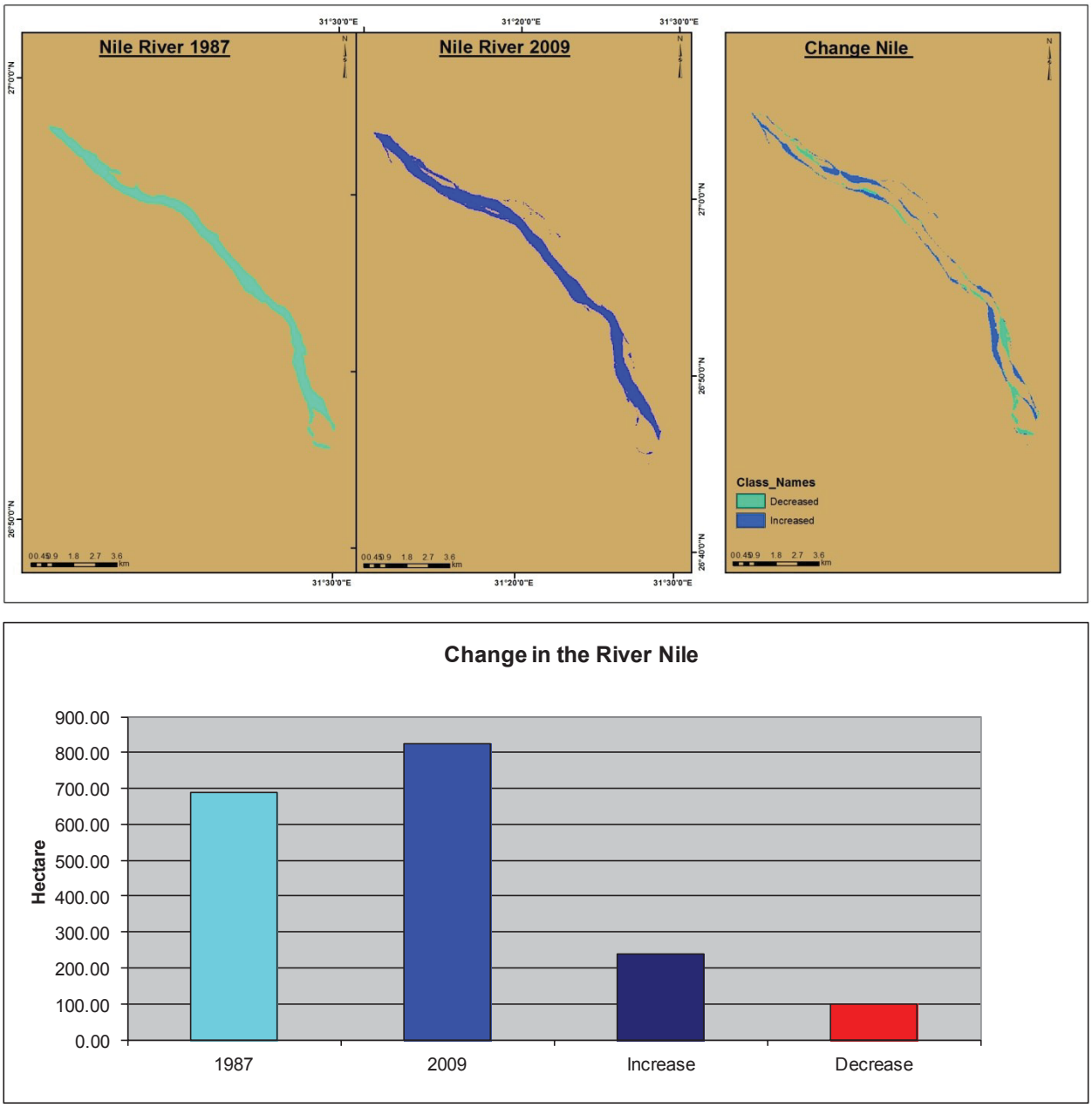

Fig. (2.7): Change detection map in the River Nile

CHAPTER THREE

Geophysical Studies

3.1. General outline

In the last period Egypt achieved a rapid agricultural development, especially in the western desert, which caused increasing demands on the water supply. The lack of surface water in this area leads to an extensive search for groundwater the main water source in the Egyptian desert. Geophysical studies are very helpful for groundwater explorations. In this study we used geoelectrical methods. These methods are widely and successfully used in the determination of the depth to the water table, the thickness of the soil, and the groundwater carrier. They are also useful in locating and mapping sand and gravel deposits. These methods are very flexible and immediately adaptable to varying problems. The electrical resistivity method measures the specific resistance of subsurface layers due to the flow of an electric current.

The electrical resistivity of rocks and minerals is an extremely variable property that depends on a number of parameters such as the porosity, permeability, water content, and salinity of the formation water. An increase in porosity and salinity causes a decrease in the electrical resistivity of saturated rocks; however the presence of clays and conductive minerals can also decrease the resistivity. The increase of temperature also leads to a reduction of the electrical resistivity, due to the solubility, as well as the mobility, of ions in the electrolytes. The electrical conductivity of rocks is mainly caused by the electrolytic conductivity of the pore fluids, as most mineral grains are insulators. Thus, resistivity of rocks is strongly dependent on the physic-chemical conditions of the water in the pores and interstices, the amount of water, and the manner in which the water is distributed.

3.2. Principles of the electrical method

The principle of vertical electrical sounding was established in the 1920s (e.g. Gish and Rooney, 1925). In the electrical resistivity method a current is applied to the ground by contractive current electrodes. Any subsurface variation in conductivity alters the current flow within the earth. The current flow in the ground through the two current electrodes causes a potential difference, which can be measured with a second pair of electrodes (potential electrodes), placed in line between them. The basis for the current flowing through the earth's materials is Ohm's law,

$$(\Delta V = IR) \qquad (1)$$

Where, **ΔV** (mV) is the potential difference between two points, **I (**MA**)** is the current flowing between these points and **R** (Ω) is the resistivity of the medium between these two points.

If **I** is the current passing through an electrode placed on a flat piece of earth of resistivity**ρ**, the electric potential at a point distance **a** from the electrode is given by:

$$V = \frac{\rho I}{2\pi a} \tag{2}$$

The simplest method of conducting a resistivity survey is to arrange the four electrodes in a straight line on the surface. Figure (3.1) shows a layout of the current and potential electrodes. The current electrodes are A and B and the potential electrodes are M and N. The M electrode is at distances r1 and r2 from the current electrodes and N electrode is at distances r3 and r4 from the current electrodes, respectively. The electric potential VM at the M electrode will be:

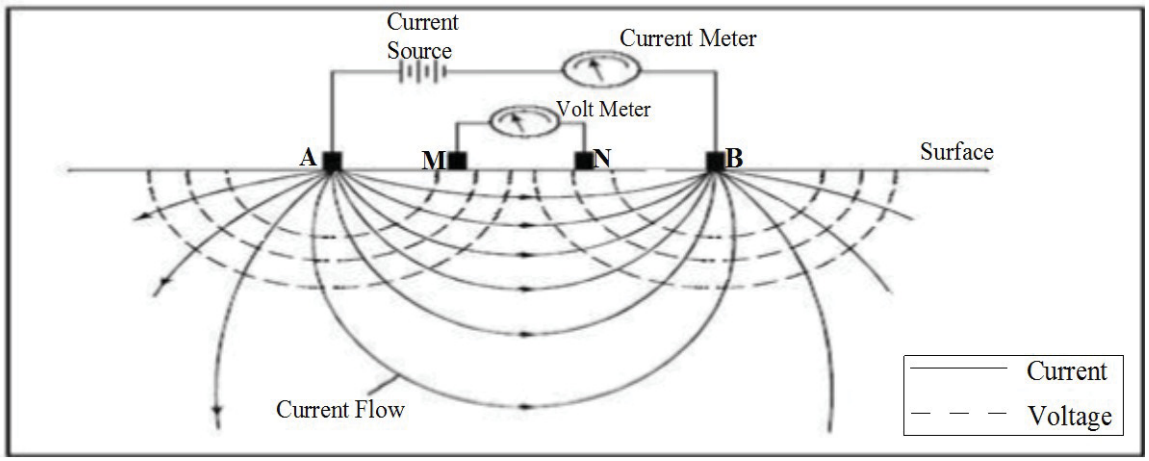

Fig. (3.1): A sketch of the layout of the current electrodes (A&B) and potential electrodes (M&N)

$$VM = \frac{I\rho}{2\pi}\left(\frac{1}{r1} - \frac{1}{r2}\right) \tag{3}$$

And the potential VN at the N electrode will be:

$$VM = \frac{I\rho}{2\pi}\left(\frac{1}{r3} - \frac{1}{r4}\right) \tag{4}$$

The difference potential ΔV measured by the voltmeter will be:

$$\Delta V = VM - VN \tag{5}$$

$$\Delta V = \frac{I\rho}{2\pi}\left(\frac{1}{r1} - \frac{1}{r2} - \frac{1}{r3} + \frac{1}{r4}\right) \quad (6)$$

Then

$$\rho = \frac{2\pi\Delta V}{I}\left[\frac{1}{\frac{1}{r1} - \frac{1}{r2} - \frac{1}{r3} + \frac{1}{r4}}\right] \quad (7)$$

where ρ is called the apparent resistivity ρa

$$\rho a = (\Delta V / I)\, K \quad (8)$$

$$K = \left[\frac{2\pi}{\frac{1}{r1} - \frac{1}{r2} - \frac{1}{r3} + \frac{1}{r4}}\right] \quad (9)$$

and where **K** is the geometrical factor which depends on the electrode layout or configuration (Wenner, Schlumberger, Dipole-Dipole).

3.3. Field instruments

In this study we used the Terrameter SAS 300 to carry out the geoelectrical survey. Additional accessories included batteries, calibrating resistors for checking the instrument, steel electrodes of about 0.85m in length and 2.5 cm in diameter, field cables characterized by plastic-insulation with a single conductor and low electrical resistance 0.5 mm^2 (two 500m reels for the potential lines and two 1000m reels for the current lines), hammers, a Brunton compass, wood marks, a GPS instrument, and wireless telephone.

3.4. Electrode configuration

The most widely used electrode configurations are, the Wenner, Schlumberger, and Double dipole arrays. The selection of one of these arrays depends on the aim of the investigation. Each configuration has a specific mathematical formula used during data processing. In the present investigation, the Schlumberger configuration was used. The Schlumberger method is the most used technique in electrical prospecting. In this array, four electrodes are placed along a straight line on the earth's surface (Fig.3.2). The outer electrodes are for the current, and the in-between electrodes are the potential ones. The separating distance between the potential electrodes (MN) is small compared with the total length of the array (AB), usually less than one fifth of the total length.

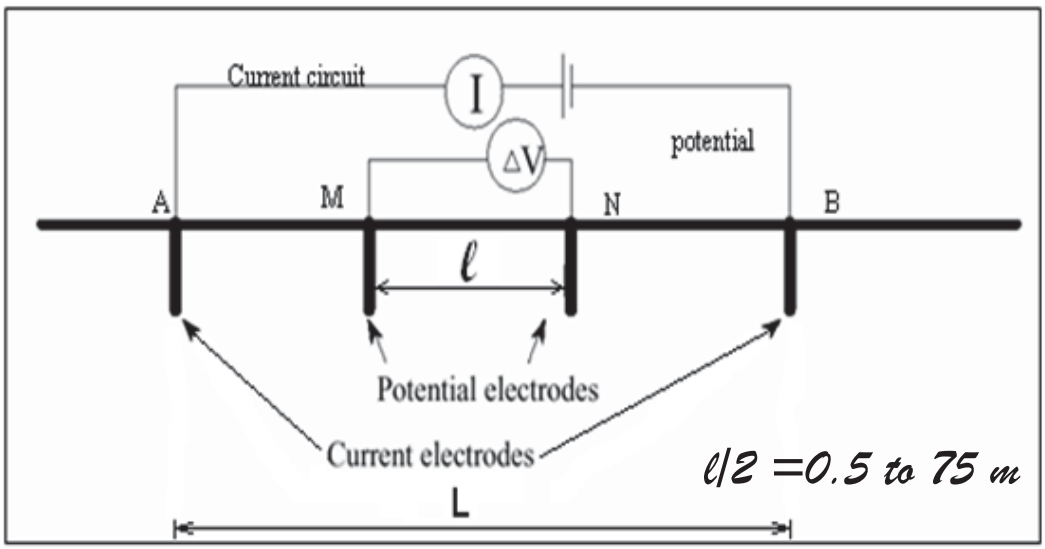

Fig (3.2): Schlumberger electrode array

3.5. Field data acquisition

29 vertical electrical soundings (Fig. 3.3) in Schlumberger array were carried out in the area under investigation to detect the groundwater conditions, including depth, thickness, and location of the aquifer. The resistivity Schlumberger sounding was carried out with half-spacing in the range of 300m to 1000m, depending on the topography of the area.

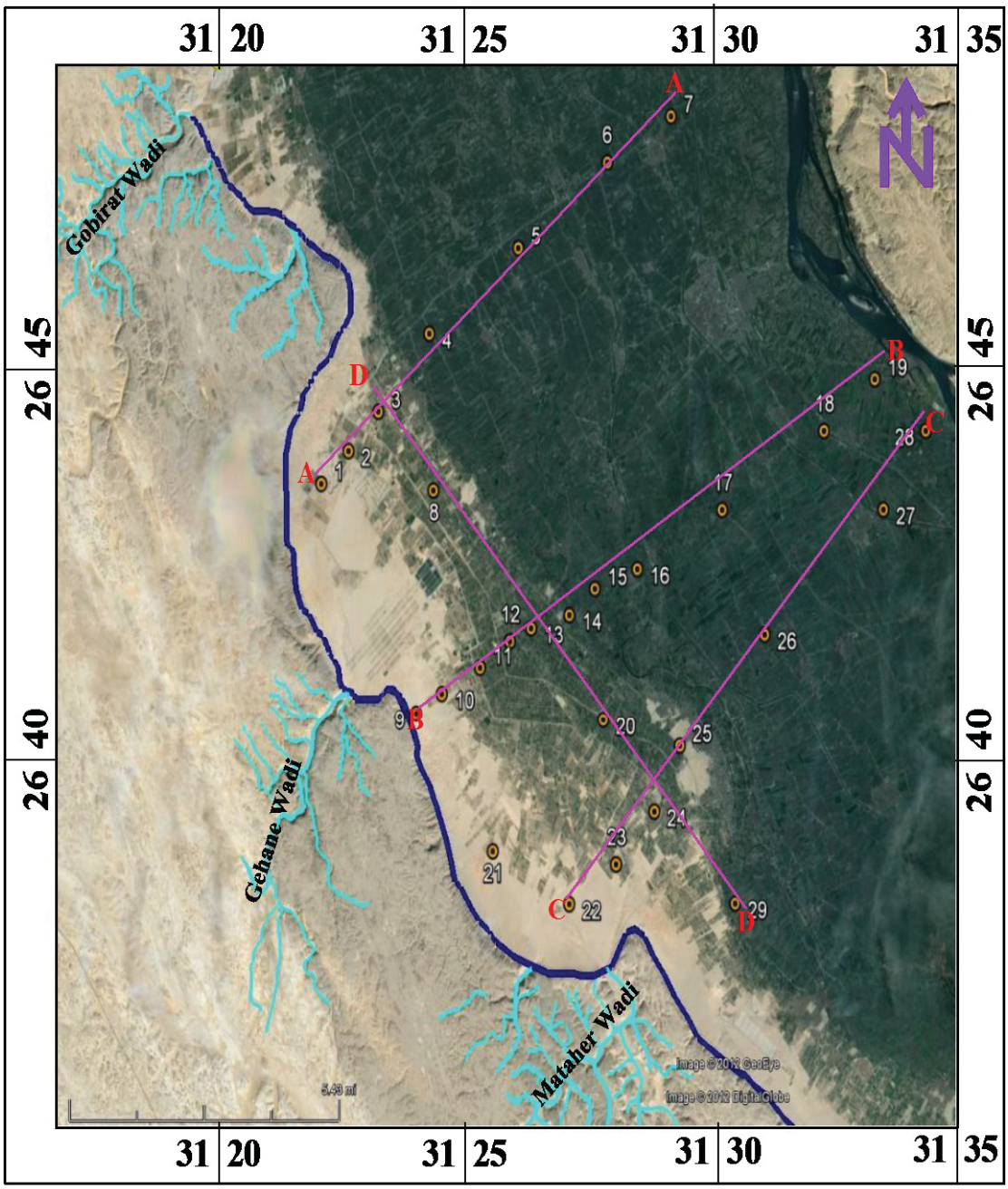

Fig.(3.3): Location of the measured VES

3.6. Data processing and interpretation

The analytic methods depend on the computerized interpretation of the vertical sounding curves over horizontally stratified media, which invert the sounding curves into their resistivity transform curves as described by Kuntez and Rocroi (1970), Zohdy (1975, 1989), and Anderson (1976) … etc.

3.6.1. The qualitative interpretation

The main purpose of the qualitative interpretation of the geoelectrical resistivity soundings is to determine the number of geoelectrical layers, as well as thicknesses (or depth) and relative

resistivities. This is done by plotting the field data of the apparent resistivity "ρa" against the half spacing of the current electrode (AB/2). The plotted field curves (VES curves) guide the subsequent process of quantitative interpretation.

3.6.2. The quantitative interpretation

The quantitative interpretation of the vertical electrical soundings (VES) is principally focused on the determining the thicknesses (or depth) and true resistivities of the geoelectrical layers belong interpreted. This can be done graphically or analytically. The graphical interpretation can be performed by using master curves and utilizing the curve matching techniques of Koefoed (1976) and Orellana and Mooney (1966). In the present study, the vertical electrical sounding was interpreted analytically using the following steps.

-An automatic iterative program (ATO) of Zohdy (1989) was applied to the 29 field sounding curves. This program is fully automatic, i.e. without any control from the interpreter. It does not require an initial model that includes the number of layers, their resistivities, and their thickness. It gives a number of layers equal to the number of points on the digitized VES curve in addition to the extrapolated VES points. This considers a multilayer model.

-The multi-layer model may be reduced to a fewer number of layers either by using a computer routine (Zohdy, 1973; Zohdy and Bisdrof, 1975) based on Dar Zarrouk functions (Maillet, 1947; Orellana et al. 1966; Zohdy, 1973 and 1974), or by simply drawing bold horizontal and vertical lines through the multilayer model. In this study, the multilayer model was manually reduced to a simplified one, in which the number of layers ranged from 3 to 5 layers, by drawing bold lines through the multilayer model. This step was guided, in fact, by the available geological and hydrogeological information about the area.

- Then, the reduced model was recalculated iteratively by a computer program called RESIST by Velpen (1988). The Velpen program depends on the iteration process, and it needs an initial model containing the resistivity and thickness of each layer. It iterates the observed data many times until a reasonably small discrepancy between the observed and calculated resistivity or a best fit between them is obtained. It also gives an error for every measured point and an average error of all the digitized points laying on the smoothed curve.

- A third computer program called IPI2Win (Moscow State University 2003) was used in the final stage of interpretation. This program is designed for interpreting vertical electrical sounding and/or induced polarization 1D data curves along a single profile. It is presumed that a user is an experienced interpreter willing to solve the geological problem posed, as well as to fit the sounding curves. Special attention is paid to the user-friendly interactive interpreting. Due to handy controls the interpreter is able to choose from a set of equivalent solutions the one that best fits both the geophysical data (i.e. providing the least amount of fitting error) and geological data (i.e. geologically sensible resistivity cross-sections).

Depending on the geologic information and the results of the previous programs, a good starting model for each VES station is used during the inverse modeling operation by using IPI2Win program. This way, all the available layer thicknesses that we obtained from some of the wells are introduced as a ground truth. Also, reliable geoelectric cross-sections are constructed by reinterpreting some VES according to the results obtained from interpreting the neighboring ones. The final models, which were calculated using these programs, are shown in Figures (3.4 to 3.11).

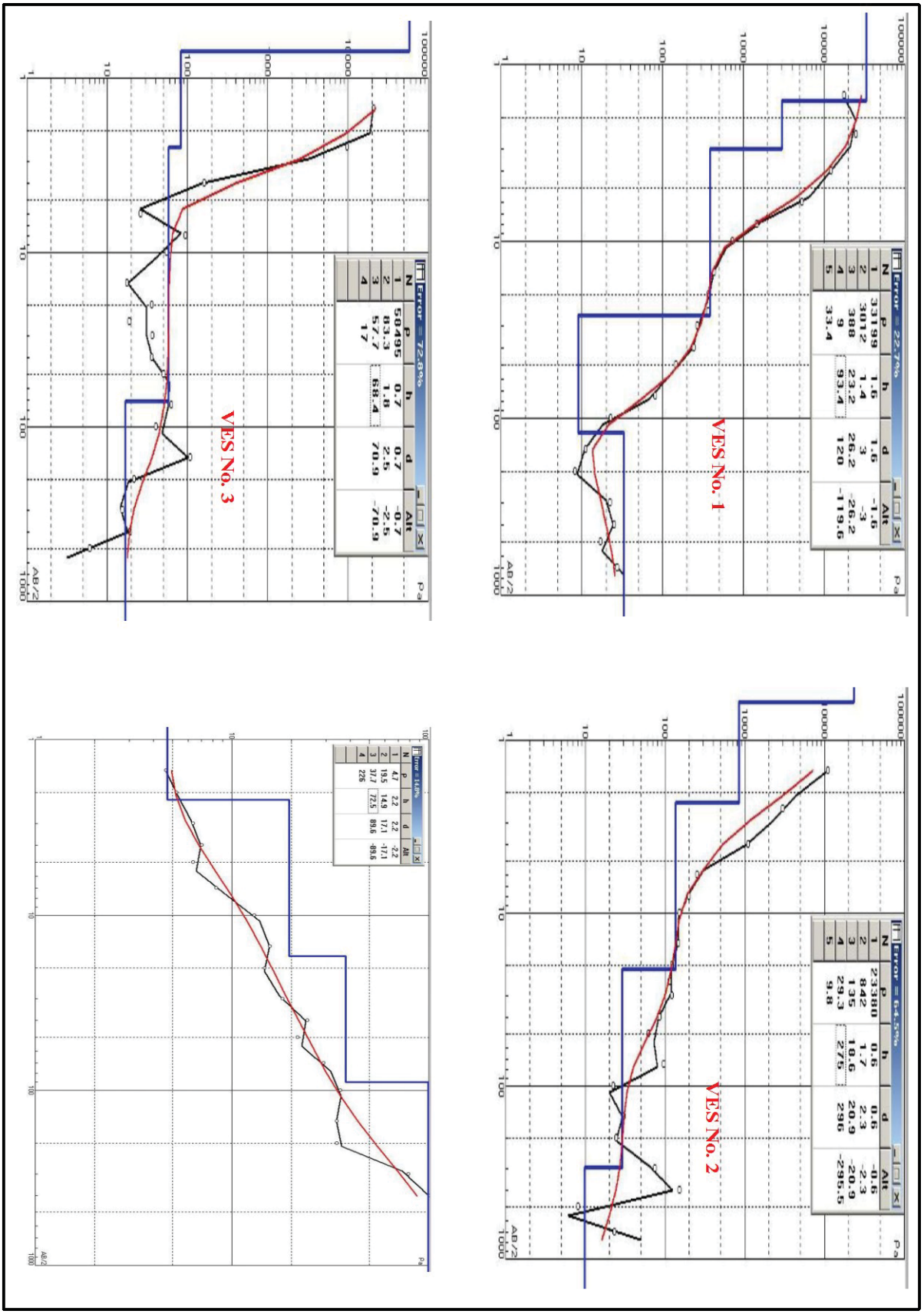

Fig. (3.4): The qualitative interpretation of VESs from 1 to 4

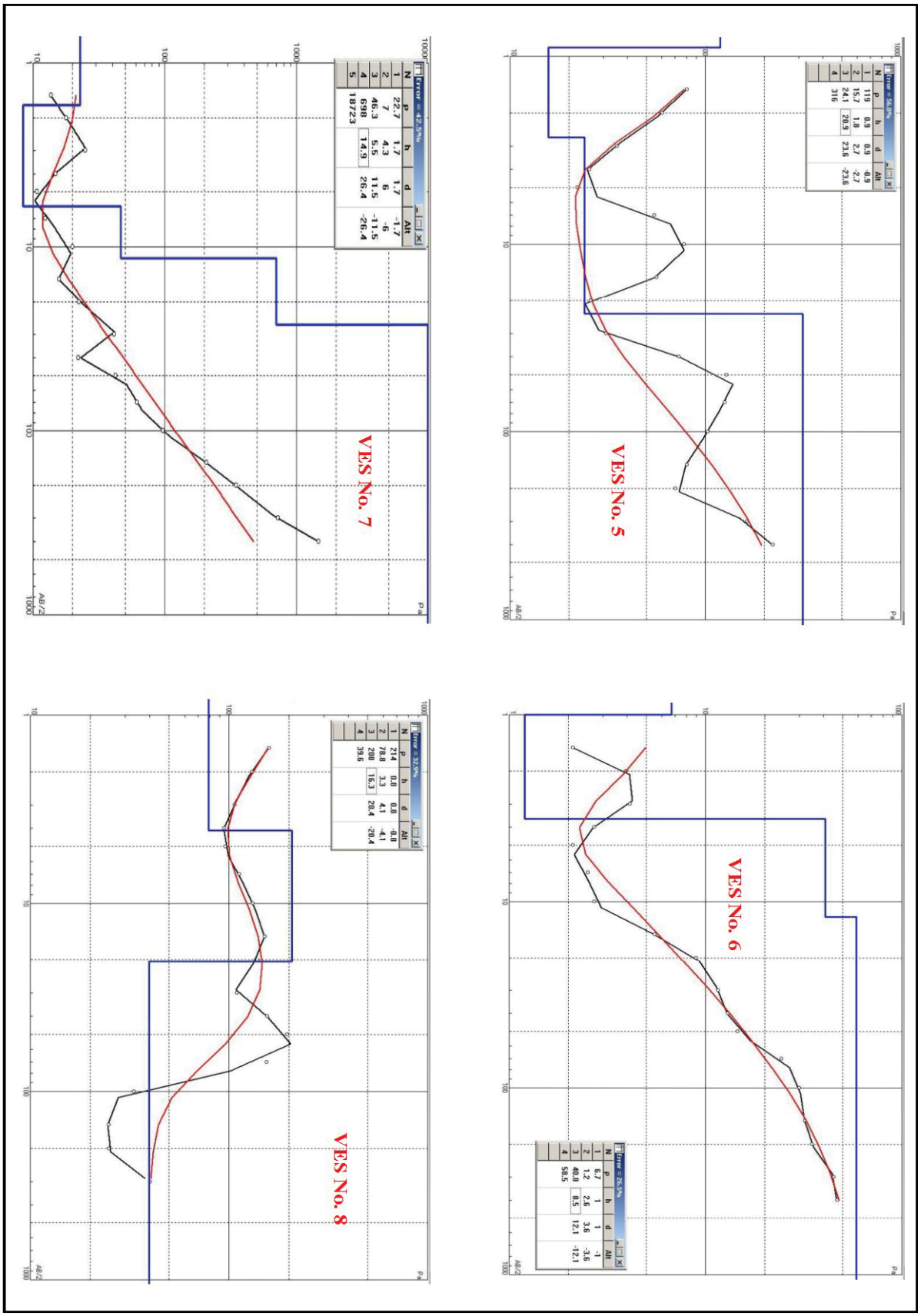

Fig. (3.5): The qualitative interpretation of VESs from 5 to 8

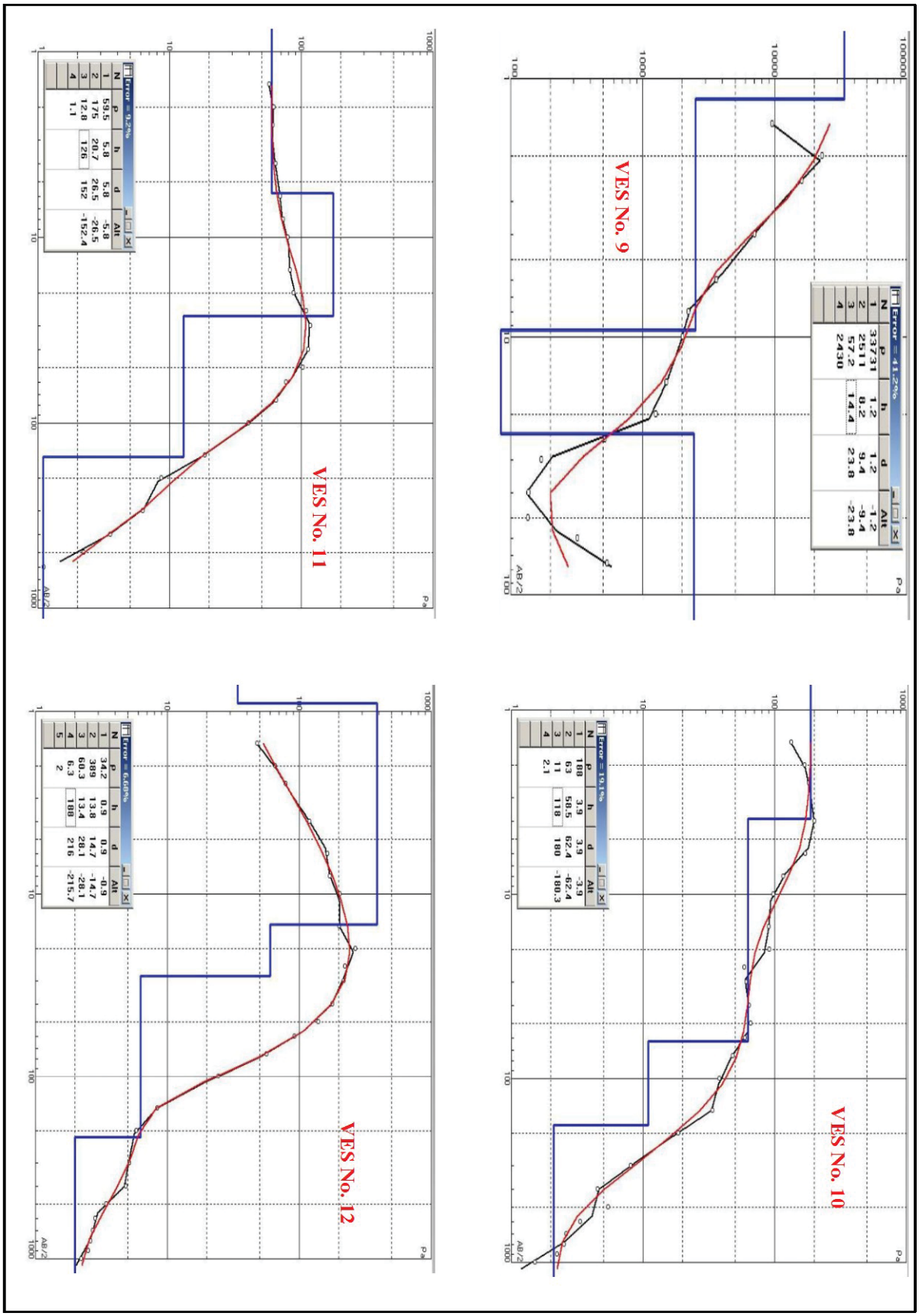

Fig. (3.6): The qualitative interpretation of VESs from 9 to 12

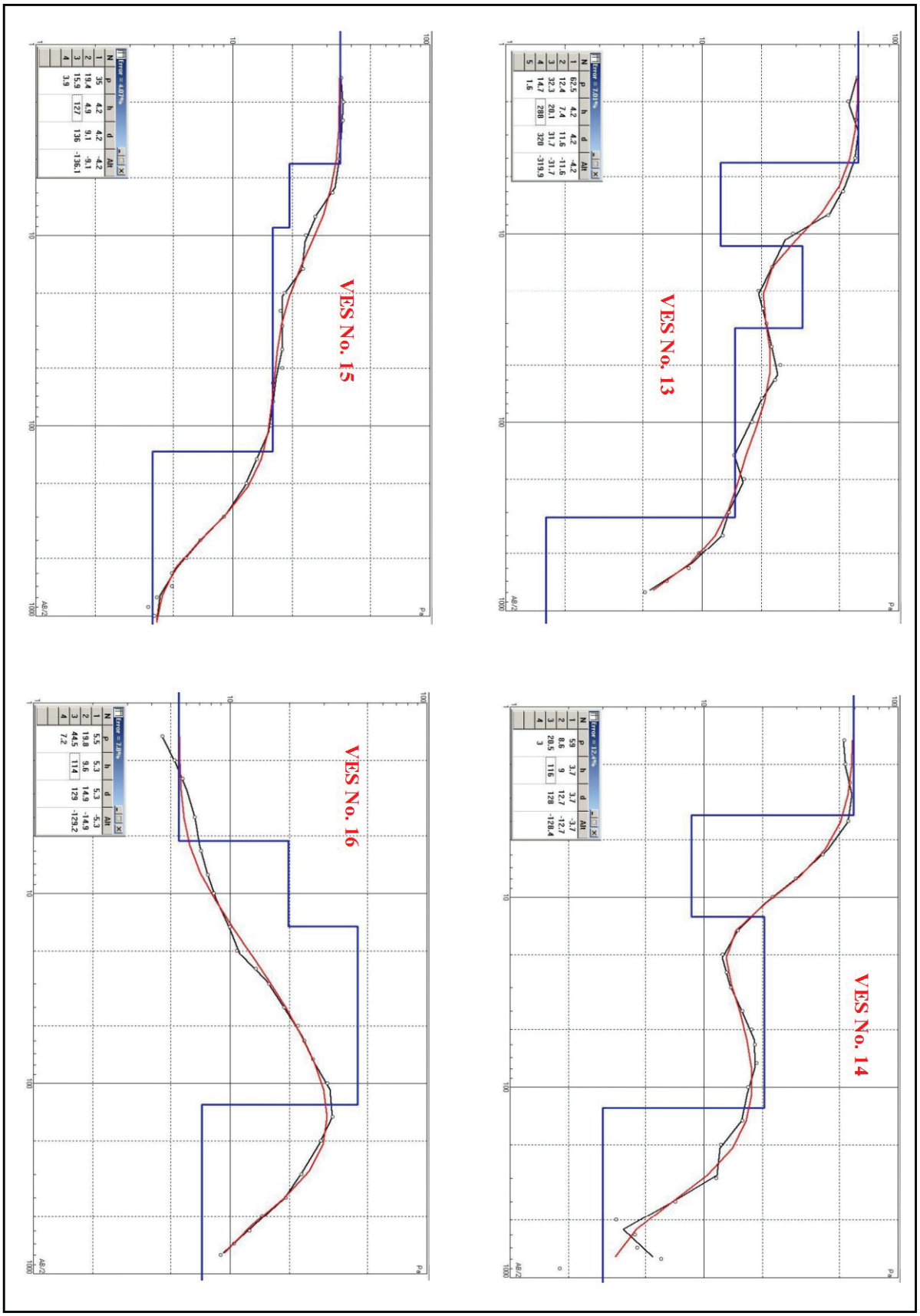

Fig. (3.7): The qualitative interpretation of VESs from 13 to 16

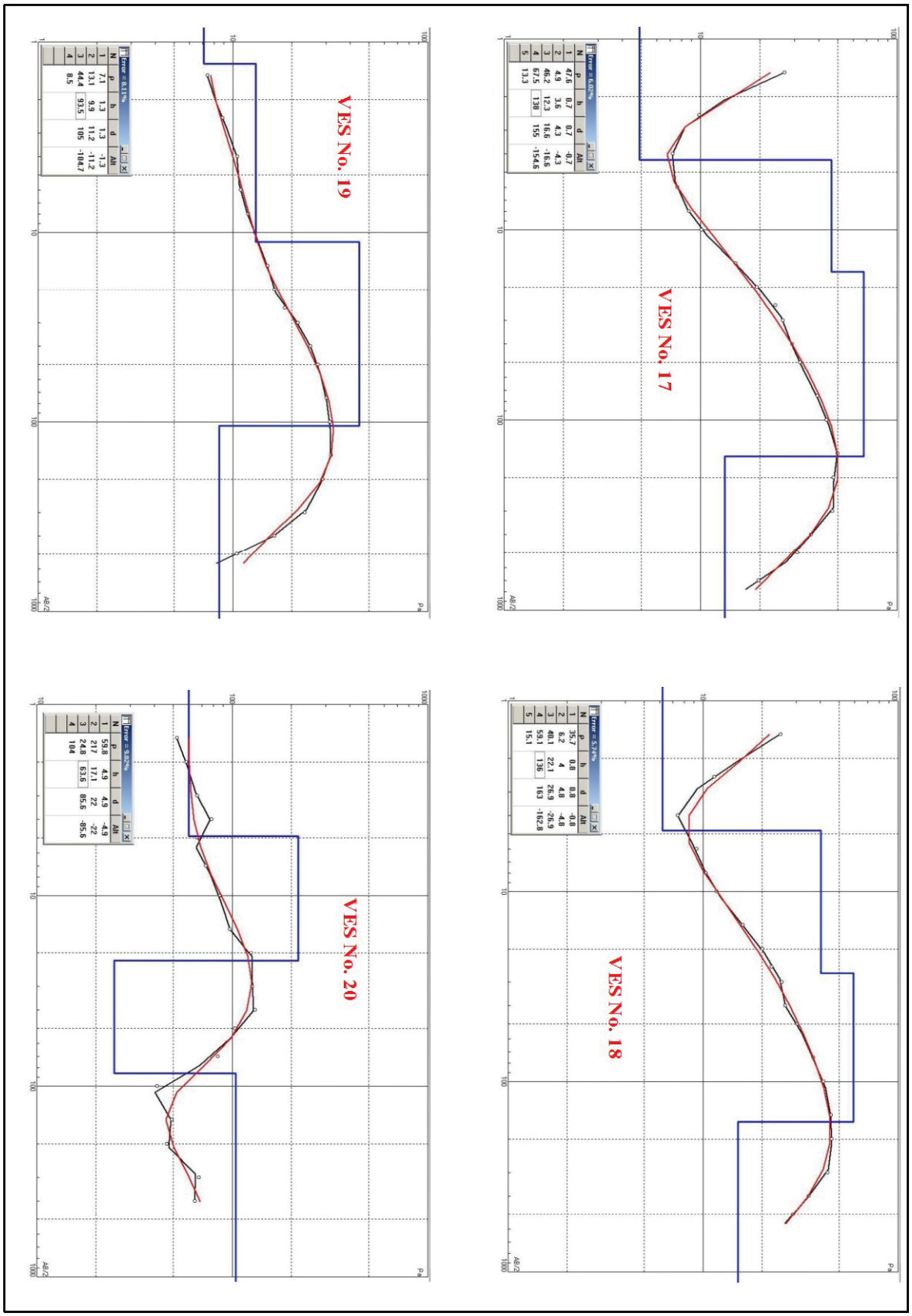

Fig. (3.8): The qualitative interpretation of VESs from 17 to 20

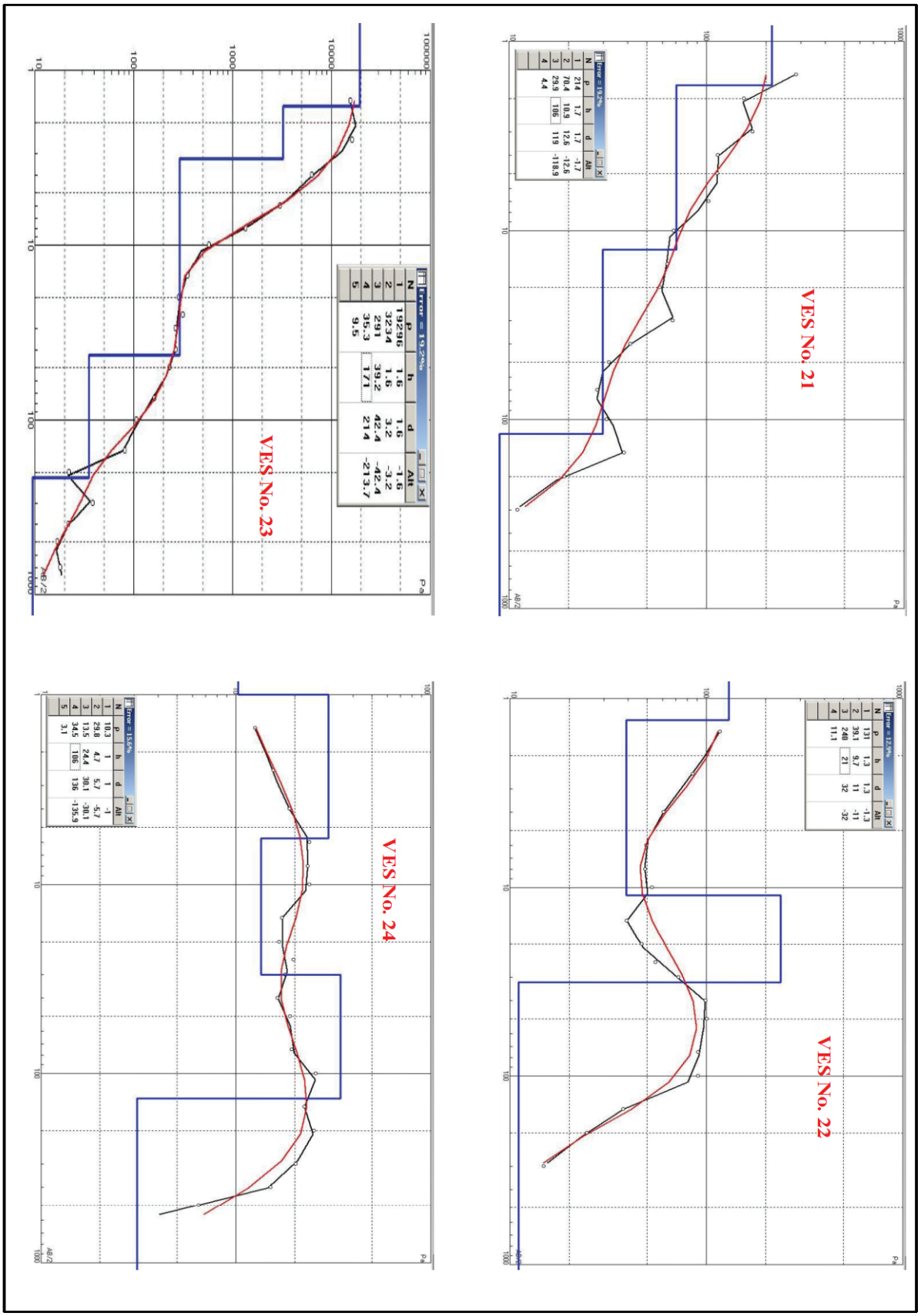

Fig. (3.9): The qualitative interpretation of VESs from 21 to 24

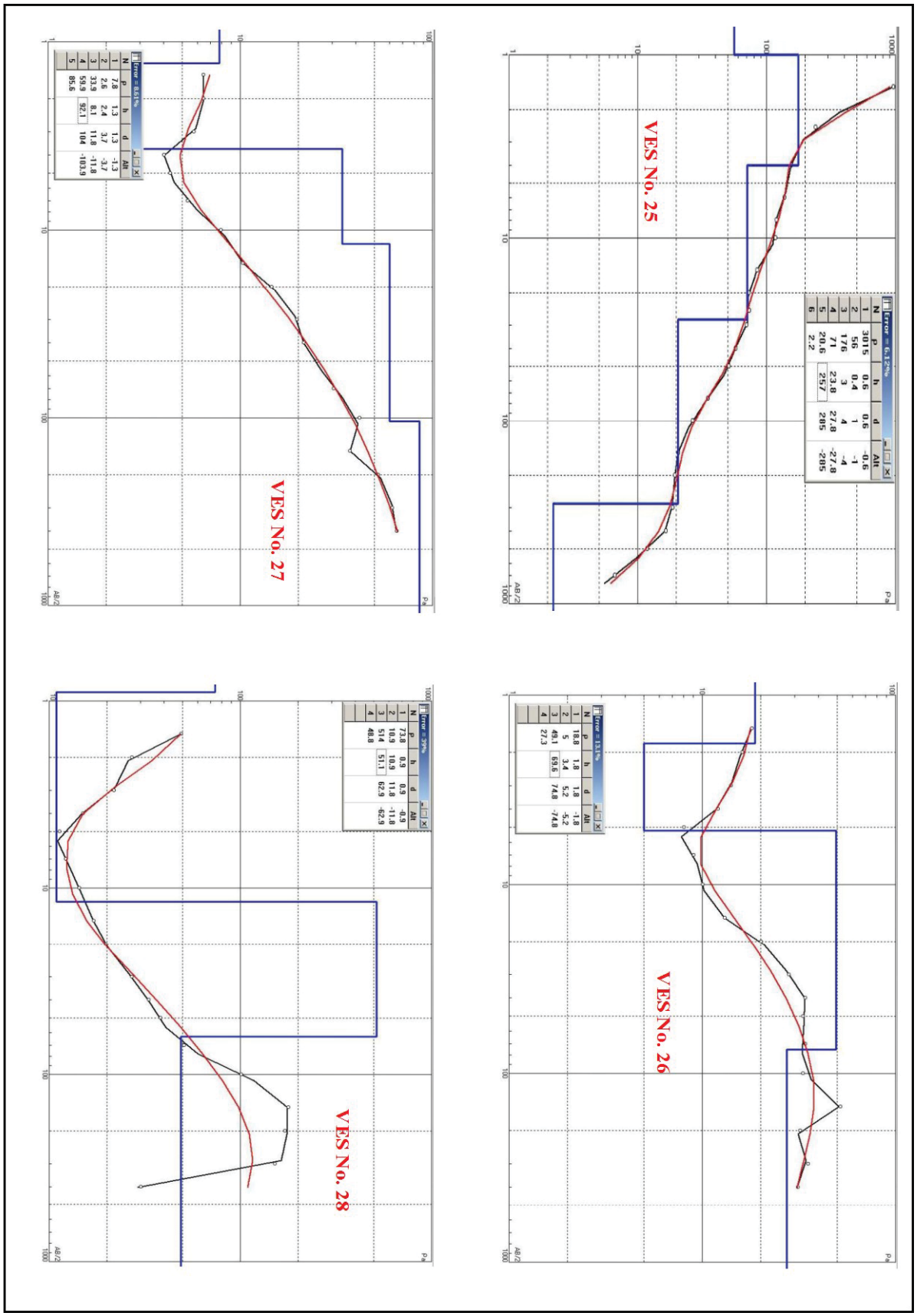

Fig. (3.10): The qualitative interpretation of VESs from 25 to 28

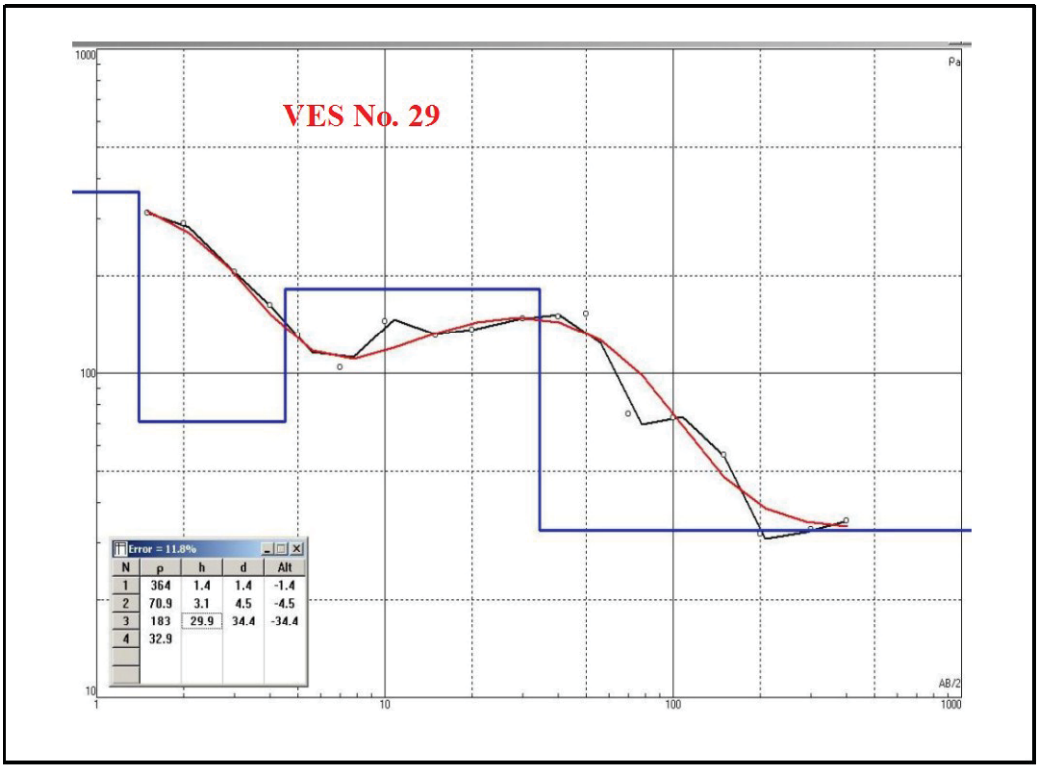

Fig. (3.11): The qualitative interpretation of VES No. 29

3.7. Results and discussion of interpreted geoelectric data

The results obtained from the interpretation of the individual sounding curve, were used to construct a subsurface picture of the area. This was done by constructing of geoelectrical cross sections and maps.

3.7.1. Geoelectric cross sections (Fig. 3.3)

3.7.1.1. Geoelectric cross section A-A\

This cross section lies in the northern part of the study area directed from the southwest to the northeast starting with VES No. 1 in the west (near limestone plateau), passing through VES no. 2,3,4,5,6, and ending at VES No. 7. (Fig.3.12). Along this section, the surface layer is composed of sand, gravel, and rock fragments in the west and clay in the east, with the thickness ranging from 1 to 5m. The second layer is composed of wet sand, which belongs to the Holocene period. The thickness varies from 6m in the east to 34m in the west and, the resistivity ranges from 129 to 325ohm.m.

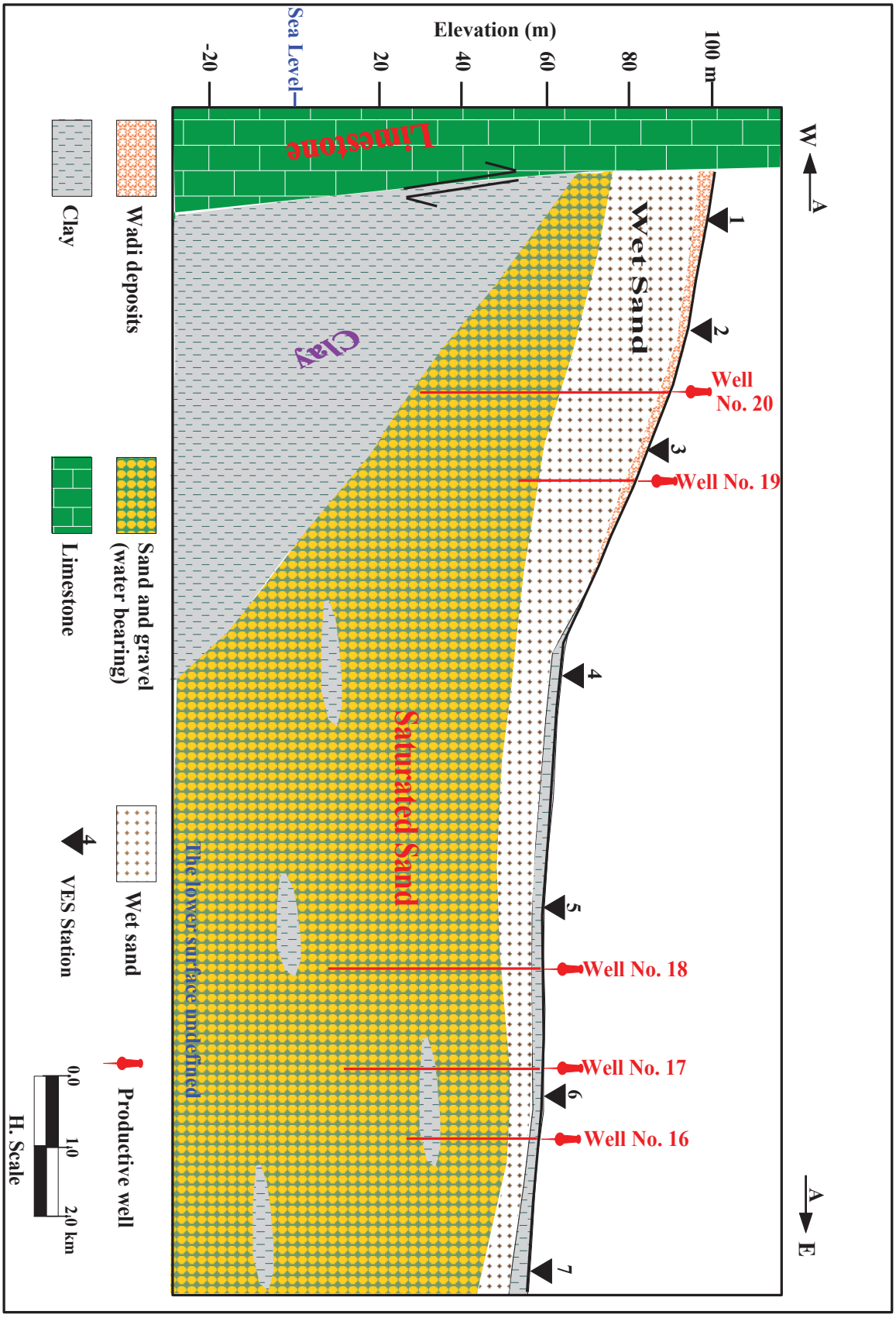

Fig. (3.12): Geoelectrical cross section A-A

The third layer of the cross section has resistivity values ranging from 29 to 91ohm.m. These resistivity values correspond to water saturated sand and gravel intercalations with clay lenses. The thickness of this layer increases towards the east and ranges from 18m in the west

under VES No. 1 to 90m under VES No. 5. The thickness under VES No. 6 and VES No. 7 is not defined because of the limitations of the instrument. The fourth layer acts as the base of the aquifer and has low resistivities, ranging from 0.9 to 5 ohm. M. The thickness in the western part reaches to 50m. This clay layer is underlain by limestone, though in the east part of the cross section it is not defined (VES No. 4 and VES No. 5). The third layer of this cross section represents the main aquifer in the study area, and it corresponds to the Pleistocene age.

3.7.1.2. Geoelectric cross section B-B

This section passes through the center of the study area and includes VES stations Nos. 9, 10, 11, 12, 13, 14, 15, 16, 17, 18, and 19 (Fig. 3.13). This cross section has the following layers:

The first layer belongs to the Holocene period and is varies in its composition from the west to the east. In the west dry sand, gravel, and rock fragments (Wadi deposits) with high resistivities are most common, while in the eastern part of the cross section, low resistivities responding to clay are visible. The thickness of this layer varies from 1m to 4m.

The second layer underlying the surface layer is characterized by high resistivities corresponding to wet sand and gravel. The thickness of this layer ranges from 5 to 18m. This layer is not seen under VES No. 9 due to the erosion and uplift of limestone along the fault plain.

The third layer belongs to the Pleistocene and is composed of sand and gravel intercalated with clay lenses. The third layer represents the main aquifer and has thicknesses ranging from 60m in the west to 143.2m in the east under VES No. 17, while the thickness under VES No. 18 was not detected because of the limitations of the instrument. The resistivity of this layer varies between 28.6 and 95.6ohm.m. The fourth layer characterized by low resistivity corresponding to Pliocene impermeable clay acts as the base of the aquifer. The resistivity of this layer varies from 0.8 to 14.8ohm.m, and the thickness is not defined.

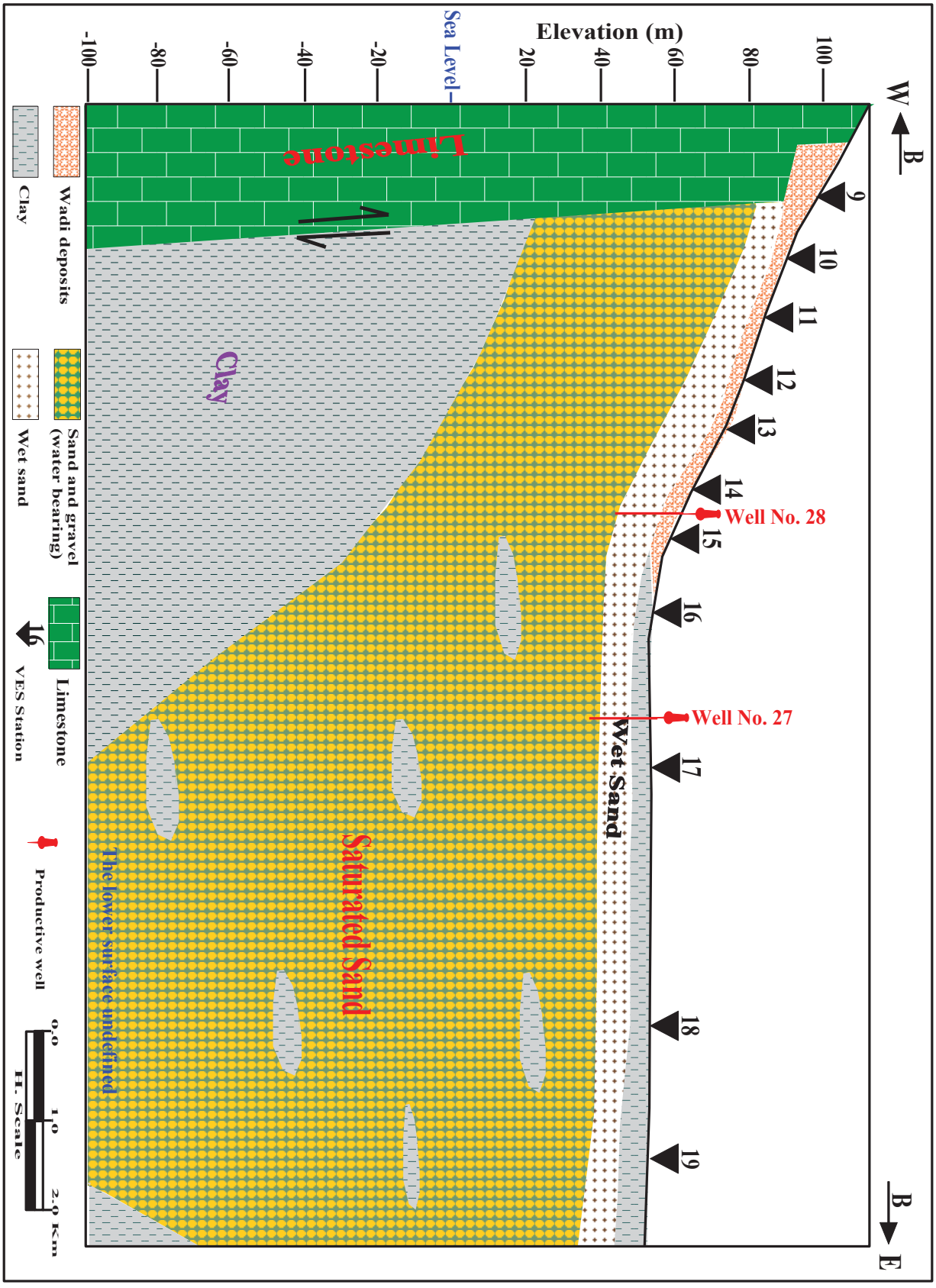

Fig. (3. 13): Geoelectrical cross section B-B

3.7.1.3. Geoelectric cross section C-C

This section includes VES stations No. 22, 23, 24, 25, 26, 27, and 28 and passes through the southern part of the study area as shown in (Fig. 3.14). The first layer (surface layer) has

various resistivity values throughout, due to the presence of wadi deposits in the west and clay in the east. This layer is thin and varies from 1 to 2.7m.

The second layer shows resistivity variation between 111.8 and 290ohm.m and thickness variation between 10 and 19m. This layer is composed of wet sand. The third geoelectric layer is the main water-bearing formation in this cross-section. It consists of the sand and gravel with resistivity values ranging from 30 to 99ohm.m. The thickness of this layer decreases in the west and increases in the east of the cross section. But it's not defined under VES No. 26 and 27. The thickness ranges from 30m under VES No. 22 to 110m VES No. 25.

The fourth geoelectric layer, which is from the Pliocene age, represents the base of the water-bearing layer, and its resistivity values range from 1.7 to 12.9ohm.m.

3.7.1.4. Geoelectric cross section D-D

This profile crosses the other profiles and is oriented NW-SE (Fig. 3.15). This cross section shows four layers. The surface layer is composed of clay in the center and wadi deposits (sand, gravel, and rock fragments) in the north and south of the section, where the section approaches the escarpment. The thickness of this layer varies from 1 to 6m. The second layer is composed of wet sand and shows resistivities from 129 to 325ohm.m with thicknesses between 5m at VES No. 29 to 34m at VES No. 3. The third layer represents the water-bearing formation (Quaternary aquifer) and is composed of sand and gravel. The thickness of this layer ranges from 60m to 90m, with resistivities between 28 and 91ohm.m. The last layer in the cross section is represented by impermeable clay, which acts as the base of the aquifer. The characteristic resistivity ranges from 1 to 12ohm.m, though the bottom is undefined.

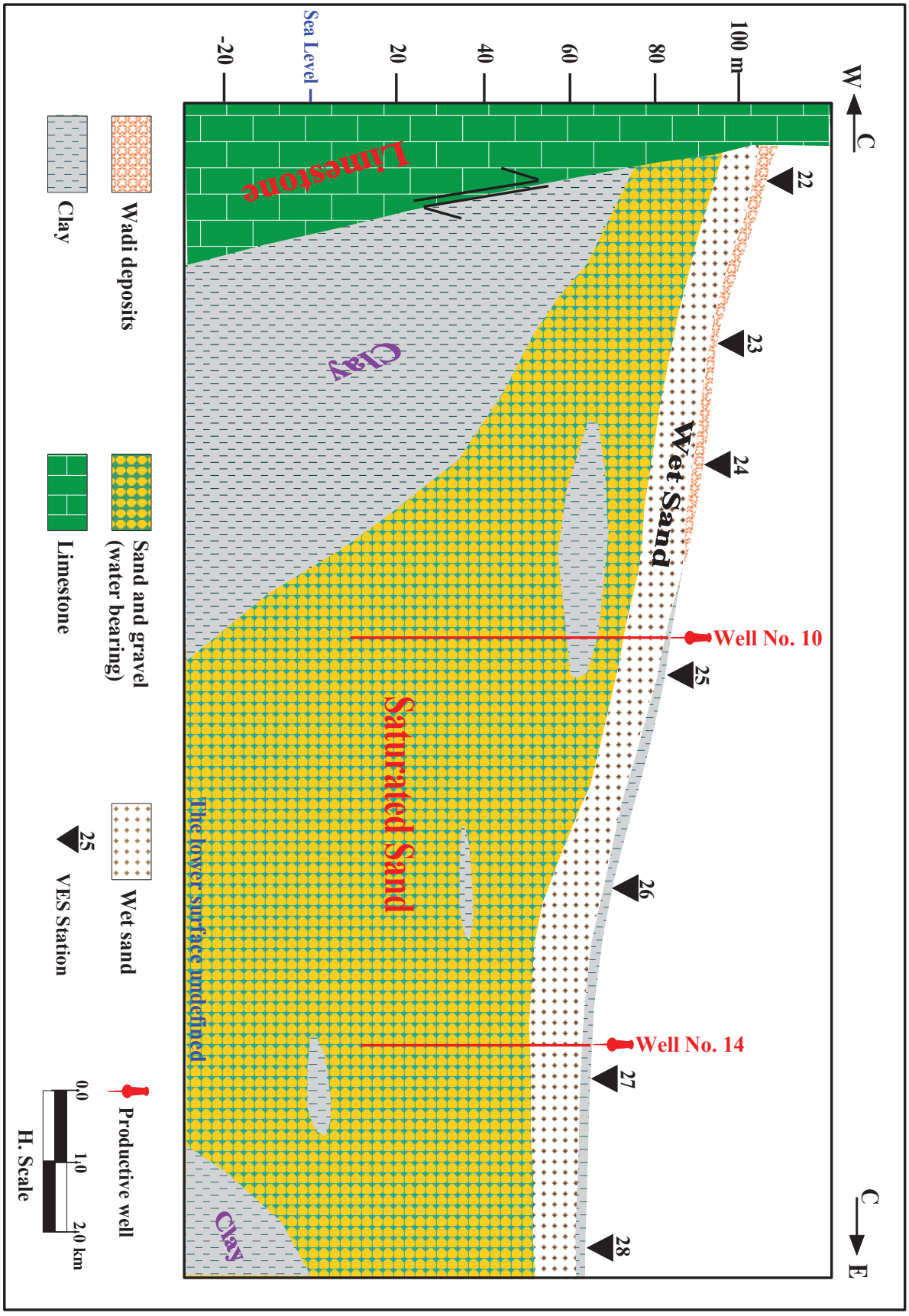

Fig. (3. 14): Geoelectrical cross section C-C

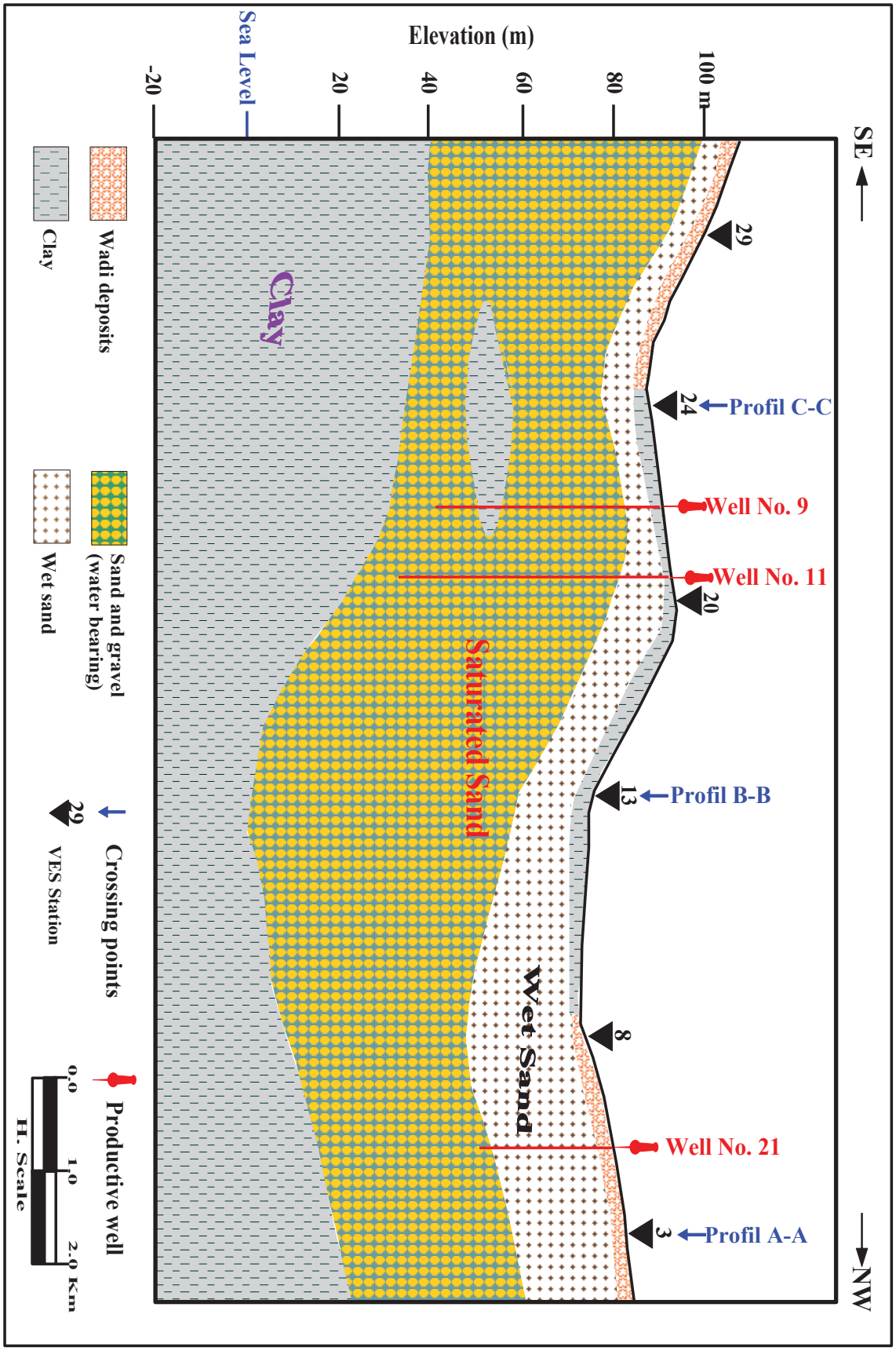

Fig. (3. 15): Geoelectrical cross section D-D

3.7.2. Maps

3.7.2.1. Isopachyte map of the saturated layer (Fig. 3.16):

This map shows the distribution of the thickness of the Quaternary aquifer in the study area. The Pleistocene aquifer becomes thicker towards northeast, most likely due to a different path of the River Nile during the pre-Pleistocene era.

3.7.2.2. The resistivity contour map of the Quaternary aquifer (Fig. 3.17):

The resistivity of the Pleistocene aquifer shows the average values of about 40ohm.m in the area of cultivated land (adjacent to the Nile) increase and reach about 90ohm.m in the west. This could be due to decreasing saturation when approaching the scarp area. The resistivity contour map shows the western part of the area has a high resistivity while the eastern part has low resistivity, due to the presence of a dry wadi deposit.

3.7.2.3. Groundwater table above sea level (Fig. 3.18):

The groundwater table above sea level (data from VES) contour map shows, that high values are present in the southwest and low values in northeast. From these values we concluded the groundwater flows from the southwest toward the River Nile.

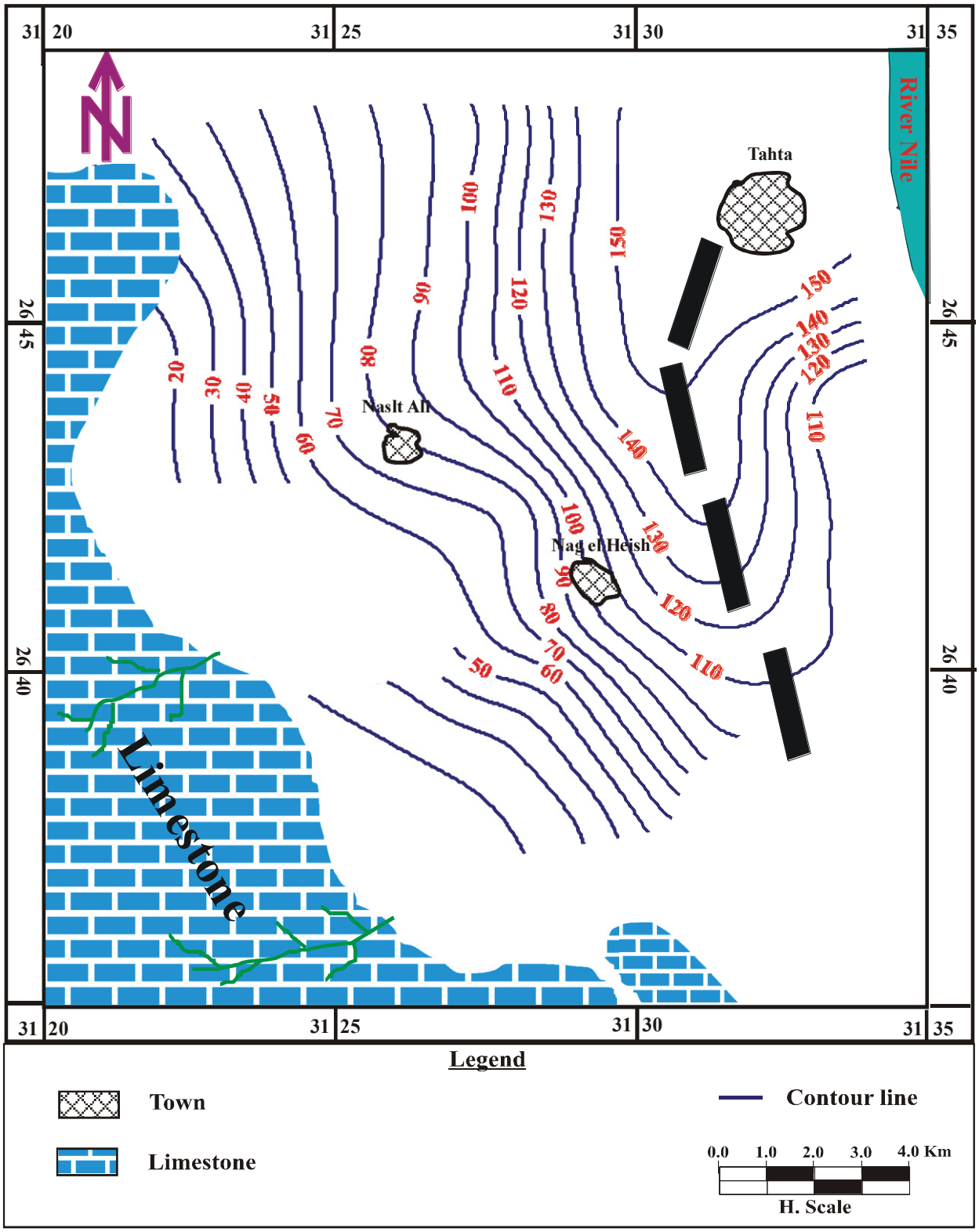

Fig. (3.16): Isopachyte map of the saturated layer

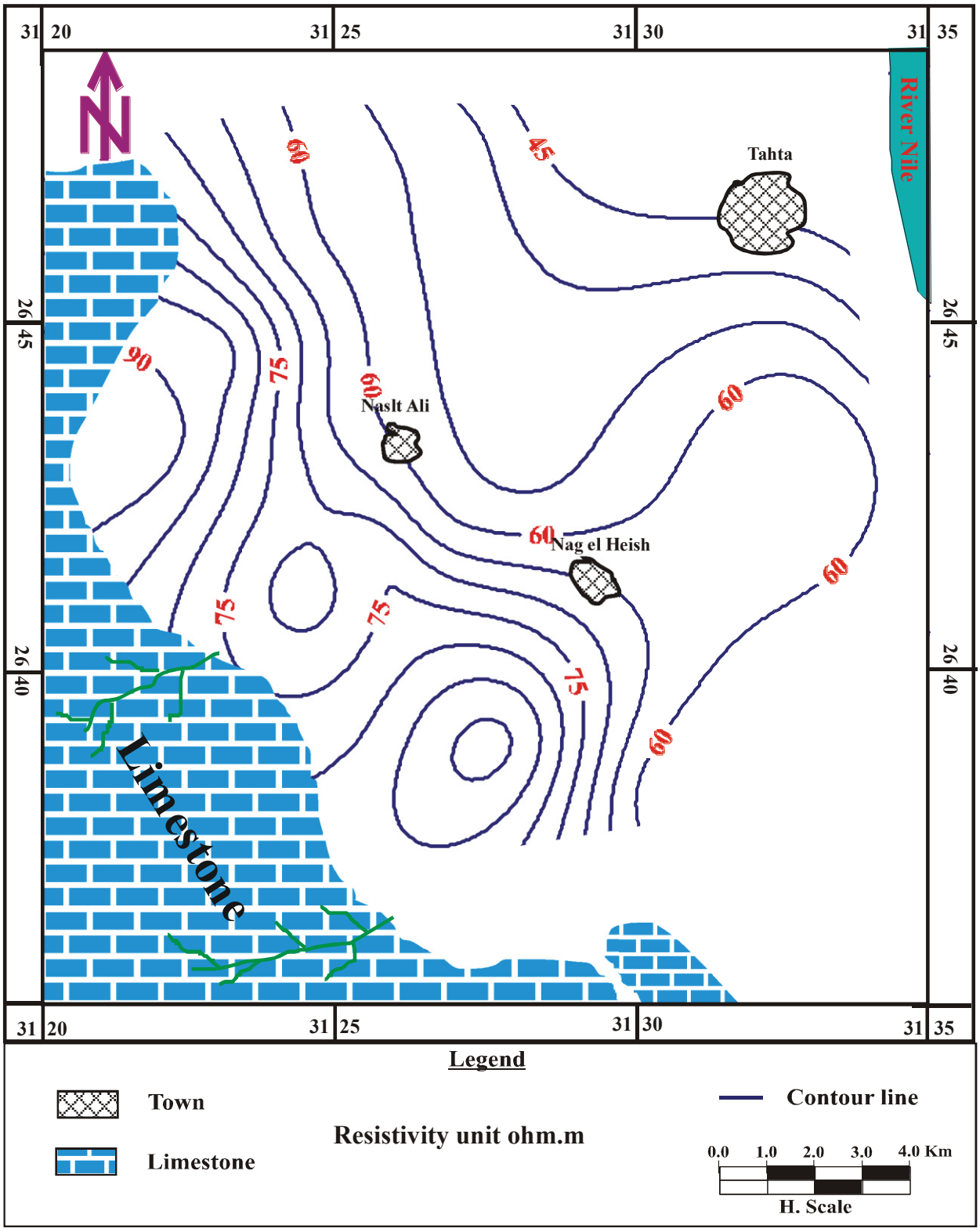

Fig. (3.17): True resistivity contour map of the Quaternary aquifer

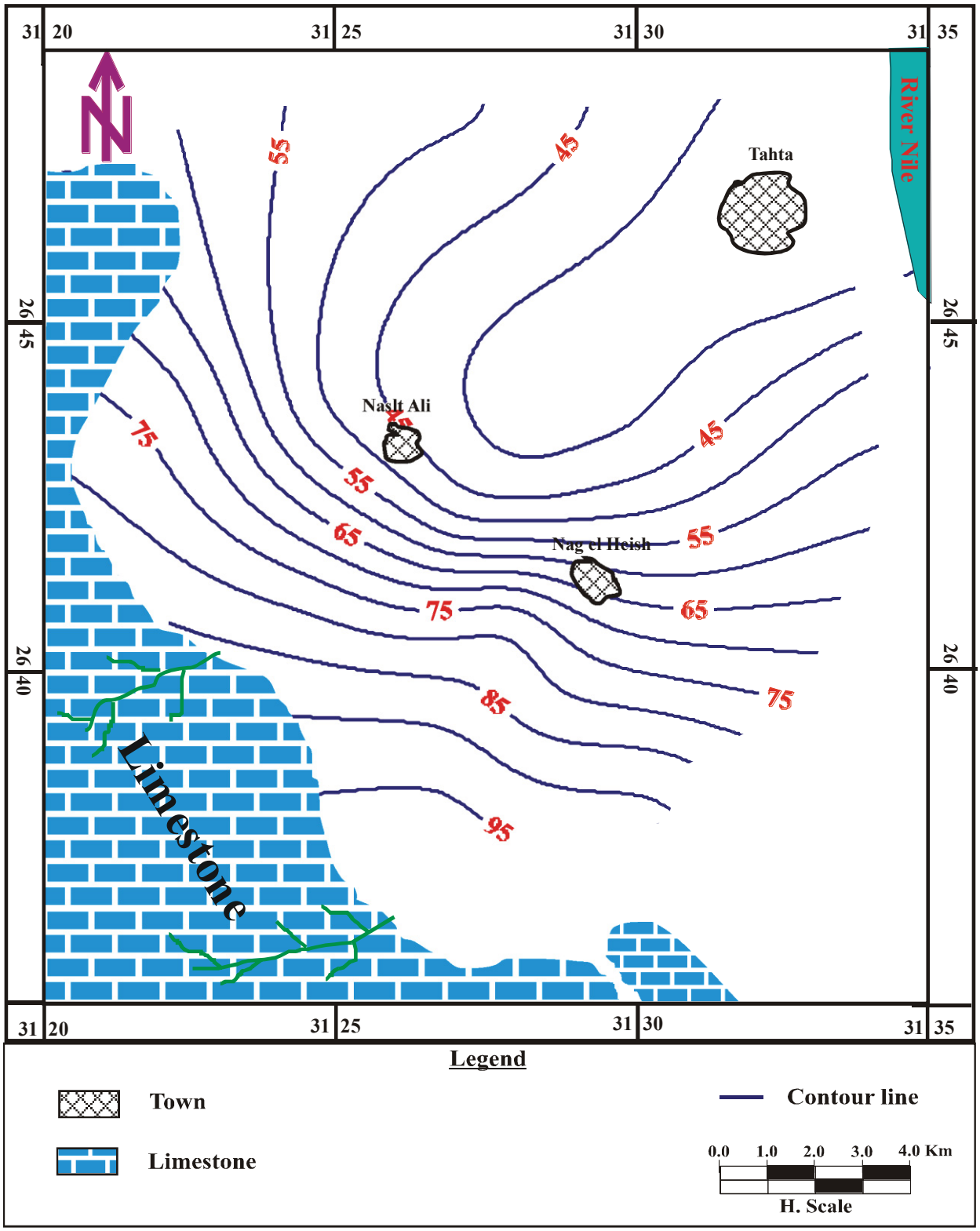

Fig. (3.18): Groundwater table above sea level (m)

CHAPTER FOUR

Hydrogeology and Hydrogeochemistry Studies

4.1. Hydrogeological data:

The groundwater is considered the principal source of water for irrigation and domestic purposes in the study area. The water bearing formation has a widely geographical distribution in the study area and differs greatly in their extension, potentialities and source of recharge.

In the reclaimed lands the main of problems of the irrigation processes are represented by the system of flood irrigation which is not suitable for the soil texture (sands and gravels), in addition, to the lack of drainage system. This causes some hydrogeological problems such as deterioration of soil, increase of the groundwater salinity and water- logging area. Under these circumstances; proper soil treatment, change the irrigation system, improve the drainage system and water management, are so important.

The data for the hydrogeological study are coming from fifty six wells in case of 1989 and twenty eight wells 2011 (tables 4.1 and 4.2). These wells are distributed in the study area, and were the base for the maps showing the hydrogeological conditions (Fig. 4.1). The hydrogeological data includes; ground level which measured direct by G.P.S, depth of water and total depth of drilling ware collected from the framer (owner of the wells).

4.1.1. Water bearing formation and the aquifer properties

The Nile Valley in the study area is characterized by one aquifer system (Quaternary aquifer) (Fig. 4.2) in a hydrogeological sense. This aquifer consists of fluvial sands with minor conglomerate and clay. It is covered by Neonile silt and fine-grained sands, constituting the base of the cultivated lands. Along the eastern and western fringes, the Neonile silty layer is replaced by recent sediments. One can describe the aquifer system in the floodplain as being under semi-confined condition, in the desert fringes under unconfined condition. The permeable thickness of the aquifer system varies from 150m in the central part of the flood plain to about 50m in the desert fringes. The average hydraulic conductivity of the aquifer is about 70m/day; but 4cm/day for the silty top layer (Omran et al., 2006).

Table (4.1): Hydrogeological data of the water samples collected in 1989

Serial No.	Well No.	Groundwater depth from the ground surface (m)	Groundwater level above sea level (m)	Serial No.	Well No.	Groundwater depth from the ground surface (m)	Groundwater level above sea level (m)
1	1	23	62	29	50	3.8	53.7
2	3	11	60	30	51	3.8	53.2
3	4	12	62	31	52	3.4	55.1
4	5	17	63	32	62	16	57.8
5	7	17	61	33	63	26	56.8
6	9	19	56.5	34	64	12	57.2
7	10	14	55	35	65	25	56.7
8	11	4	55.5	36	66	23	56.7
9	13	8	57.5	37	68	24	56.9
10	14	2	57	38	70	25	69
11	15	8	58	39	71	25	70
12	17	2	58.5	40	72	22	64.5
13	18	1.8	57	41	73	23	59.5
14	19	3	59.5	42	74	21	60
15	23	6	57	43	75	34	65
16	24	7	56	44	76	39	65.5
17	25	9	55.8	45	78	45	67.3
18	33	19	62	46	79	22.5	67.5
19	34	1	58	47	80	16	57.5
20	36	4.5	52.3	48	81	36	63
21	38	1	55.5	49	85	5	54.9
22	39	3	53.5	50	87	6	57
23	40	1.7	55.2	51	89	4.5	56.5
24	41	4.3	56.5	52	95	28	59.2
25	44	5	51	53	96	42	67
26	45	4.5	50	54	98	23.5	67
27	48	3.9	52.7	55	101	23	64
28	49	5.9	52.5	56	102	23	58.5

Table (4.2): Hydrogeological data of the water samples collected in 2011

Serial No.	Well No.	Groundwater depth from the ground surface (m)	Groundwater level above sea level (m)	Serial No.	Well No.	Groundwater depth from the ground surface (m)	Groundwater level above sea level (m)
1	7	52	50	29	22	22	47
2	8	55	52	30	23	22	44
3	9	56	53	31	24	22	43.5
4	10	53	50	32	25	19	43
5	11	40	47.5	33	26	15	42
6	12	39	46	34	27	9	41
7	13	39	47.5	35	28	24	45.5
8	14	39	48.5	36	29	37	51
9	15	33	47.5	37	30	42	55
10	17	26	43	38	31	38	56.5
11	19	25	49	39	32	40	58.5
12	20	32	52	40	33	33	52
13	21	28	50	41	34	34	59

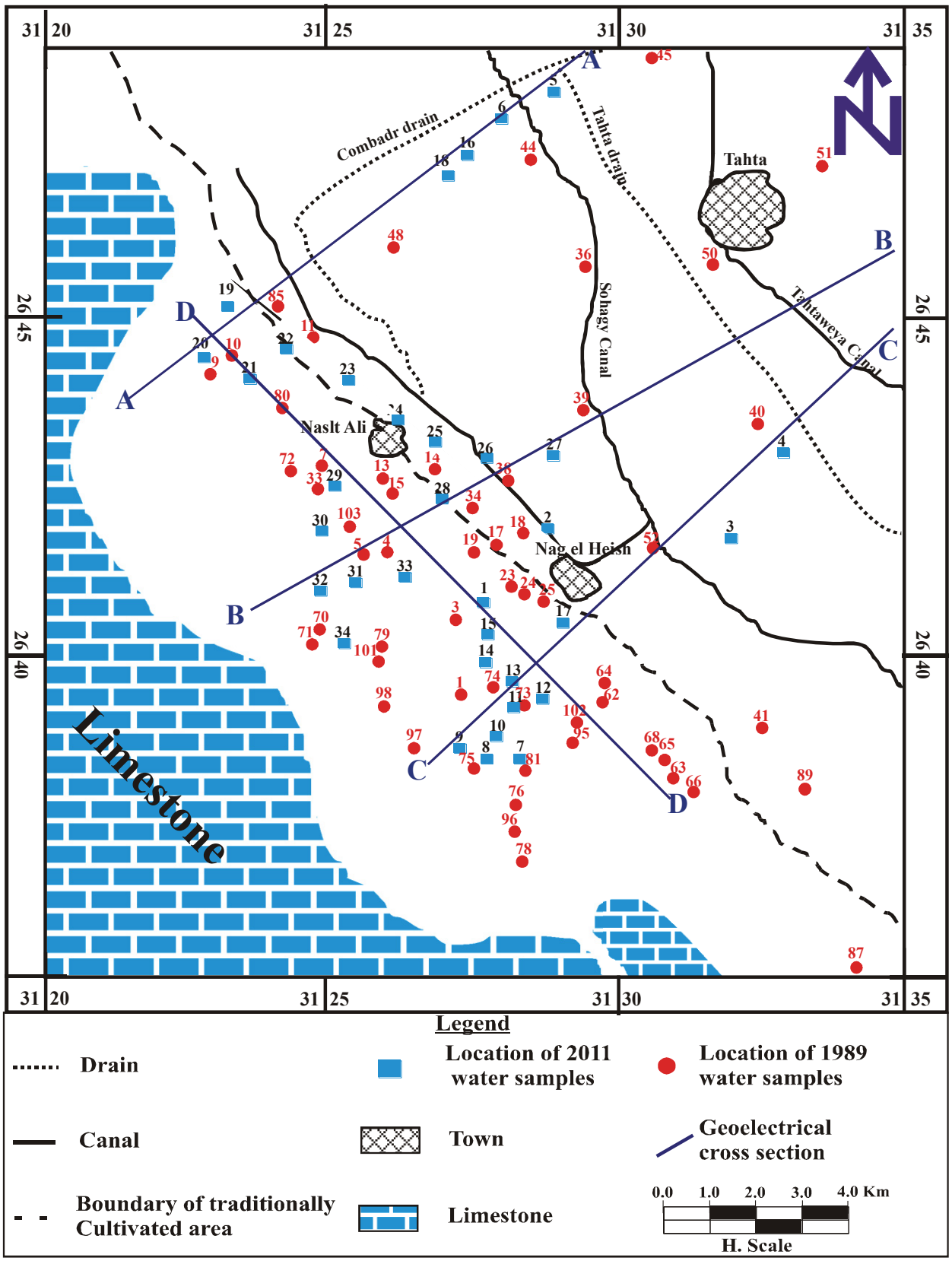

Fig. (4.1): Location of the productive wells of the study area

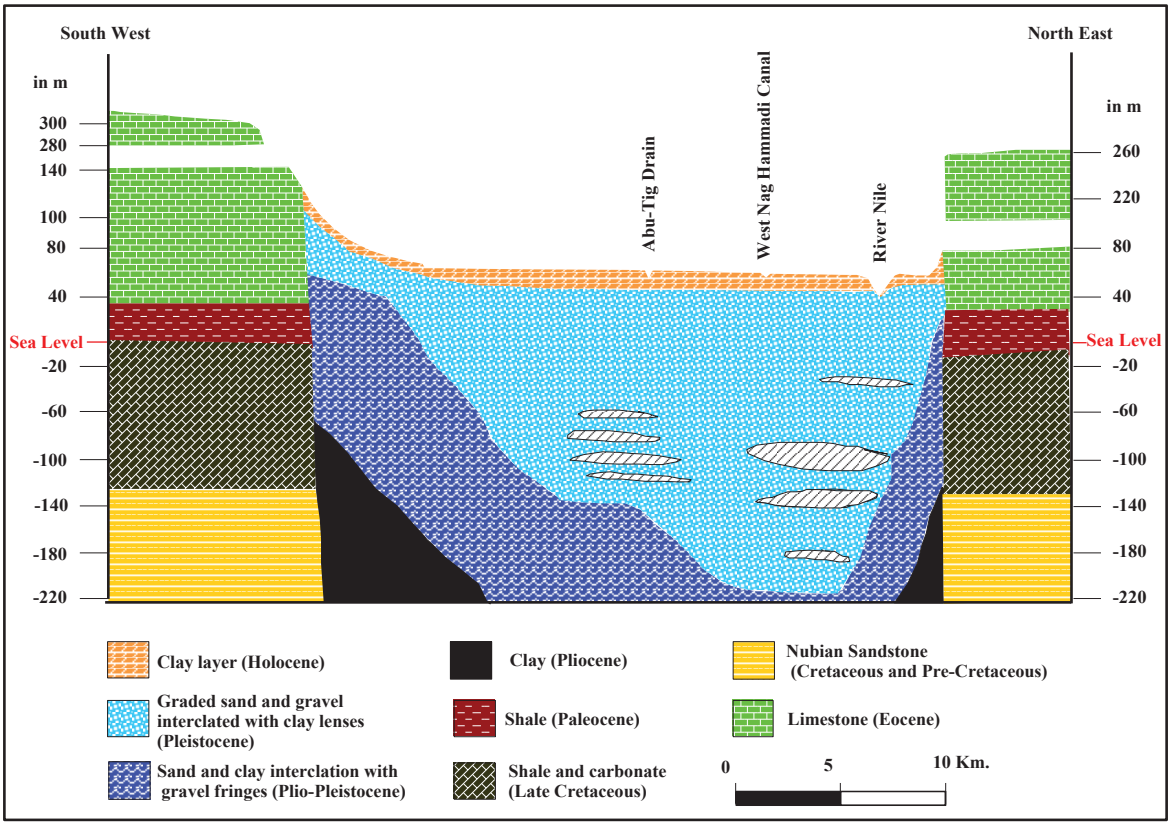

Fig. (4.2): Schematic hydrogeological cross section in Tahta area (RIGW, 1989)

4.1.2. Aquifer recharge and discharge

The Quaternary aquifer is recharged mainly from the surface water, particularly the irrigations canals, which play a main role in the configuration of the water table. The discharge of this aquifer takes place during the evaporation process. The connection to the underlying aquifer and river acts as an effluent stream in most of its parts.

4.1.3. Groundwater flow

The main direction of flow of the groundwater in the study area is towards the northeast, i.e. towards the River Nile (Fig. 4.3) due to the influence of recharging canals. There are differences between Figures 3.18 and 4.3 because the data in Figure 3.18 depends on the VES and the geoelectrical cross sections, while Figure 4.3 mainly depends on data collected from the farmers (owners of the wells). Figure 4.4 shows that the depth to the groundwater surface ranges from 9m and 56m and increases toward the west. The hydraulic gradients are relatively moderate and regular, except in the areas of water depressions, where the gradients become steeper in the north-eastern and south-western parts (Awad, A. O., 2008).

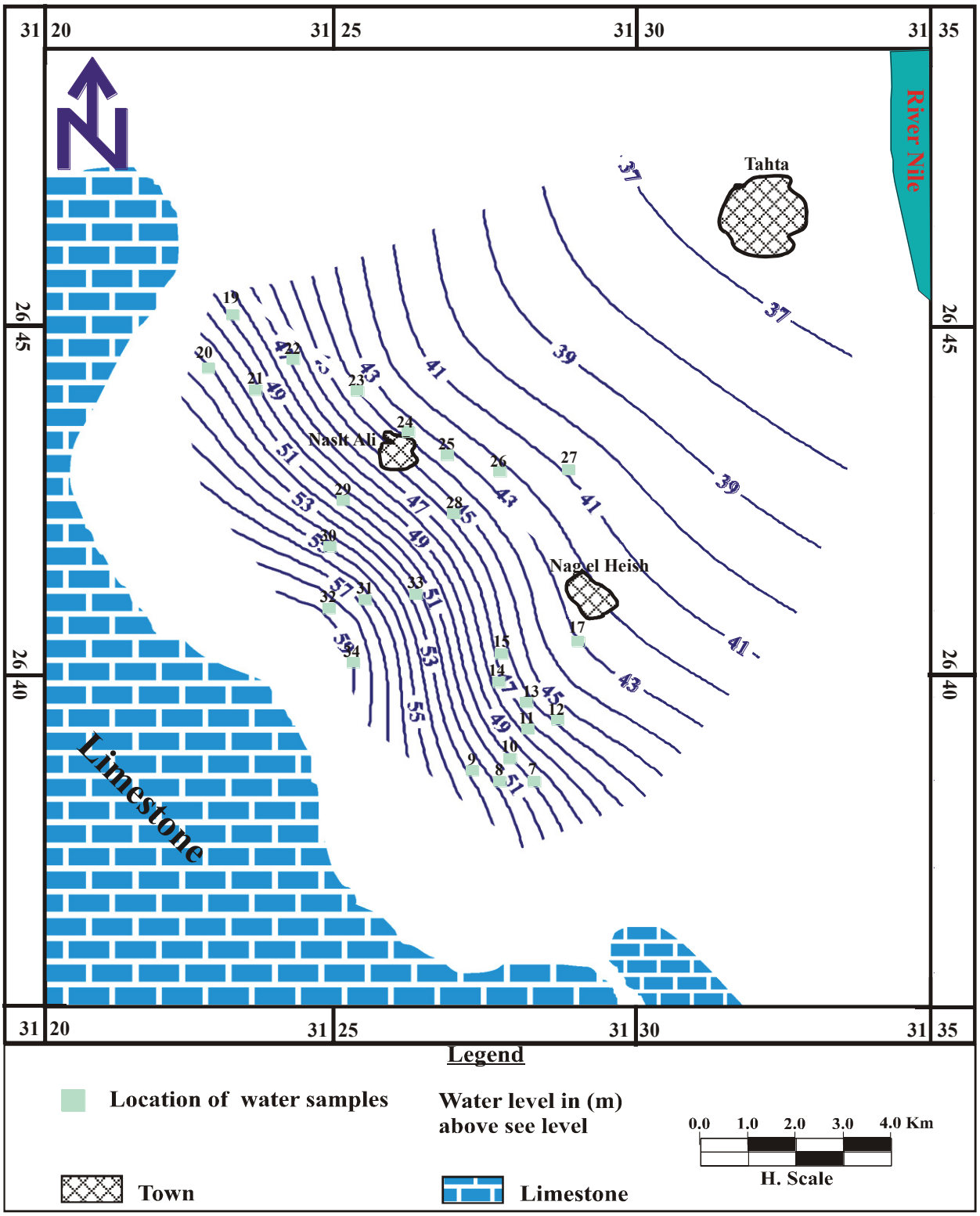

Fig. (4.3): Water level contour map 2011

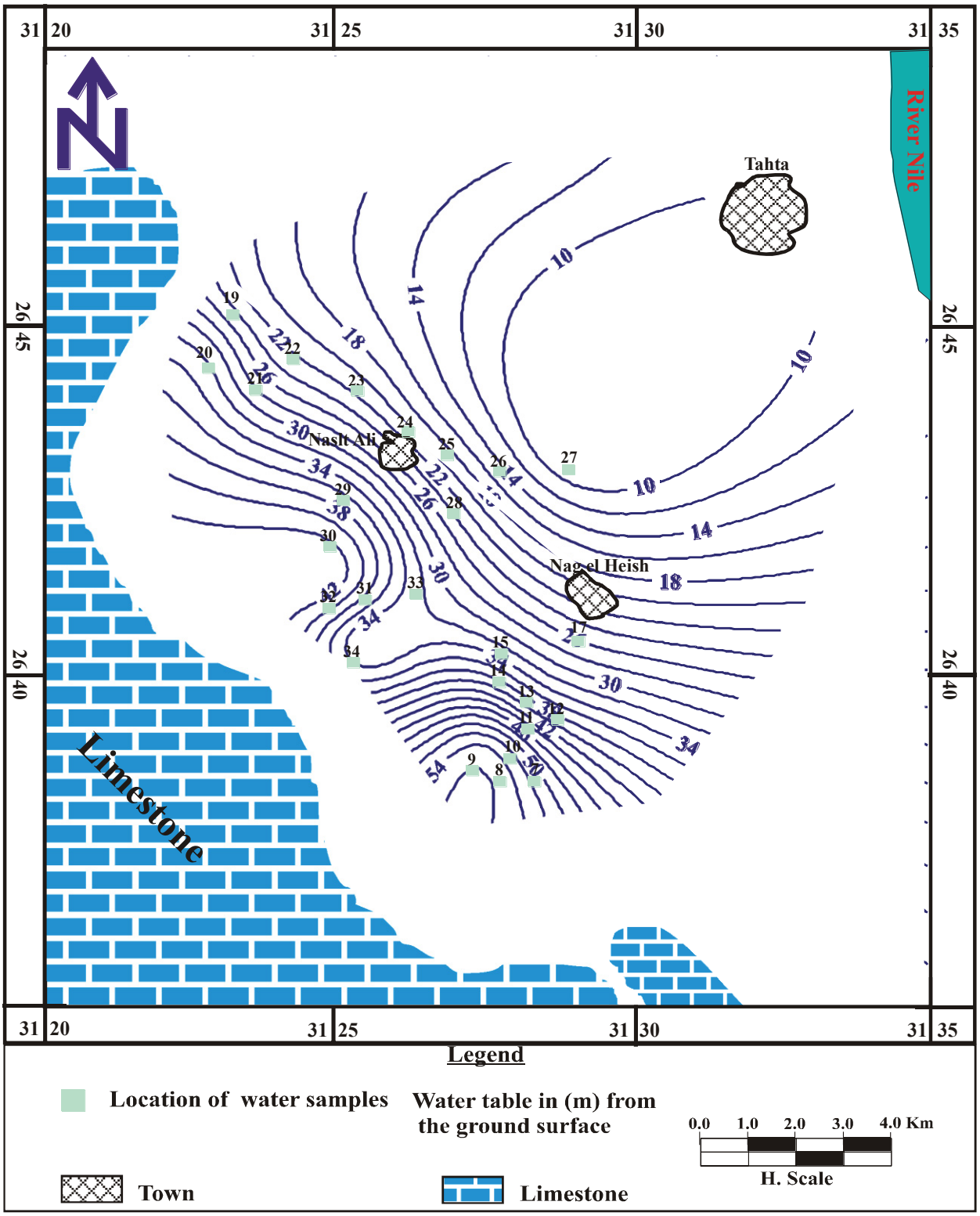

Fig. (4.4): Water table contour map 2011

4.1.4. Water logging problems

In the study area, some farmers are facing problems with the amount of groundwater and its salinity (Figs. 4.5, 4.6), hindering the agricultural development. These water problems can be seen in the field but not on the Satellite images. The hydrogeological study of this area indicates a connection between the old cultivated land and the new reclaimed area, as these two areas are irrigated by flooding. The downward flow from the increased irrigation in the new reclaimed land in the west influences the old cultivated land. Due to the high temperatures in the study area throughout most time of the year, the evaporation causes a decrease in the water supply with an increase in the soil salinity. There are many possible solutions to this problem. The new irrigation method covers the demand for water for the low-lying old cultivated land by using a conventional drainage system. The water used for irrigation is a mix of groundwater and surface water. (Blomquist, et. al. 2001).

4.2. Hydrogeochemical data

The hydrogeochemical study includes a description of the occurrence of the various constituents in the groundwater and the relation of these constituents to water use. The distribution maps of the chemical properties (Total dissolved salts (TDS) and Total hardness (TH)), ion dominance, hypothetical salt combinations, and hydrochemical coefficients were constructed and studied. Also, the chemical classification of the groundwater and the evaluation of the water samples for different purposes are discussed in this chapter. All these chemistry data give an important clue to the history of various cationic and anionic concentrations, as well as an indication of the groundwater recharge, discharge movement, and storage. The hydrogeochemical aspects in the study area are based on the chemical analysis of the 34 samples (6 surface water and 28 groundwater samples) collected in 2011(Fig. 4.1).

The groundwater samples were collected from the wells after a few hours of pumping to avoid contamination and to ensure that the samples will represent the aquifer type. While surface water samples were collected by using this sampler, the water was collected from the middle of stream at a depth of about one meter.

Fig.(4.5): Field photograph showing water logging

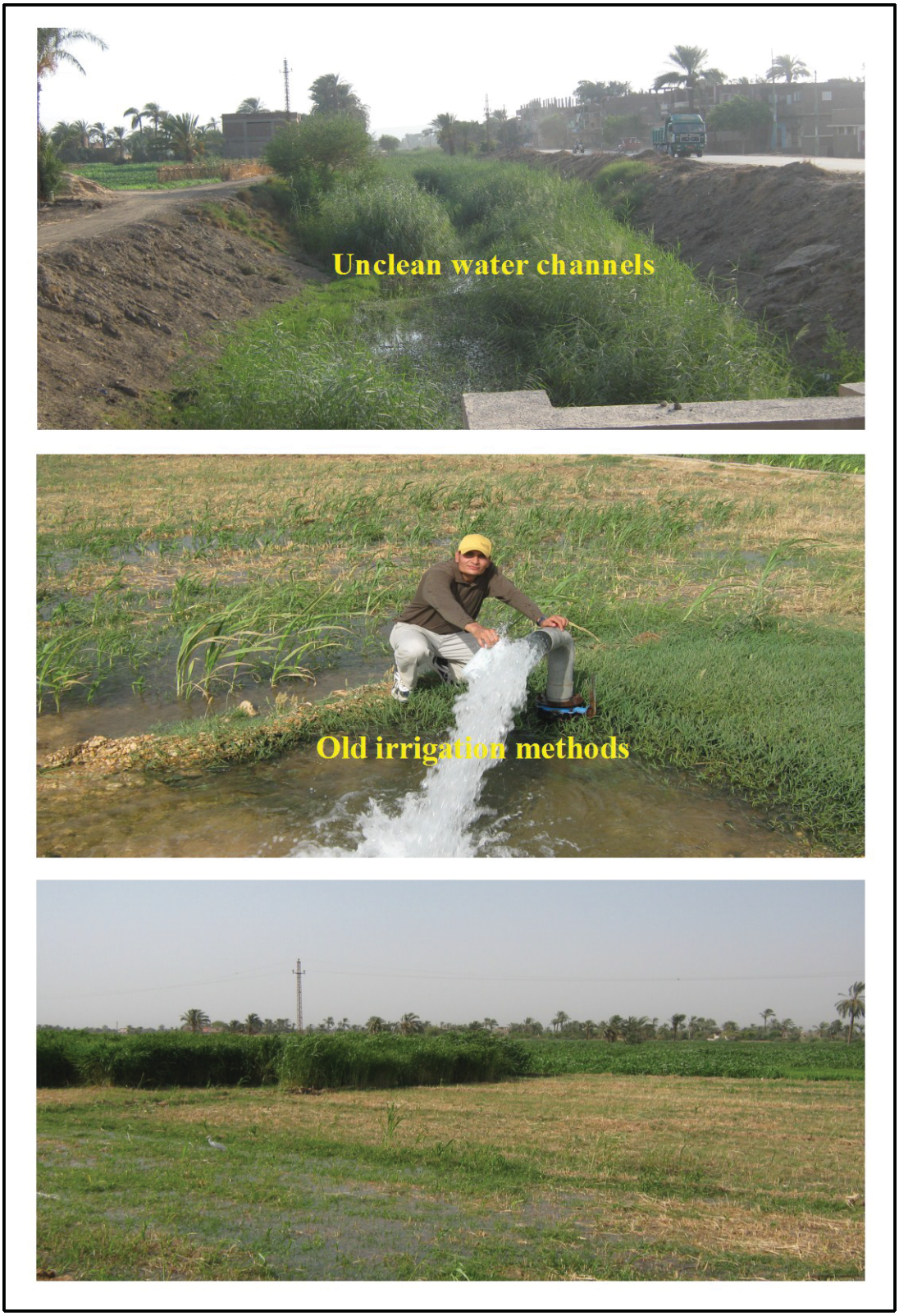

Fig. (4.5): Field photograph showing the unclean water channels and the use of old irrigation methods

In the field, the water samples were placed in (one Letter) polyethylene bottles. These bottles were tightly closed, sealed with caps, plastic inserts, and cellotape to avoid contamination or evaporation.

The hydrogen ion concentration, electric conductivity, and total dissolved salts were measured in the field. Complete chemical analysis, including major cations and anions were carried out in Central Laboratory- Water & Soil Analysis Unit, Desert Research Center, Ministry of Agriculture and Land Reclamation, Egypt.

The concentration of major ions of the collected surface and groundwater samples are given in tables 4.3 and 4.4 and expressed in ppm, epm, and epm %. The chemical characteristics of the studied water samples are discussed through the following main topics:

- Physical properties, including hydrogen ion concentration and electric conductivity
- Chemical characteristics, including total dissolved salts, total hardness, and major cations and anions
-Ion relationship, including hydrochemical coefficients, ion dominance, water type, and salt combinations
- Hydrochemical classification
- Groundwater quality

4.2.1. Physical properties

-The hydrogen ion concentration (PH) describes the acidic or basic nature of a substance. By measuring the concentration of hydrogen ions on a scale from 0 to 14 with a value of 7 (distilled water) indicating a neutral (PH), water can be classified as basic (with values greater than 7) and as acid (with values less than 7). The pH in the groundwater depends mainly on the composition of the rock and sediment the water was migrating.

-The pH of the surface water varies from 7.1 to 7.6, and the groundwater varies from 6 to 7.7. This is indicates a slightly acidic to slightly basic nature. According to BIS (1998), all the water samples showed pH values within the permissible limit of 6.5 - 8.5.

Table (4.3) : Chemical analysis data and hydrochemical parameters of the surface and ground water samples collected in 2011

S.No.	W.No.	pH	E.C	TDS	Units	Cations				Total Cations	Anions				Total Anions	TH	SAR	Hydrochemical Coefficients(epm)			Ion Dominance	water type
						Ca^{++}	Mg^{++}	Na^{+}	K^{+}		CO_3^{-}	HCO_3^{-}	Cl^{-}	SO_4^{--}				r(Na+K)/rCl	rCa/rMg	rSO4/rCl		
1	S.W	7.50	239	166.27	ppm	23.46	7.92	24	6	3.03	14.70	119.56	10.77	19.64	3.16	91.17	1.1	3.95	1.78	1.35	Na > Ca> Mg HCO_3 >SO_4 > Cl	$NaHCO_3$
					epm	1.17	0.66	1.04	0.15		0.49	1.96	0.30	0.41								
					epm%	38.71	21.78	34.43	5.08		15.49	61.98	9.59	12.94								
2	S.W	7.60	241	170	ppm	27.89	9.305	20	5	3.17	14.70	116.57	9.57	24.96	3.19	107.93	0.8	3.70	1.80	1.93	Ca >Na >Mg HCO_3 > SO_4 > Cl	$Ca(HCO_3)_2$
					epm	1.39	0.78	0.87	0.13		0.49	1.91	0.27	0.52								
					epm%	44.02	24.48	27.45	4.05		15.36	59.89	8.45	16.30								
3	S.W	7.10	930	571	ppm	60.17	29.36	100	7	9.98	14.70	295.91	62.23	150	10.22	271.06	2.6	2.58	1.23	1.78	Na >Ca >Mg HCO_3 >SO_4 >Cl	$NaHCO_3$
					epm	3.01	2.45	4.35	0.18		0.49	4.85	1.75	3.13								
					epm%	30.14	24.51	43.55	1.80		4.80	47.47	17.15	30.58								
4	S.W	7.70	230	163	ppm	21.68	7.916	24	8	2.99	11.76	122.54	8.6	20	3.06	86.709	1.1	5.15	1.64	1.72	Na> Ca> Mg HCO_3>SO_4 > Cl	$NaHCO_3$
					epm	1.08	0.66	1.04	0.21		0.39	2.01	0.24	0.42								
					epm%	36.23	22.05	34.87	6.86		12.81	65.65	7.92	13.62								
5	S.W	7.50	1535	755	ppm	36.58	24.61	210	9	13.24	29.40	266.02	148.4	164.26	12.94	192.61	6.6	2.24	0.89	0.82	Na> Mg> Ca HCO_3 > Cl >SO_4	$NaHCO_3$
					epm	1.83	2.05	9.13	0.23		0.98	4.36	4.18	3.42								
					epm%	13.81	15.49	68.96	1.74		7.57	33.69	32.30	26.44								
6	S.W	7.30	2386	1456	ppm	103.7	54.03	300	12	23.04	55.86	289.93	153.2	632.07	24.10	481.27	5.9	3.09	1.15	3.05	Na > Ca >Mg SO_4 >HCO_3 > CL	Na_2SO_4
					epm	5.19	4.50	13.04	0.31		1.86	4.75	4.31	13.17								
					epm%	22.51	19.54	56.62	1.34		7.73	19.72	17.91	54.64								
7	G.W	7.00	4360	2655	ppm	224.8	95.33	540	8	42.87	5.88	110.59	825.8	900	44.02	953.61	7.6	1.02	1.41	0.81	Na > Ca > Mg Cl > SO_4 >HCO_3	NaCl
					epm	11.24	7.94	23.48	0.21		0.20	1.81	23.26	18.75								
					epm%	26.22	18.53	54.77	0.48		0.45	4.12	52.84	42.59								
8	G.W	7.30	970	567	ppm	57.25	13.54	130	3	9.72	11.76	239.12	122.1	110	10.04	198.67	4.0	1.67	2.54	0.67	Na > Ca > Mg HCO_3 > Cl > SO_4	$NaHCO_3$
					epm	2.86	1.13	5.65	0.08		0.39	3.92	3.44	2.29								
					epm%	29.45	11.61	58.15	0.79		3.90	39.04	34.24	22.82								
9	G.W	7.60	1627	1004	ppm	80.1	37.9	210	4	16.40	17.64	158.41	225	350	16.81	355.97	4.8	1.46	1.27	1.15	Na>Ca > Mg SO_4 > Cl > HCO_3	Na_2SO_4
					epm	4.01	3.16	9.13	0.10		0.59	2.60	6.34	7.29								
					epm%	24.43	19.26	55.69	0.63		3.50	15.44	37.69	43.37								
10	G.W	7.40	5870	3533	ppm	235.6	55.76	900	7	55.74	0.00	146.46	1112	1148.9	57.66	817.75	13.7	1.25	2.54	0.76	Na >Ca >Mg Cl >SO_4 >HCO_3	NaCl
					epm	11.78	4.65	39.13	0.18		0.00	2.40	31.33	23.94								
					epm%	21.14	8.34	70.21	0.32		0.00	4.16	54.33	41.51								
11	G.W	7.20	7550	4453	ppm	248.8	84.14	1220	11	72.78	17.64	170.37	1649	1136.9	73.52	967.49	17.0	1.15	1.77	0.51	Na >Ca>Mg Cl >SO_4> HCO_3	NaCl
					epm	12.44	7.01	53.04	0.28		0.59	2.79	46.45	23.69								
					epm%	17.09	9.63	72.88	0.39		0.80	3.80	63.18	32.22								
12	G.W	7.50	1454	818	ppm	54.84	25.3	210	7	14.16	14.70	215.2	258.5	140	14.22	241.04	5.9	1.28	1.30	0.40	Na > Ca > Mg Cl >HCO_3 >SO_4	NaCl
					epm	2.74	2.11	9.13	0.18		0.49	3.53	7.28	2.92								
					epm%	19.36	14.89	64.48	1.27		3.45	24.82	51.22	20.52								
13	G.W	7.30	4550	2808	ppm	218.3	63.27	650	8	44.65	11.76	161.4	825.8	950	46.09	805.45	9.9	1.22	2.07	0.85	Na> Ca > Mg Cl >SO_4 >HCO_3	NaCl
					epm	10.92	5.27	28.26	0.21		0.39	2.65	23.26	19.79								
					epm%	24.44	11.81	63.29	0.46		0.85	5.74	50.47	42.94								
14	G.W	7.60	4110	2493	ppm	243.3	100.2	460	12	40.82	0.00	215.2	820.3	750	42.26	1019.8	6.2	0.88	1.46	0.68	Na > Ca > Mg Cl > SO_4 > HCO_3	NaCl
					epm	12.17	8.35	20.00	0.31		0.00	3.53	23.11	15.63								
					epm%	29.80	20.45	48.99	0.75		0.00	8.35	54.68	36.97								
15	G.W	7.50	3300	2379	ppm	150.4	100.2	500	26	38.28	20.58	269.01	347.1	1100	37.79	787.87	7.7	2.29	0.90	2.34	Na>Mg > Ca SO_4 > Cl >HCO_3	Na_2SO_4
					epm	7.52	8.35	21.74	0.67		0.69	4.41	9.78	22.92								
					epm%	19.65	21.82	56.80	1.74		1.82	11.67	25.87	60.64								
16	G.W	7.30	2354	1480	ppm	210.7	62.11	190	8	24.18	41.16	304.87	220.2	595.2	24.97	781.7	2.9	1.36	2.04	2.00	Ca>Na >Mg SO_4>HCO_3 > CL	$CaSO_4$
					epm	10.54	5.18	8.26	0.21		1.37	5.00	6.20	12.40								
					epm%	43.57	21.41	34.17	0.85		5.49	20.01	24.84	49.65								
17	G.W	7.30	863	452	ppm	27.01	9.13	132	2	7.90	26.46	221.18	28.72	115.9	7.73	105.01	5.6	7.16	1.78	2.98	Na > Ca> Mg HCO_3>SO_4>Cl	$NaHCO_3$
					epm	1.35	0.76	5.74	0.05		0.88	3.63	0.81	2.41								
					epm%	17.09	9.63	72.63	0.65		11.41	46.90	10.46	31.23								

[Geben Sie Text ein]

Table (4.4) : Continued

S.No.	W.No.	pH	E.C	TDS	Units	Cations				Total Cations	Anions				Total Anions	TH	SAR	Hydrochemical Coefficients(epm)			Ion Dominance	water type
						Ca^{++}	Mg^{++}	Na^{+}	K^{+}		CO_3^{-}	HCO_3^{-}	Cl^{-}	SO_4^{-}				r(Na+K)/rCl	rCa/rMg	rSO4/rCl		
18	G.W	7.60	3490	2124	ppm	175.7	91.22	440	13	35.85	29.40	251.07	478.7	770.1	34.62	814.09	6.7	1.44	1.16	1.19	Na > Ca >Mg SO_4 > CL > HCO_3	Na_2SO_4
					epm	8.79	7.60	19.13	0.33		0.98	4.12	13.48	16.04								
					epm%	24.50	21.20	53.36	0.93		2.83	11.89	38.95	46.34								
19	G.W	7.20	2854	1858	ppm	100.2	56.1	440	28	29.53	29.40	266.02	411.7	660	30.69	481.05	8.7	1.71	1.07	1.19	Na > Ca> Mg SO_4> Cl > HCO_3	Na_2SO_4
					epm	5.01	4.68	19.13	0.72		0.98	4.36	11.60	13.75								
					epm%	16.96	15.83	64.78	2.43		3.19	14.21	37.79	44.81								
20	G.W	7.70	356	184	ppm	21.1	11.2	30	10	3.55	17.64	119.56	19.15	15	3.40	98.775	1.3	2.89	1.13	0.58	Na > Ca >Mg HCO_3> Cl > SO_4	$NaHCO_3$
					epm	1.06	0.93	1.30	0.26		0.59	1.96	0.54	0.31								
					epm%	29.73	26.30	36.75	7.22		17.29	57.65	15.86	9.19								
21	G.W	7.70	1883	1242	ppm	50.2	42.1	330	12	20.67	17.64	236.13	172.3	500	19.73	298.59	8.3	3.02	0.72	2.15	Na> Mg> Ca SO_4 > Cl>HCO_3	Na_2SO_4
					epm	2.51	3.51	14.35	0.31		0.59	3.87	4.85	10.42								
					epm%	12.14	16.97	69.40	1.49		2.98	19.62	24.60	52.80								
22	G.W	6.00	6700	4448	ppm	235.84	112.26	1100	6	69.13	17.64	134.5	1197	1712	72.17	1050.8	14.7	1.42	1.26	1.06	Na >Ca >Mg SO_4> Cl > HCO_3	Na_2SO_4
					epm	11.79	9.36	47.83	0.15		0.59	2.20	33.71	35.67								
					epm%	17.06	13.53	69.19	0.22		0.81	3.06	46.71	49.42								
23	G.W	7.70	3300	2017	ppm	148.4	20.14	510	3	31.35	26.46	218.19	299.2	900.72	31.65	453.43	10.4	2.64	4.42	2.23	Na> Ca> Mg SO_4> Cl > HCO_3	Na_2SO_4
					epm	7.42	1.68	22.17	0.08		0.88	3.58	8.43	18.77								
					epm%	23.67	5.35	70.73	0.25		2.79	11.30	26.63	59.29								
24	G.W	7.90	3060	2140	ppm	179.7	65.3	420	18	33.15	17.64	179.34	299.2	1050	33.83	717.42	6.8	2.22	1.65	2.60	Na > Ca >Mg SO_4> Cl > HCO_3	Na_2SO_4
					epm	8.99	5.44	18.26	0.46		0.59	2.94	8.43	21.88								
					epm%	27.10	16.42	55.09	1.39		1.74	8.69	24.91	64.66								
25	G.W	7.60	4100	2642	ppm	197.3	58.7	600	7	41.02	20.58	239.12	538.5	1100	42.69	734.21	9.6	1.73	2.02	1.51	Na > Ca > Mg SO_4 > Cl >HCO_3	Na_2SO_4
					epm	9.87	4.89	26.09	0.18		0.69	3.92	15.17	22.92								
					epm%	24.05	11.92	63.59	0.44		1.61	9.18	35.53	53.68								
26	G.W	6.60	3860	2196	ppm	176.5	42.87	540	7	36.06	32.34	206.24	454.8	839.05	34.75	617.13	9.4	1.85	2.47	1.36	Na >Ca > Mg SO_4> Cl > HCO_3	Na_2SO_4
					epm	8.83	3.57	23.48	0.18		1.08	3.38	12.81	17.48								
					epm%	24.48	9.91	65.12	0.50		3.10	9.73	36.86	50.30								
27	G.W	7.30	1957	1278	ppm	104.9	25.3	280	11	19.81	23.52	230.15	158	560	20.67	366.04	6.3	2.80	2.49	2.62	Na > Ca> Mg SO_4>HCO_3 >Cl	Na_2SO_4
					epm	5.25	2.11	12.17	0.28		0.78	3.77	4.45	11.67								
					epm%	26.48	10.64	61.46	1.42		3.79	18.25	21.52	56.43								
28	G.W	7.60	1154	725	ppm	99.69	18.9	120	7	11.96	26.46	260.04	43.08	280	12.19	326.7	2.9	4.45	3.16	4.81	Na > Ca > Mg SO_4>HCO_3> Cl	Na_2SO_4
					epm	4.98	1.58	5.22	0.18		0.88	4.26	1.21	5.83								
					epm%	41.69	13.17	43.64	1.50		7.23	34.97	9.95	47.85								
29	G.W	7.30	1700	978	ppm	39.83	8.66	280	3	14.96	26.46	185.31	71.8	455.55	15.43	135.09	10.5	6.06	2.76	4.69	Na > Ca > Mg SO_4>HCO_3> Cl	Na_2SO_4
					epm	1.99	0.72	12.17	0.08		0.88	3.04	2.02	9.49								
					epm%	13.31	4.82	81.35	0.51		5.72	19.68	13.11	61.50								
30	G.W	6.80	6820	4063	ppm	338.6	57.76	1020	12	66.40	17.64	152.43	1149	1392.1	64.45	1083.2	13.5	1.38	3.52	0.90	Na > Ca> Mg Cl > SO_4 > HCO_3	NaCl
					epm	16.93	4.81	44.35	0.31		0.59	2.50	32.36	29.00								
					epm%	25.50	7.25	66.79	0.46		0.91	3.88	50.21	45.00								
31	G.W	7.00	1187	698	ppm	28.64	19.4	190	3	11.39	17.64	188.3	47.87	297.64	11.22	151.35	6.7	6.18	0.89	4.60	Na> Mg> Ca SO_4 > HCO_3 > Cl	Na_2SO_4
					epm	1.43	1.62	8.26	0.08		0.59	3.09	1.35	6.20								
					epm%	12.58	14.20	72.55	0.68		5.24	27.50	12.01	55.25								
32	G.W	7.80	4260	2816	ppm	215.5	37.57	660	4	42.70	29.40	149.45	394.9	1400	43.72	692.7	10.9	2.59	3.44	2.62	Na > Ca > Mg SO_4> Cl > HCO_3	Na_2SO_4
					epm	10.78	3.13	28.70	0.10		0.98	2.45	11.12	29.17								
					epm%	25.23	7.33	67.20	0.24		2.24	5.60	25.44	66.71								
33	G.W	7.60	2191	1391	ppm	67.35	39.9	350	2	21.96	35.28	304.87	143.6	600	22.72	332.36	8.3	3.77	1.01	3.09	Na > Ca > Mg SO_4 > HCO_3 > Cl	Na_2SO_4
					epm	3.37	3.33	15.22	0.05		1.18	5.00	4.05	12.50								
					epm%	15.33	15.14	69.29	0.23		5.18	22.00	17.81	55.02								
34	G.W	7.30	5790	3783	ppm	277	140.1	800	16	60.72	29.40	125.53	658.2	1800	59.08	1268.2	9.7	1.90	1.19	2.02	Na > Ca > Mg SO_4> Cl > HCO_3	Na_2SO_4
					epm	13.85	11.68	34.78	0.41		0.98	2.06	18.54	37.50								
					epm%	22.81	19.23	57.29	0.68		1.66	3.48	31.38	63.47								

[Geben Sie Text ein]

-Electric conductivity is a numerical expression of the physical property of water to carry an electric current. There are relations between the electric conductivity and the total dissolved salts. More specifically when the total dissolved salts increases, the electric conductivity increases as well. The electrical conductivity (EC) ranges from 230 to 2386 µS/cm for the surface water and from 356 to 7550 µS/cm for the groundwater. The surface water and about 46% of the studied water samples showed conductivity values above the permitted limit of 3000 µS/cm (BIS 1998).

4.2.2. Chemical properties of the water samples

The chemical properties of the water samples include the total dissolved solids, the total hardness, and the distribution of major cations and major anions.

Total dissolved solids (TDS) is a measure of the combined content of all inorganic and organic substances contained in a liquid as a molecular, ionized, or micro-granular (colloidal sol) suspended form. Hem (1970) classified the water according to TDS into the following categories (Table 4.5)

Table (4.5): TDS classification according to Hem (1970)

Water type	TDS (ppm)
Fresh water	< 1000
Slightly saline water	1000-3000
Moderately saline water	3000-10,000
Very saline water	10,000-35,000
Briny water	> 35,000

In the studied water samples, the salinity of the surface water is lower than in the fresh water, except one sample where the salinity of the groundwater occurs to be in between. The TDS varies between 184 and 4448 PPM. The increase of salinity is attributed to leaching processes and the dissolution of limestone during extensive relieve of, as well as during evaporation of the irrigation water. The iso-salinity contour map (Fig. 4.7) shows the increase of the salinity from east to west, reflecting the impact of the leaching effect on the limestone in the west.

Total hardness (TH): Hardness of water is defined as the concentration of multivalent cations. Multivalent cations are metal ions with a charge greater than 1+, such as Ca^{2+} and Mg^{2+}.

These ions are easily precipitated and react with soap to form a scum which is difficult to remove. Hardness of water causes encrustations in containers or conduits where water is heated or transported. The total hardness of water is divided into two types, carbonate and non-carbonate. Carbonate hardness (or temporary hardness) dissipated in the water during heating includes calcium and magnesium, as well as bicarbonate and a small amount of carbonate. The non-carbonate hardness (or permanent hardness) remains after heating and is caused by the amount of calcium and magnesium in combination with sulphate, chloride, and nitrate ions. According to Todd (1980), Hem (1985, 1989), Ragunath (1987), the total hardness (TH) in ppm can be determined with the following equation:

$$TH = 2.497\ Ca^{2+} + 4.115 Mg^{2+}.$$ (Ca^{2+} and Mg^{2+} are all measured in ppm)

The classification of the surface and groundwater based on hardness (Sawyer and McCarthy, 1967) is presented in the following table:

Table (4.6): Sawyer and McCarty's classification of groundwater based on hardness

TH as $CaCO_3$ (mg/L)	Water classes	Surface water	Groundwater
< 75	Soft	----	----
75 – 150	Moderately hard	3 samples 50%	3 samples 11%
150 – 300	Hard	2 samples 33%	4 samples 14%
> 300	Very hard	1sample 17%	21 samples 75%

The high levels of total hardness of the groundwater samples reflect the high dissolution of the limestone, (Fig. 4.8) which is similar to the salinity discussed above.

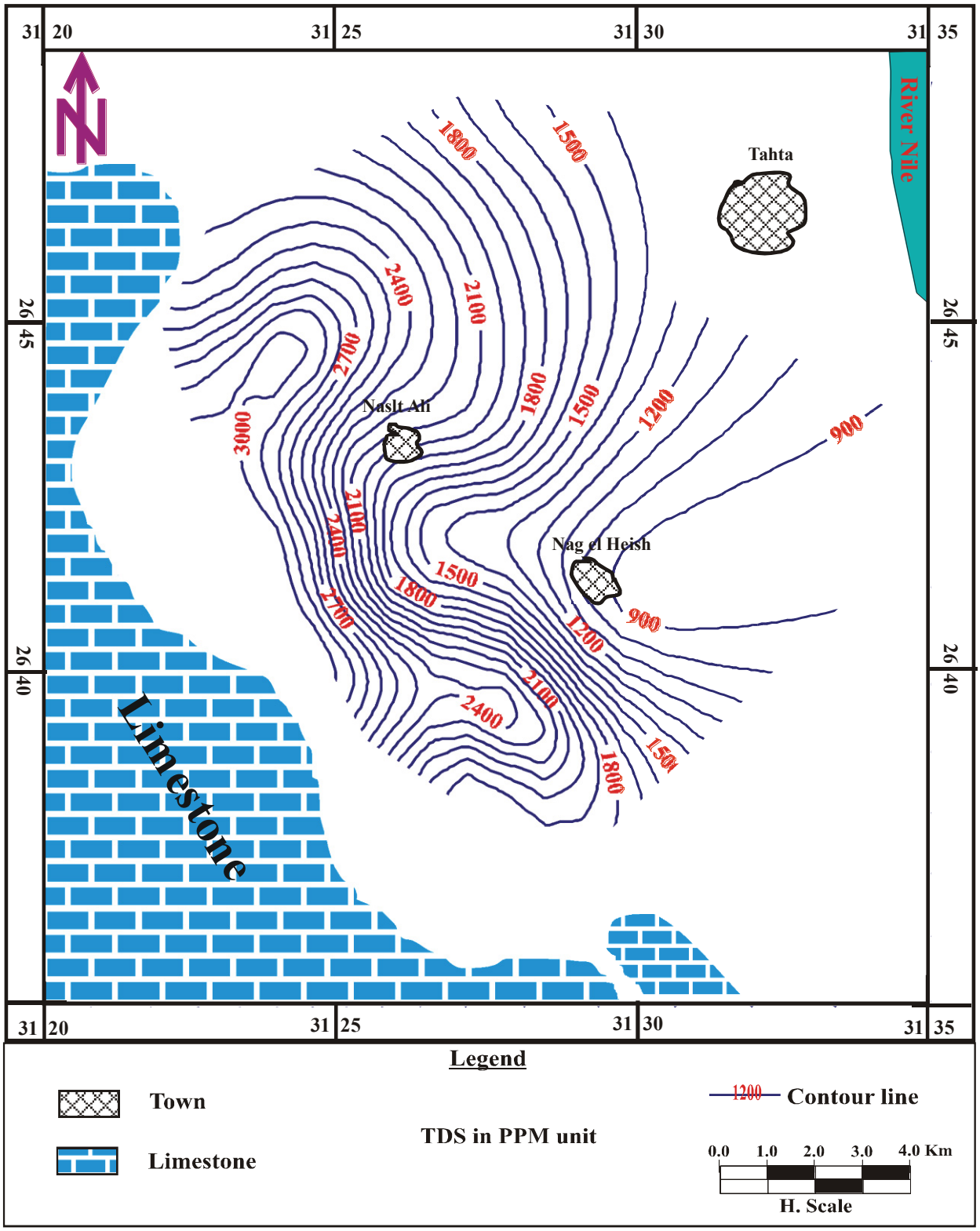

Fig. (4.7): Iso-salinity contour map 2011(groundwater samples)

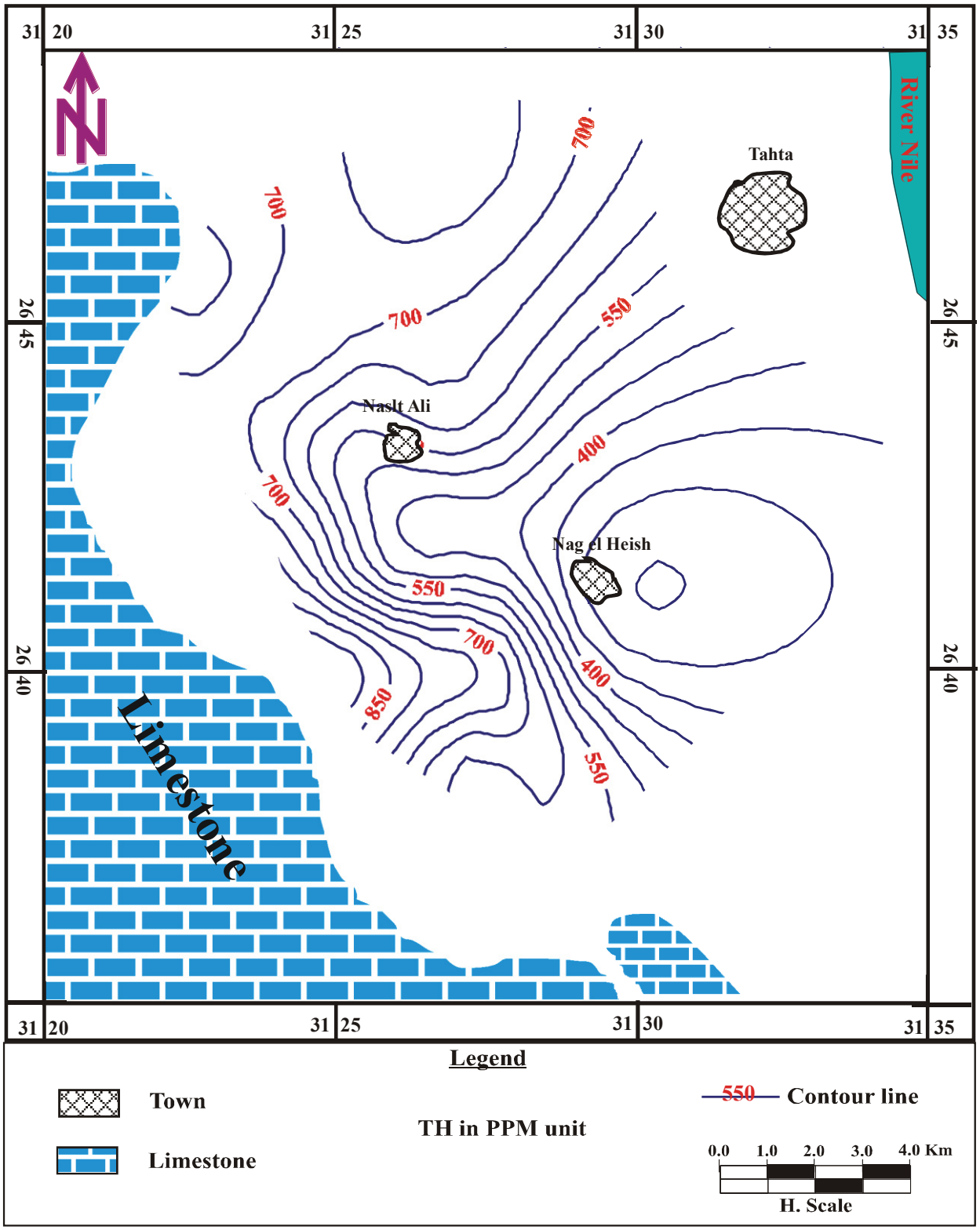

Fig. (4.8): Hardness contour map 2011 (groundwater samples)

4.2.2.1. Major ion concentration and distribution:

Calcium is one of the principal cations in most natural fresh water and is dissolved more or less from all rocks and soils. Calcium ions are widely distributed in the carbonate sediments. The calcium concentration of the studied water samples varies from 22 to 104ppm and from 21 to 339ppm in the surface and groundwater respectively. The iso-calcium contour map (Fig. 4.9) shows the calcium concentration increasing towards the west and northwest.

The distribution of magnesium ions is similar to that of calcium ions, affecting the water quality. Magnesium occurs in many rock types; however, the concentration is usually significantly less than for calcium. The concentration of magnesium in the studied water samples varies from 8 to 54ppm and 9 to 140ppm in the surface and groundwater respectively. The iso-magnesium contour map (Fig. 4.10) shows an increase of Mg^{++} towards the west and northwest.

Sodium and potassium ion concentrations: In arid regions, all natural waters contain sodium and potassium in high concentrations, particularly in shale and clay sediments. The concentration of sodium in the water samples ranges from 25 to 312ppm and from 30 to 1220ppm in the surface and groundwater respectively. The increases in the sodium distribution reflect the dissolution of shale and clay in the area. The sodium and potassium distribution are shown in (Fig. 4.11).

Bicarbonate ion concentration: Carbon oxide dissolved in water causes a weak acid, increasing the leaching of rocks. Carbonates are particularly susceptible. Bicarbonate concentrations of more than 200ppm are not common in groundwater and the higher concentrations can occur where CO_2 is produced within the aquifer. The bicarbonate distribution in the surface water varies between 132 and 346ppm, while in the groundwater it varies between 111 and 305ppm. From the iso-bicarbonate contour map (Fig. 4.12) we see the concentration of HCO_3 ion increases towards the east to the surface water.

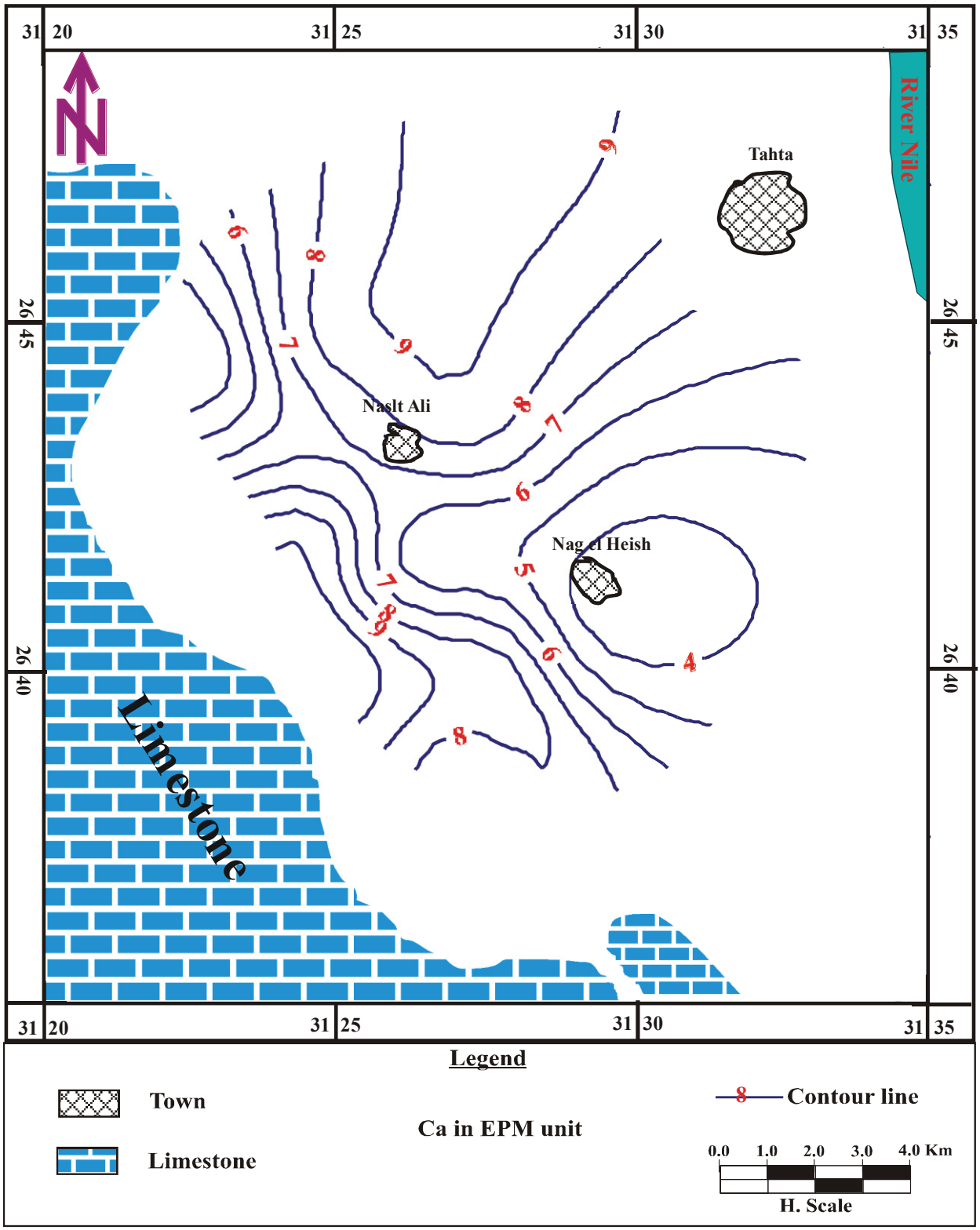

Fig. (4.9): Iso-calcium contour map 2011 (groundwater samples)

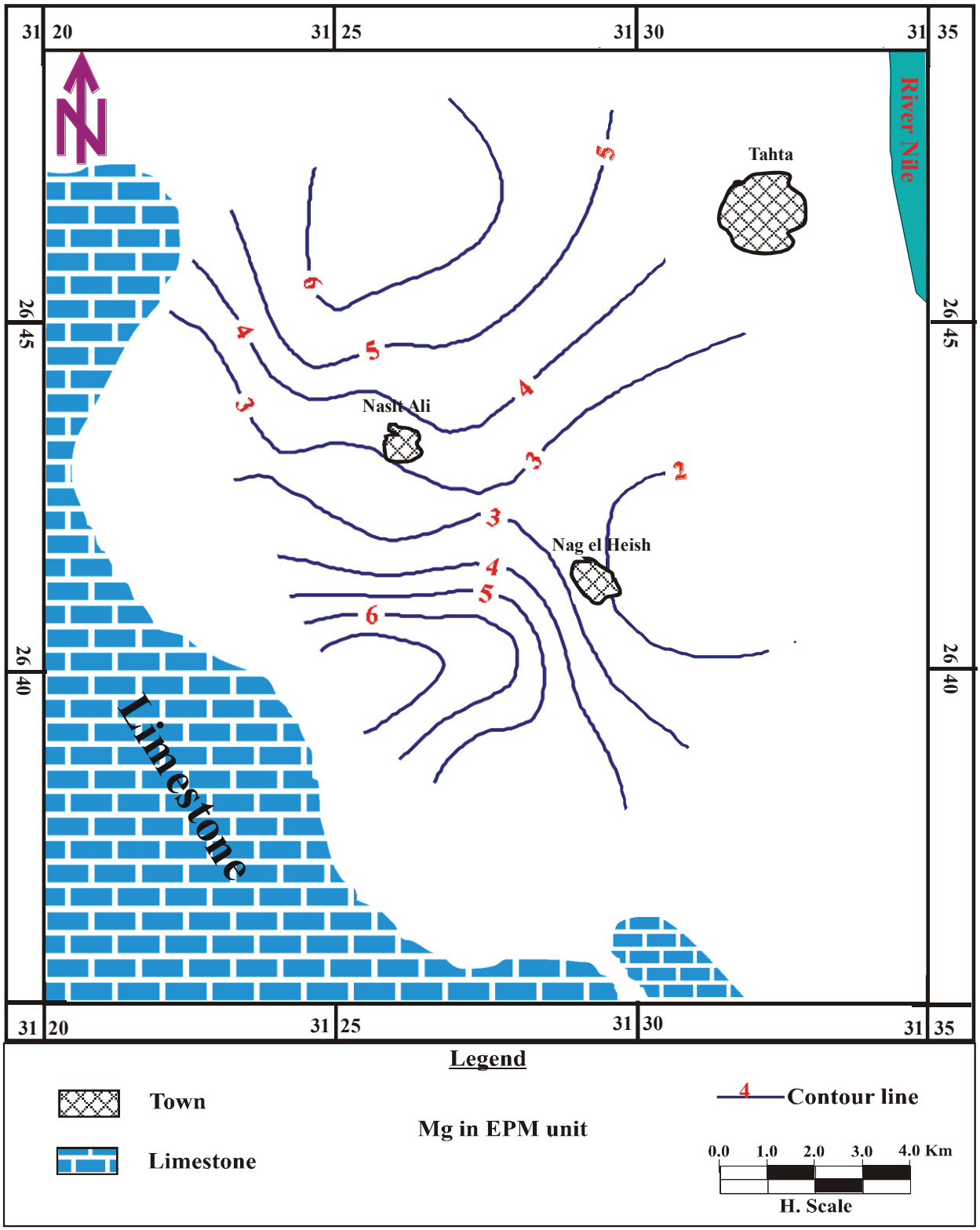

Fig. (4.10): Iso-magnisum contour map2011 (groundwater samples)

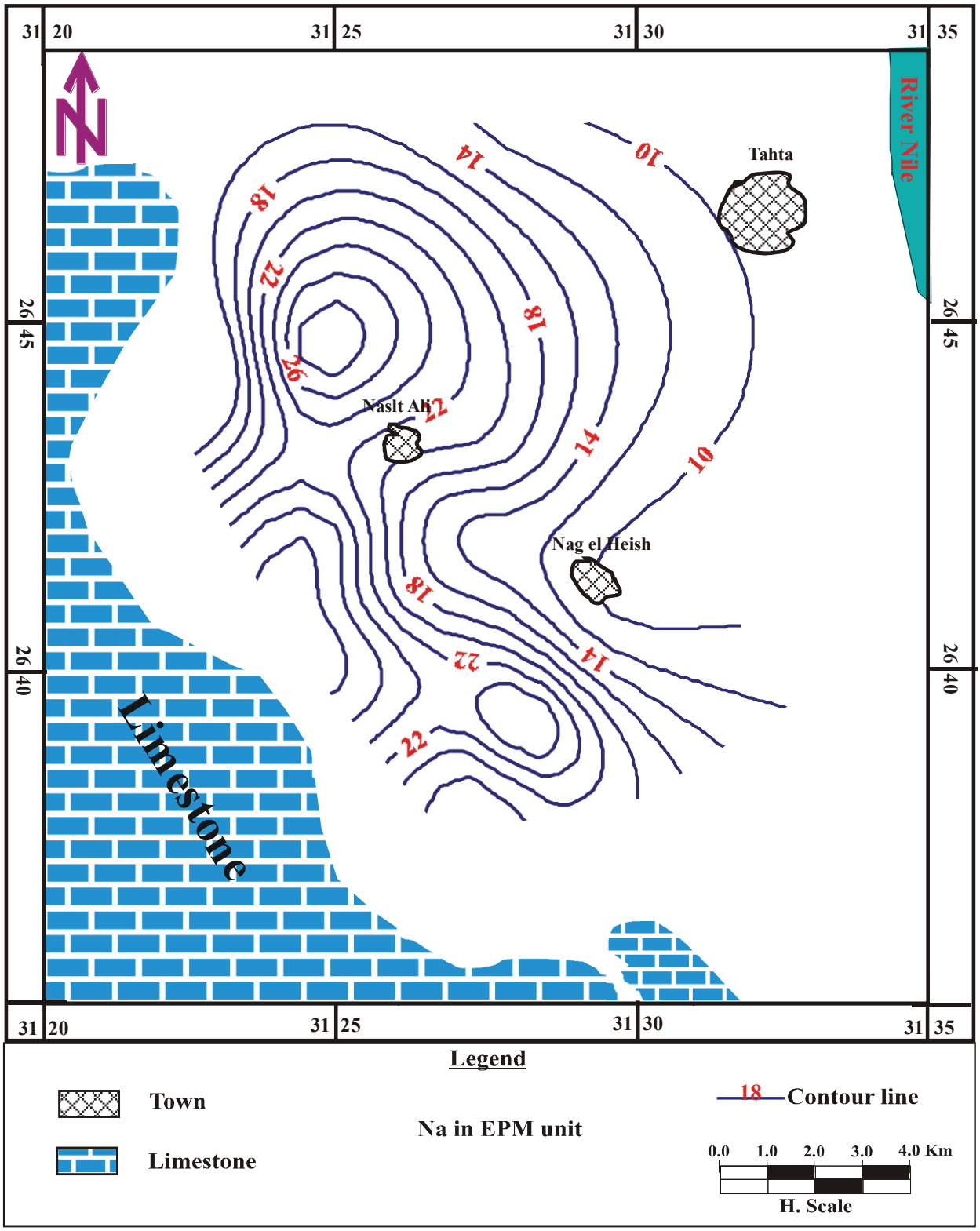

Fig. (4.11): Iso-sodium contour map 2011 (groundwater samples)

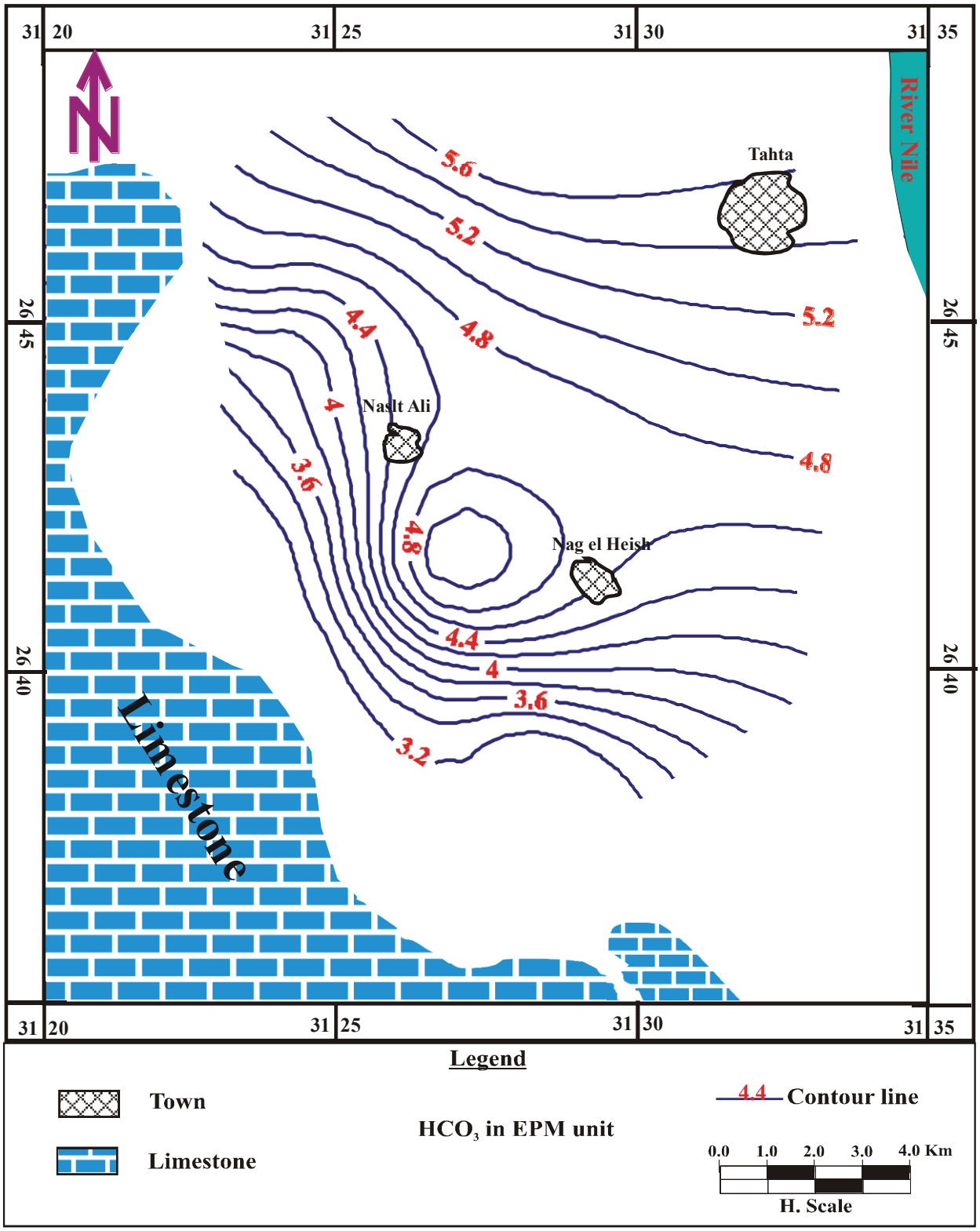

Fig. (4.12): Iso-bicarbonate contour map 2011(groundwater samples)

Sulfate ion concentration: In natural waters the sulfate concentration is usually below 300ppm, except in wells affected by acid mine drainage. In some brines, the sulfate concentration may be up to 200,000ppm. The sulfate concentration ranges from 20 to 632ppm in the surface water samples and from 15 to 1800ppm in the groundwater samples. Figure 4.13 shows the distribution of sulfate in the study area increasing toward the west due to the presence of new reclaimed areas. Fertilizers are used extensively in this area to improve the soil quality in the new reclamation project, but they also influence the water quality.

The chloride ion concentration of surface water varies from 9 to153ppm, while the chloride concentration of the groundwater shows values between 19 and 1649ppm. The increase of chloride ions indicates human and animal sewage contamination. The distribution of chloride is shown in Fig. 4.14.

4.2.2.2. Ion relationship

(I)-Hydrochemical coefficients (ion ratios):

Ion ratios are useful in detecting the previous hydrochemical process that affected the water quality in terms of groundwater contamination, mixing, leaching, and ion exchange. It gives a coherent picture of the hydrochemical similarities and differences between different water types. The used ion ratios (rNa/rCl, rSO4/rCl and rCa/rMg) (Tables 4.3 and 4.4) are of particular importance in the present study as follows:

(rNa + rK/rCl) ratio; This relationship between the alkali metals and chloride ions is a good indicator of the chemical maturity or contamination of the water. When the alkaline values are less than one, it means that Na replaces Ca and Mg in their halogens. From 1 to 1.2, alkaline replaces Ca and Mg in their sulphates and a small part of their carbonates. A value above 1.2 means alkaline replaces Ca and Mg in the carbonates. Surface water and 89% of the groundwater samples have ratios higher than 1.2, indicating the replacement of Ca and Mg in the carbonates. 4% of the groundwater samples have ratio less than one which shows that Na replaces Ca and Mg in the halogen. 7% of the groundwater samples show values from 1 to 1.2, indicating the alkaline replacement of Ca and Mg in their sulphates and minor in the carbonates.

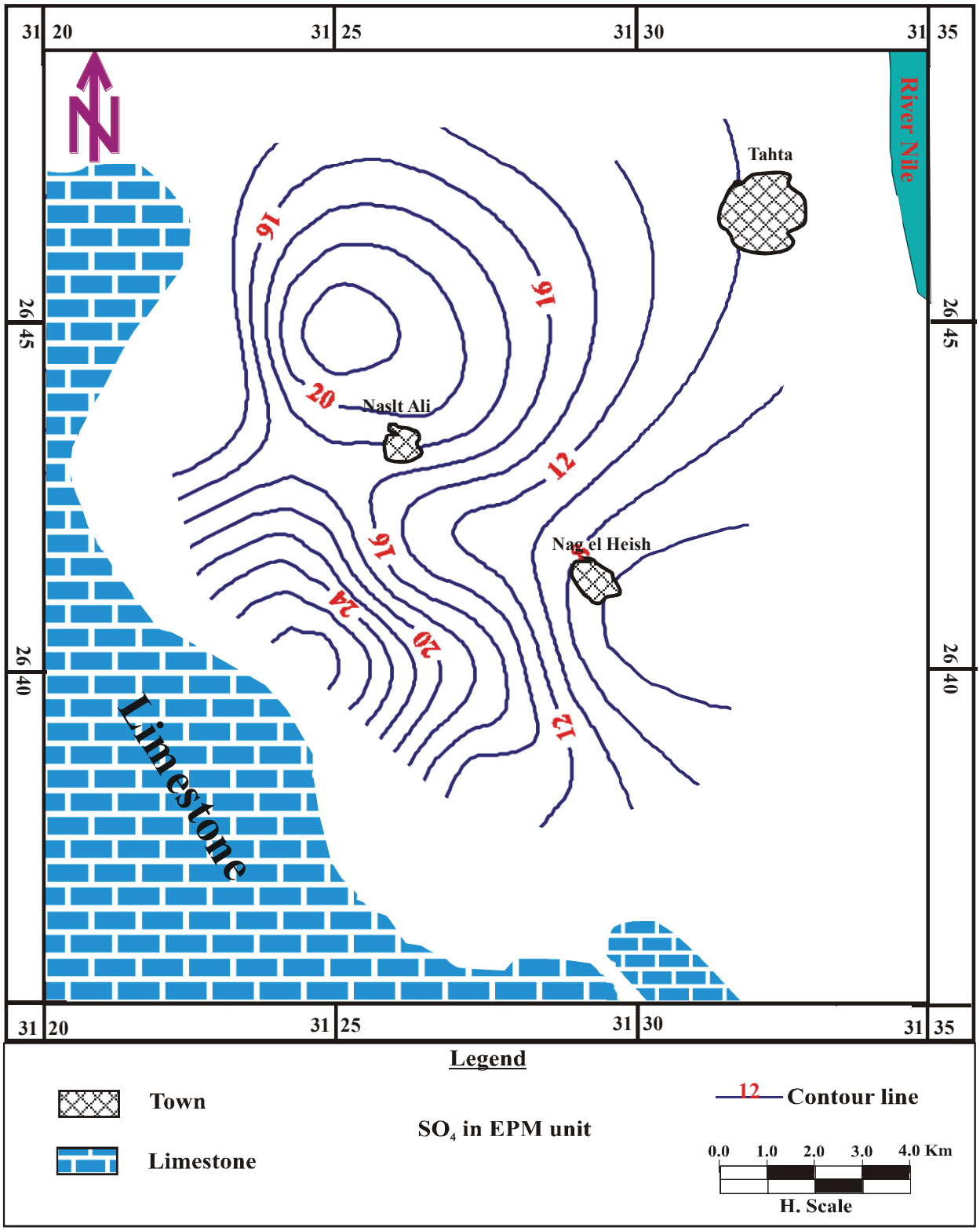

Fig. (4.13): Iso-sulfate contour map 2011 (groundwater samples)

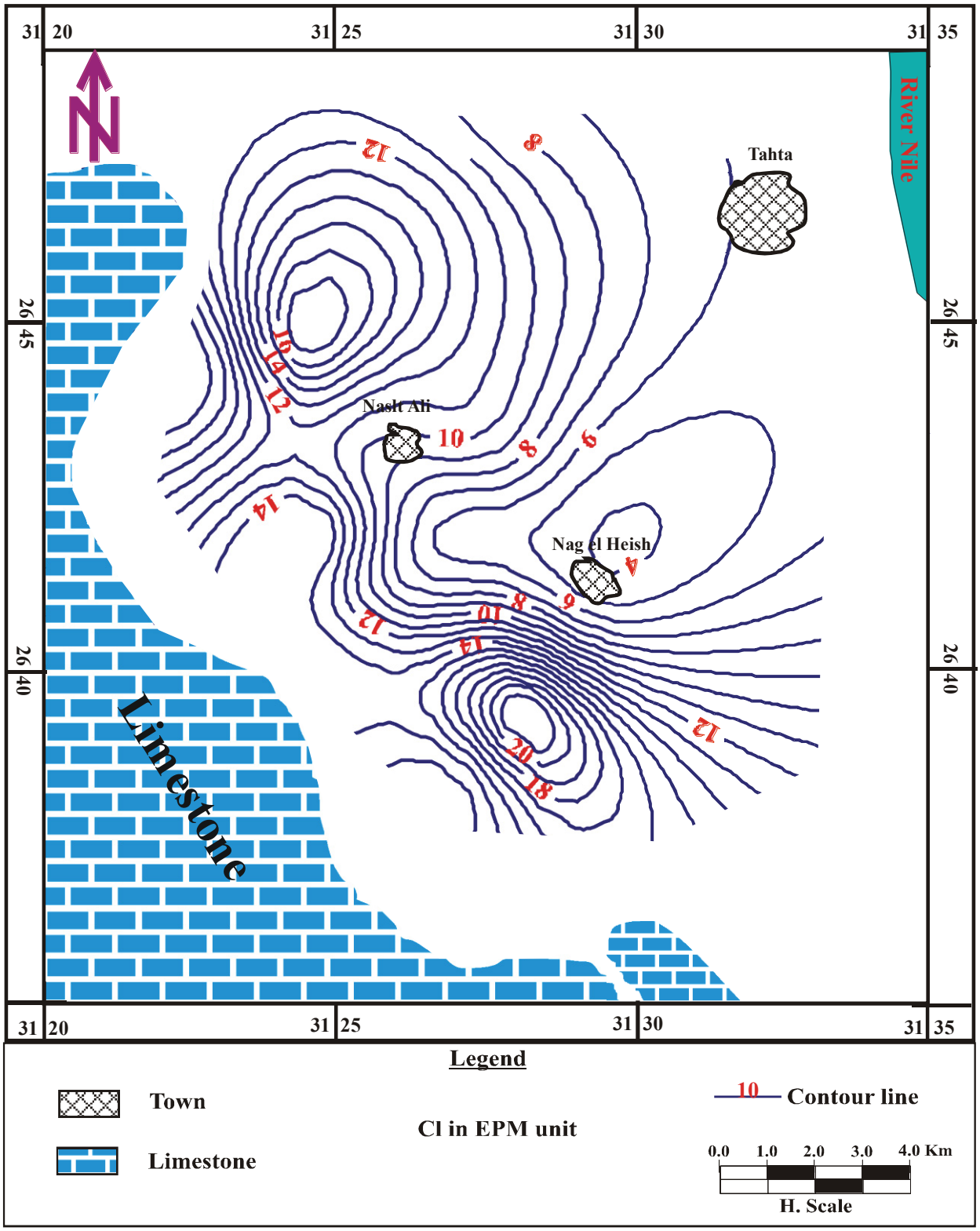

Fig. (4.14): Iso-chloride contour map 2011 (groundwater samples)

(rSO_4/rCl) ratio; the ratio of sulphate to chloride is a useful guide for detecting any oversupply of sulphates in the groundwater. The majority of the surface water and groundwater samples have an oversupply of sulphate over chloride, attributed to the extensive and increasing use of fertilizers.

(rCa/rMg) ratio; the rCa/rMg ratio is highly influenced by the activity of the Base Exchange process. This ratio is an important factor for studying groundwater content in limestone aquifers. High values may indicate surface water mixing or CO_2-$CaCO_3$ interaction. Most of the surface and groundwater samples have a higher Ca ion oversupply than Mg. The majority of these ratios are close to those of the Nile water, proving the dominant recharge of the aquifer from the River Nile. The ion ratio shows the similarity between the surface water and groundwater, indicating that, the surface water is the main source of groundwater recharge.

(II)- Ion dominance and water type:

The ion dominance and water types of groundwater samples from the study area are represented in Tables 4.7 and 4. 8. Concerning the ion dominance, sodium is the dominant cation, while the dominant anions are greatly variable. The dominant chemical water types of the surface water samples are $NaHCO_3$, $Ca(HCO_3)_2$, and Na_2SO_4, while the dominant water types of the groundwater samples are Na_2SO_4, NaCl, and $NaHCO_3$. The sodium bicarbonate dominated water type indicates the recharge of the groundwater in the study area is from the Nile water through the irrigation canals. The sodium chloride and sodium sulfate water types represent the water samples from the western study area, indicating the extensive use of fertilizers.

Table (4.7): Ion dominance of the studied water samples

Ion dominance	Surface water	Groundwater
HCO_3> Cl> SO_4/ Na> Ca (or Mg)> Mg (or Ca)	17%	7%
Cl> HCO_3> SO_4/ Na> Ca (or Mg)> Mg (or Ca)	---	4%
Cl> SO_4> HCO_3/ Na> Ca (or Mg)> Mg (or Ca)	---	21%
SO_4> Cl > HCO_3/ Na >Ca (or Mg)> Mg (or Ca)	---	43%
HCO_3> SO_4> Cl / Ca (or Mg)> Na> Mg (or Ca)	67%	4%
SO_4 > HCO_3> Cl / Na >Ca (or Mg)> Mg (or Ca)	----	18%
HCO_3> SO_4> Cl / Na> Ca (or Mg)> Mg (or Ca)	16%	--
SO_4 > HCO_3> Cl / Ca (or Mg)> Na > Mg (or Ca)	--	3%

Table (4.8): Water type of the studied water samples

Water type	Surface water	Groundwater
$NaHCO_3$	67%	11%
NaCl	--	25%
Na_2SO_4	17%	61%
$Ca(HCO_3)_2$	16%	--
$CaSO_4$	--	3%

(III)-Hypothetical salt combinations:

By using the Bar-graph method of Collins (1923), the salt combination of the water samples of the actual results are shown in Figures 4.15 and 4.16. In this method of representation, the concentrations of the cations are plotted on the left half, while the anions are plotted on the right. The following table shows the sequences of salt combinations of the surface and groundwater collected from the study area.

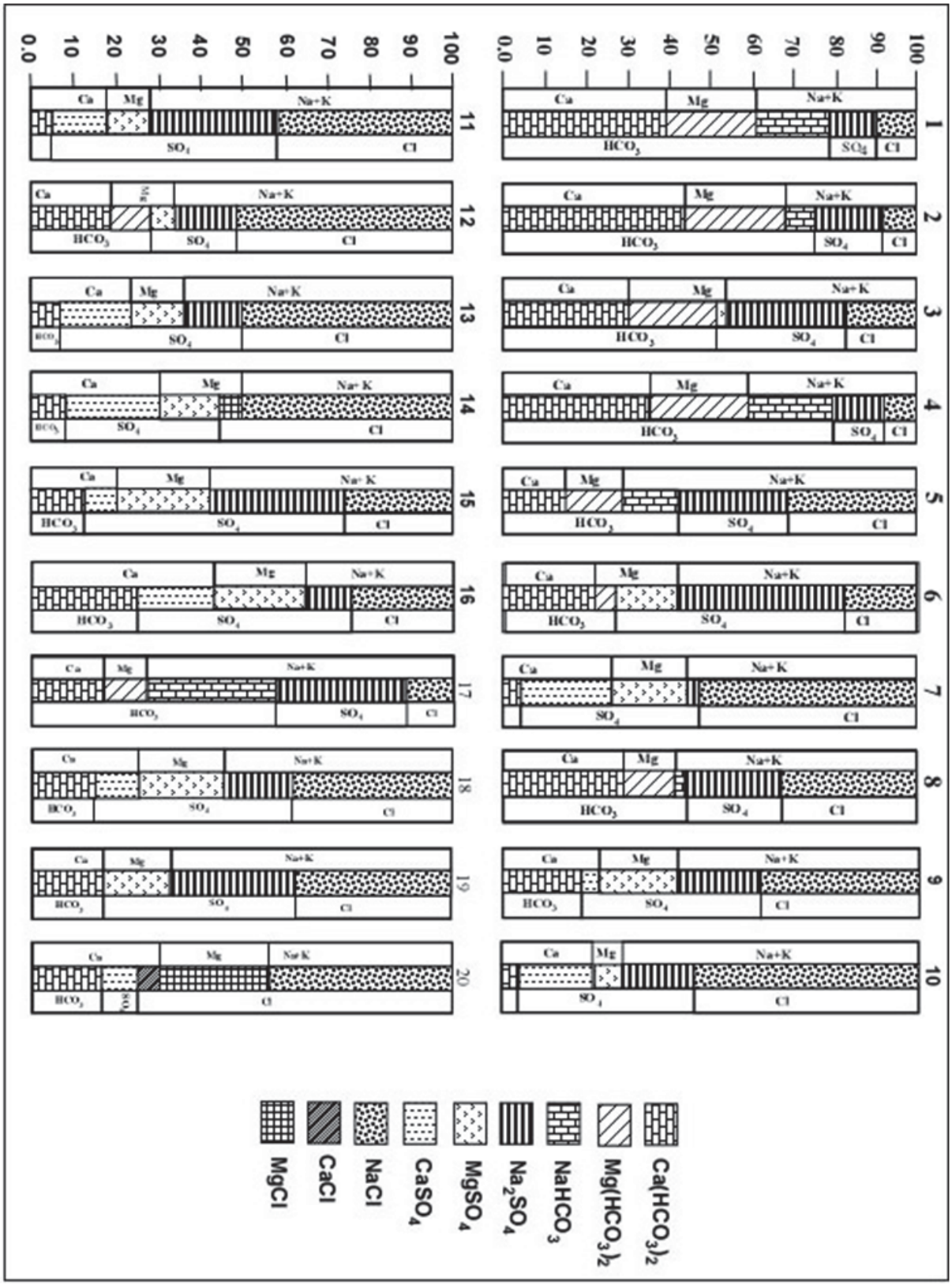

Fig. (4.15): Bar-graph method of the study water samples

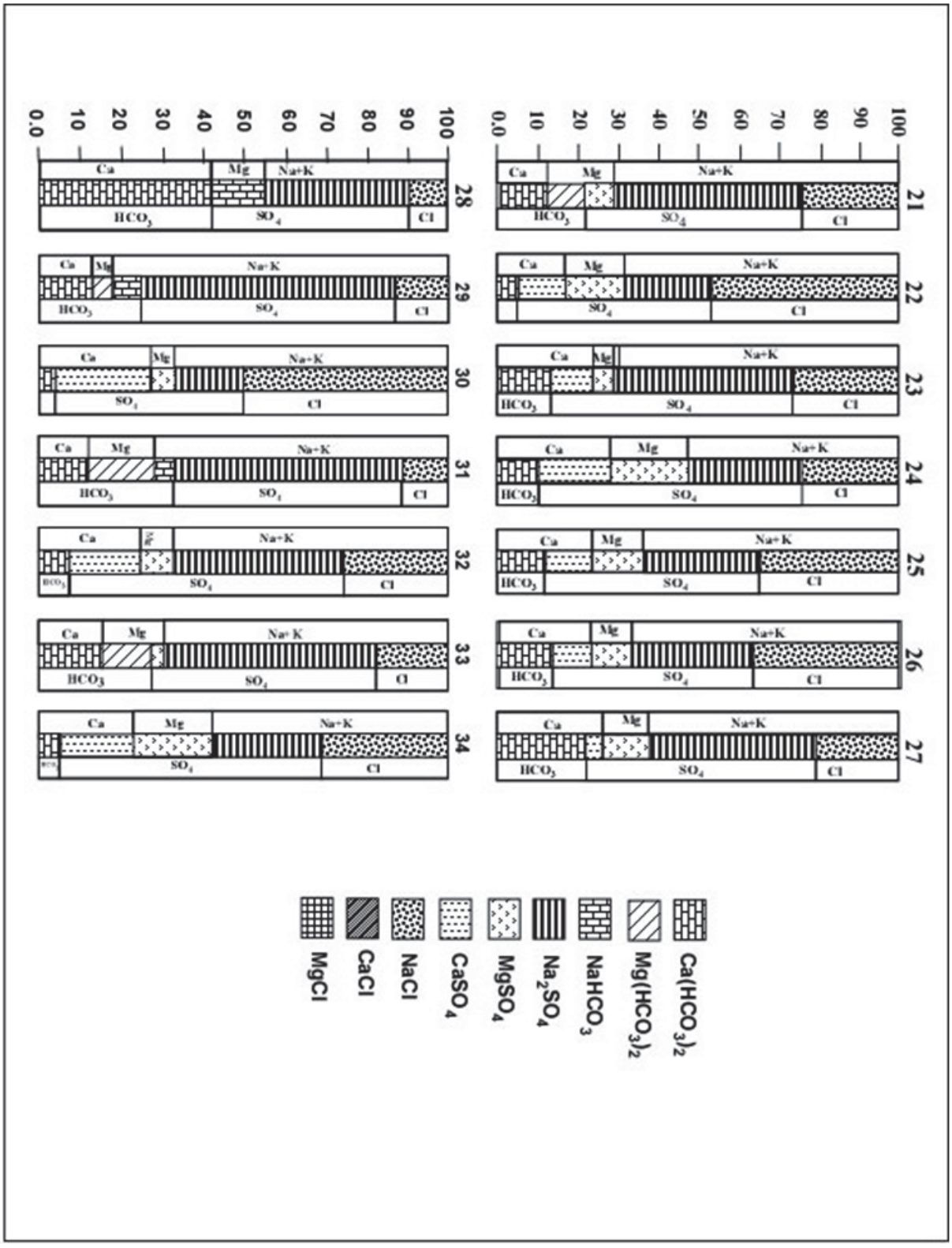

Fig. (4.16): Bar-graph method of the study water samples

Table (4.9): Salt combination of the study water samples

Salt combination	Surface water	Groundwater
$Ca(HCO_3)_2$, $Mg(HCO_3)_2$, $Na(HCO_3)_2$, Na_2SO_4, and NaCl	67%	26%
$Ca(HCO_3)_2$, $Mg(HCO_3)_2$, $MgSO_4$, Na_2SO_4, and NaCl	33%	15%
Ca(HCO3)2, CaSO4, MgSO4, Na2SO4, and NaCl	--	53%
$Ca(HCO_3)_2$, $MgSO_4$, Na_2SO_4, and NaCl	--	6%

4.2.2.3. Hydrochemical classification:

(I)-Application of Piper trilinear diagram

One of the most useful graphs for representing and comparing water types is the trilinear diagram introduced by Piper (1944). In these graphs the cations are expressed as a percentage of total cations in milli-equivalent per liter and plotted as a single point on the left triangle, while anions are expressed as a percentage of the total anions and appear as a point in the right triangle. These two points are then projected into the central diamond-shaped area. The trilinear diagram shows the similarities and differences between the groundwater samples, since the samples with similar qualities will tend to plot together as groups. The central diamond-shaped area can be divided into four sectors. Sector (1) represents primary alkalinity characters where the characteristic salt is calcium bicarbonate (meteoric origin). Sectors (2, 3) illustrate mixing water types (meteoric and marine water). Sector (4) reflects marine origin and secondary salinity properties, where sodium chloride salts are predominate.

By representing the water samples from the study area in the Piper diagram (Fig. 4.17), we can see that most of them are in sector 1 which reflects meteoric origin. This indicates that the main source of recharge comes from the surface water by way of the irrigation canals.

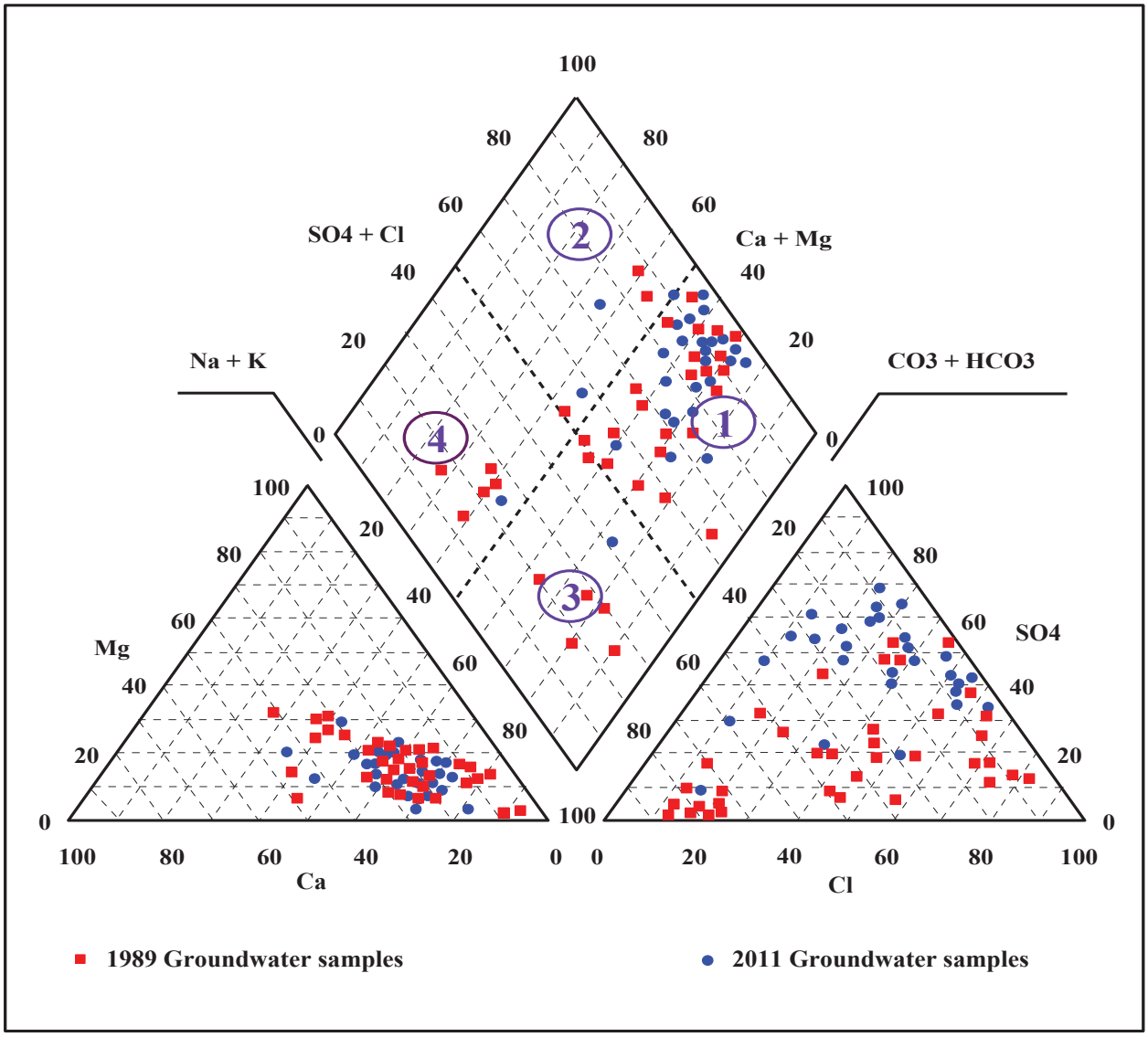

Fig. (4.17): Piper diagram of the studied water samples

(II)-Application of the Grid system method

Atwa (1979) introduced a method for water classification that's based on the reacting values of the three major anions and the three major cations expressed as epm percent. Figure (4.18) shows the grid system. The figure is divided into nine equally sized main grids. A further subdivision is possible based on cations or anions, which are presenting small amounts. The results of the investigated water samples are plotted in the grids, where each point represents a sample. The pattern of distribution immediately gives an idea about the major and minor classes of waters encountered. The water samples of the study are mainly the sodium sulfate and sodium chloride types.

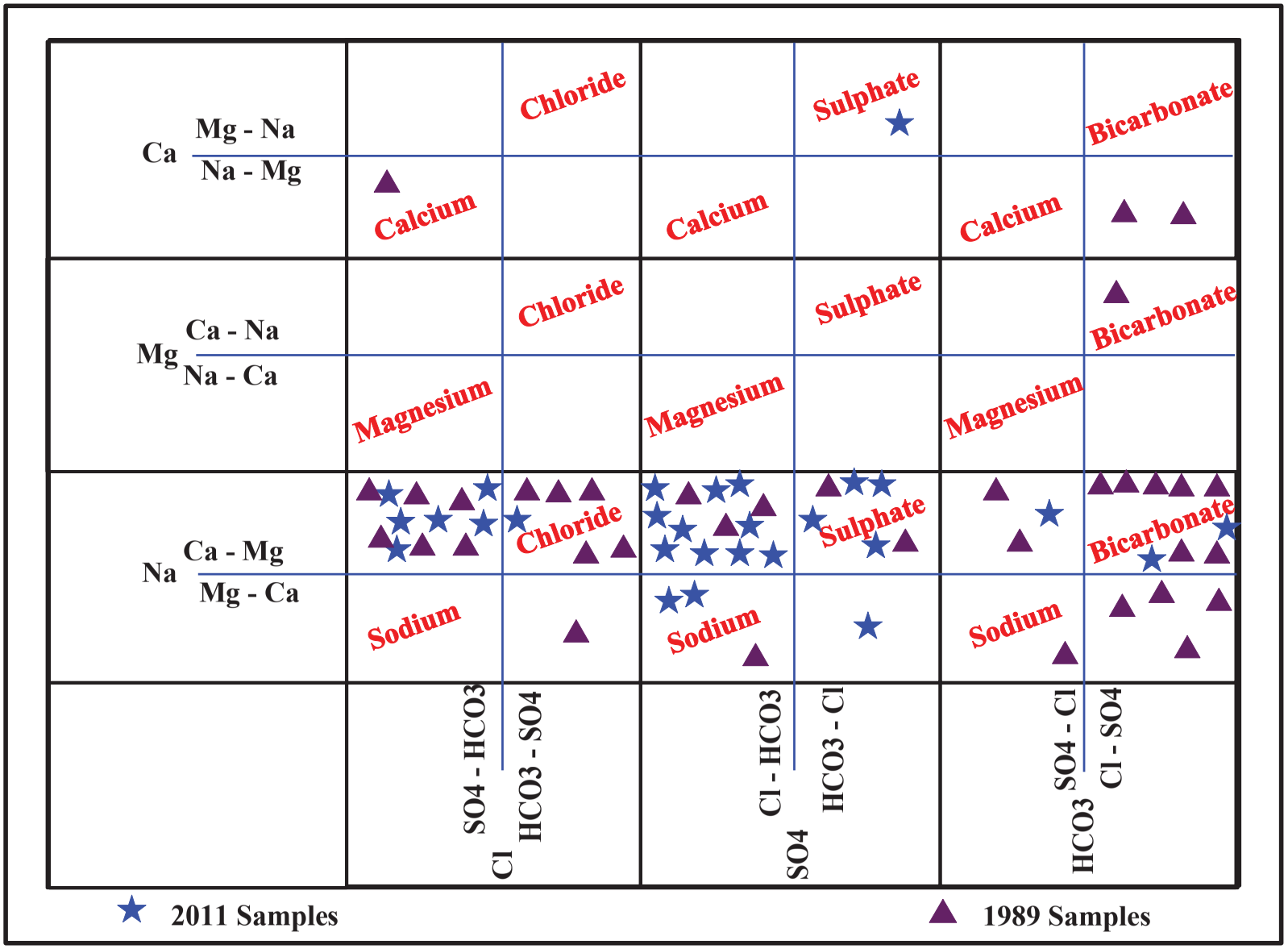

Fig. (4.18): Grid system classifacation of the studied water samples

4.2.2.4. Groundwater quality and availability for use

Quality of groundwater is defined as the physical, chemical, and biological properties of the water. The physical properties include temperature, color, turbidity, and taste. Naturally, groundwater contains ions leached from minerals in the soils, rocks and sediments as the water migrates. These ions includes both the major ions (Na^{+}, Ca^{2+}, Mg^{2+}, HCO^{3-}, Cl^{-}, SO_4^{2-}) and the minor ions (NO^{3-}, NO^{2-}, F^{-},CO^{3-}, K^{+}, Mn^{2+}, and Fe^{2+}). The concentration of these ions characterizes the groundwater and often reflects the geological origin and groundwater flow regime.

Many factors affect water quality. Understanding these factors is necessary in deciding the well depth and the best water quality for particular uses. Climate variations (rainfall, evaporation, etc.), the permeability and chemical composition of the sediments saturated by groundwater, and the depth of the groundwater from the surface are the major factors that directly or indirectly affect the groundwater quality.

(I)-Evaluation of groundwater quality for drinking;

Generally, drinking water has to be free from colour, specific taste, turbidity, and excessive amounts of dissolved salts. By examining the groundwater samples from the study area in the context of international standards for human drinking water and the Egyptian Committee for Water (2007) (Table 4.10), it is clear that the majority of the surface water is suitable for drinking water, while the majority of the groundwater samples (71%) are unsuitable due to their high salinity (1200ppm to 4453ppm) and major ions more than the permissible limits. The remaining samples (29%) are suitable for drinking due to their low levels of salinity (>1200) and also the major ions within the permissible limits.

Table (4.10): Water quality guidelines for human drinking and domestic uses (Egyptian Higher Committee for water, 2007)

Chemical constituent or parameter	European[1] Standards mg/l	International[2] Standards Mg/l	Egyptian maximum[3] permissible limit in mg/l	World[4] Health Organization guidelines mg/l
Aluminum	0.05 to 0.2	--	0.2	0.2
Arsenic	< 0.05	< 0.05	0.0	--
Barium	<1.00	<1.00	1.0	--
Boron	1.00	--	--	--
Cadmium	< 0.01	< 0.01	0.005	--
Calcium	75 - 200	75 - 200	200	--
Chloride	--	--	500	250
Copper	< 0.05	0.05 -1.5	1.00	1.00
Cyanides	<0.05	< 0.05	0.05	--
Fluoride	--	1.4 - 2.4	0.8	--
Hardness as $CaCO_3$	2 10 meq / l	2 – 100 meq/l	500 meq/l	--
Iron (total)	<0.1	0.10 – 1.0	0.3 – 1.0	0.3
Lead	<0.1	<0.1	0.05	--
Magnesium **If SO4> 250 mg/l** **If SO4< 250 mg/l**	 <30 <125	 <30 <125	150	--
Manganese	<0.05	0.10 – 0.5	0.05	0.1
Mercury total	<0.01	<0.01	0.001	--
Nitrate as N Recommended Acceptable Not recommended	<50 for babies Less than three months 50 -100 for older children and adults >100	----	10	--
TDS	--	500 - 1500	1200	1000
PH	7 – 8.5	--	--	6.5 – 9.2
Sodium	--	200	--	200
Sulfates	<250	250	250 - 400	400
Zinc	<5	3	5.00 - 15	5.0

1- World Health Organization, 1971

2- World Health Organization, 1972

3- Egyptian standards for drinking and domestic uses (Higher Committee for Water, 1995)

4- Guidelines for drinking water quality, 1996, World Health Organization.

(II)- Evaluation of groundwater quality for irrigation purposes:

Water quality, soil types, and cropping practices play important roles in a suitable irrigation practice. Excessive amounts of dissolved ions in irrigation water affect plants and agricultural soil physically and chemically, thus reducing the productivity. The physical effect of these ions lowers the osmotic pressure in the plant structure cells, hindering the water from reaching the branches and leaves. The chemical effects disrupt plant metabolism. The important chemical constituents affecting the suitability of the irrigation water are:

-*Salinity index or total dissolved salts as computed by measured EC values.* High concentrations of salinity (electrical conductivity) in irrigation water affect crop yield through the inability of the plant to complete with ions in the soil solution for water. Based on Bauder et al. (2007), the studied water samples have been classified (Table 4.11). From this classification, we found half of the surface water samples are categorized under excellent quality, and the other half under permissible quality. While about half of the groundwater samples are categorized under unsuitable, the other half ranged between good qualities to doubtful for use in irrigation.

Table (4.11): Classification of water samples based on E.C

EC (µS/cm)	Water salinity range	Surface water	Groundwater
< 250	excellent quality	50%	--
251–750	good quality	---	3%
75 –2000	permissible quality	50%	32%
2001–3000	Doubtful	--	11%
>3000	Unsuitable	--	54%

-SAR or sodicity index: Another important factor for water quality is the sodium concentration, which expresses reactions with the soil and a reduction in its permeability. A high sodium-content in water is generally unsuitable for irrigation, as higher sodium concentrations may deteriorate the soil characteristics. Therefore, SAR is considered a better measure of sodium (alkali) risks in irrigation, as SAR of water is directly related to the absorption of sodium by the soil. It is a valuable criterion for determining the suitability of the water for irrigation. Excessive sodium content relative to calcium and magnesium reduces the soil's permeability and thus inhibits the supply of water needed for the crops. The classification of water samples of the study area based upon SAR values according to Bauder

et.al. (2007) show that the surface and groundwater of the study area lie below excellent water values.

-According to the U.S. Laboratory Staff's diagram (Richards 1954); Figure 4.19 shows that most of the surface water samples are suitable for irrigation purposes in addition to 54% of the groundwater. 46% appear to be unsuitable for irrigation purposes under normal conditions due to their high salinity.

-Percent sodium: Methods of Wilcox (1995) and Richards (1954) have been used to classify and understand the basic character of the chemical composition of groundwater, since the suitability of the groundwater for irrigation depends on the mineralization of water and its effect on plants and soil. Percent sodium can be determined using the following formula:

$$\text{Na \%} = \frac{(\text{Na+K})*100}{(\text{Ca+Mg+Na+K})} \quad \text{(epm)}$$

When the concentration of sodium is high in irrigation water, sodium ions tend to be absorbed by clay particles, displacing Mg^{2+} and Ca^{2+} ions. This exchange process of Na^{+} in water for Ca^{2+} and Mg^{2+} in soil reduces the permeability and eventually causes poor internal drainage in the soil. Air and water circulation is restricted during wet conditions, and such soils usually become hard when dry (Saleh et al. 1999). According to Eaton's (1950) classification table (4.12), we found that most of the surface water and 39% of groundwater is safe while 61% of the groundwater samples are unsafe.

Table (4.12): Sodium percent and water class (Eaton 1950)

Sodium %	Water class	Surface water	Groundwater
>60	Unsafe	17%	61%
<60	Safe	83%	39%

Wilcox (1948) classified groundwater for irrigation purposes by correlating the percent sodium (i.e., sodium in irrigation waters) and the electrical conductivity. Looking to Wilcox's (1995) diagram (Fig. 4.20), the groundwater collected from west Tahta shows the following percentages, 54% unsuitable, 14% doubtful to unsuitable, 21% permissible to doubtful, 7% good to permissible, and 4% excellent to good.

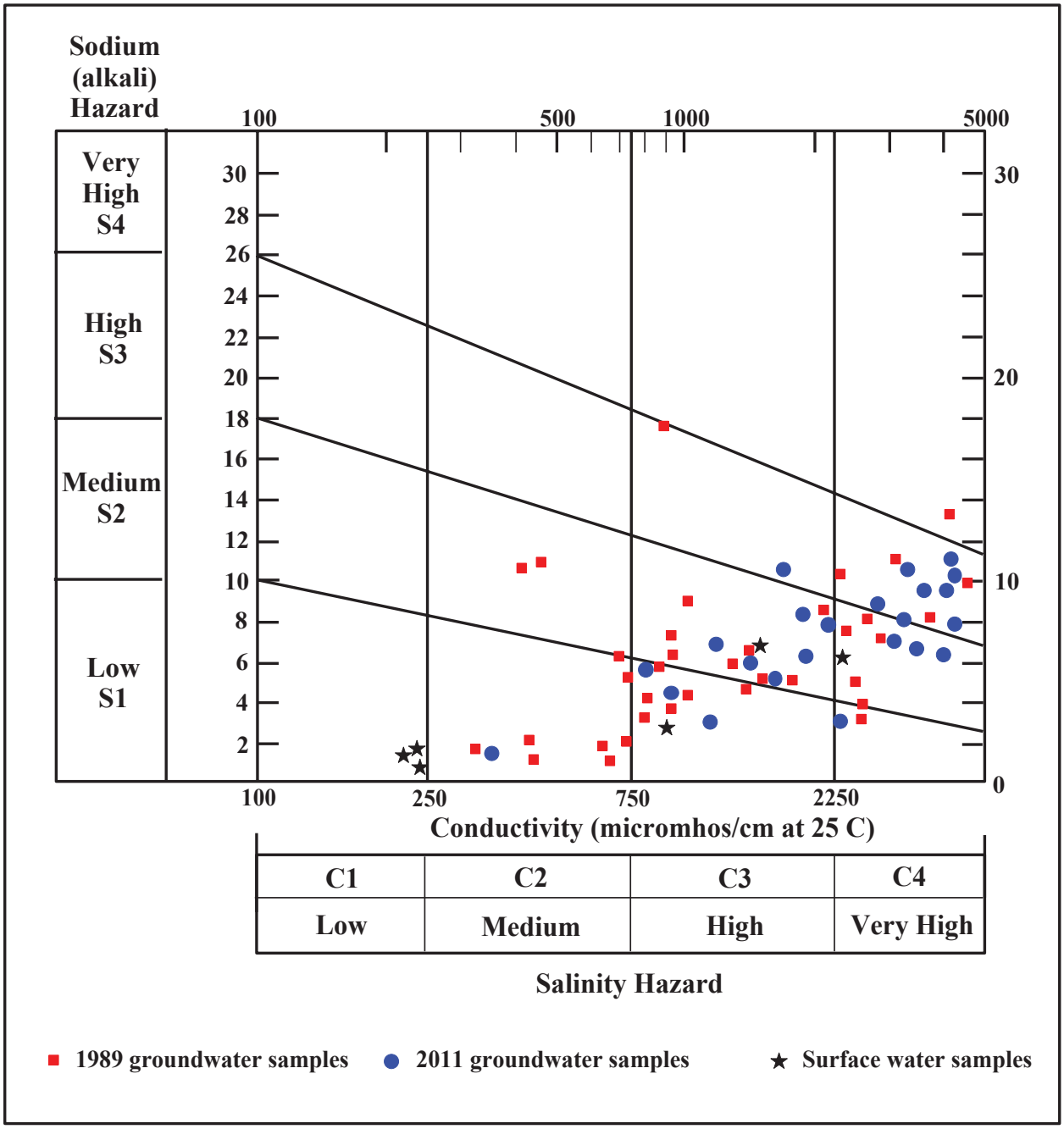

Fig. (4.19): Wilcox diagram for the studied water samples

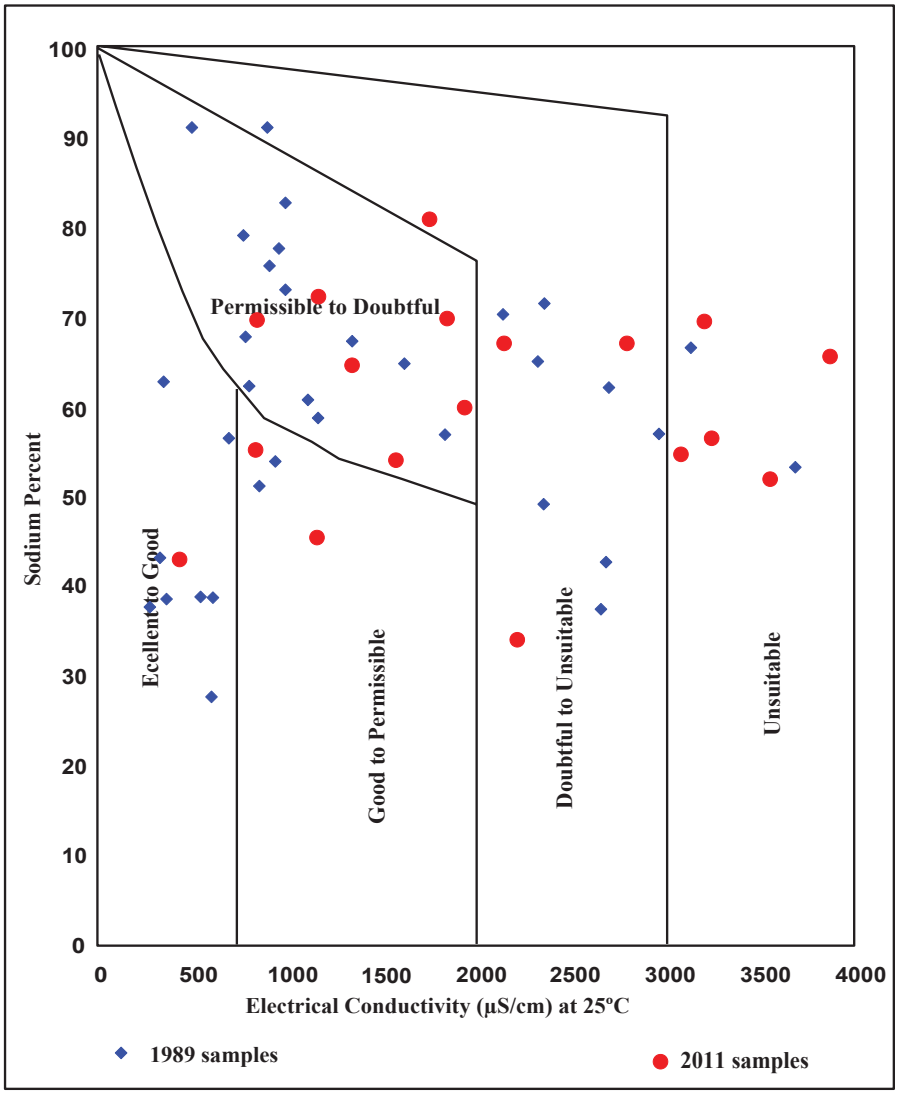

Fig. (4.20):Groundwater classification for irrigation purposes

-Residual sodium carbonate; in addition to the SAR and Na %: The excess amount of carbonate and bicarbonate in groundwater, in addition to the amount of calcium and magnesium, influences the suitability of groundwater for irrigation. Water having a high concentration of bicarbonate shows a tendency for precipitation of calcium and magnesium as the water in the soil becomes more concentrated. An excess quantity of sodium bicarbonate and carbonate is considered detrimental to the physical properties of soils, as it causes dissolution of organic matter in the soil, which in turn leaves a black stain on the soil surface when it dries. As a result, the relative proportion of sodium in the water is increased in the form of sodium carbonate, and this excess, denoted by RSC, is calculated as follows (Eaton 1950; Ragunath 1987):

$$RSC = (CO_3 + HCO_3) - (Ca + Mg)\ (epm)$$

By classifying the water samples from the study area in accordance with the RSC table (4.13), we concluded that most of the water samples are suitable for irrigation.

Table (4.13): Groundwater quality based on RSC (Richards, 1954)

RSC (epm)	Remark on quality
<1.25	Good
1.25–2.5	Doubtful
>2.5	Unsuitable

4.2.2.5. Mechanisms controlling groundwater chemistry

Lastly, to know the groundwater chemistry and the relationship of the chemical components of the water to their respective aquifers, such as the chemistry of the rock types, the chemistry of precipitated water, and the rate of evaporation, Gibbs (1970) has suggested a diagram in which the ratio of dominant anions and cations are plotted against the value of TDS. The chemical data of the groundwater samples are plotted in the Gibbs diagram (Fig. 4.21). The majority of the groundwater samples collected from the study area suggest that the chemical weathering of rock-forming minerals are influencing the groundwater quality through the dissolution of the host rock.

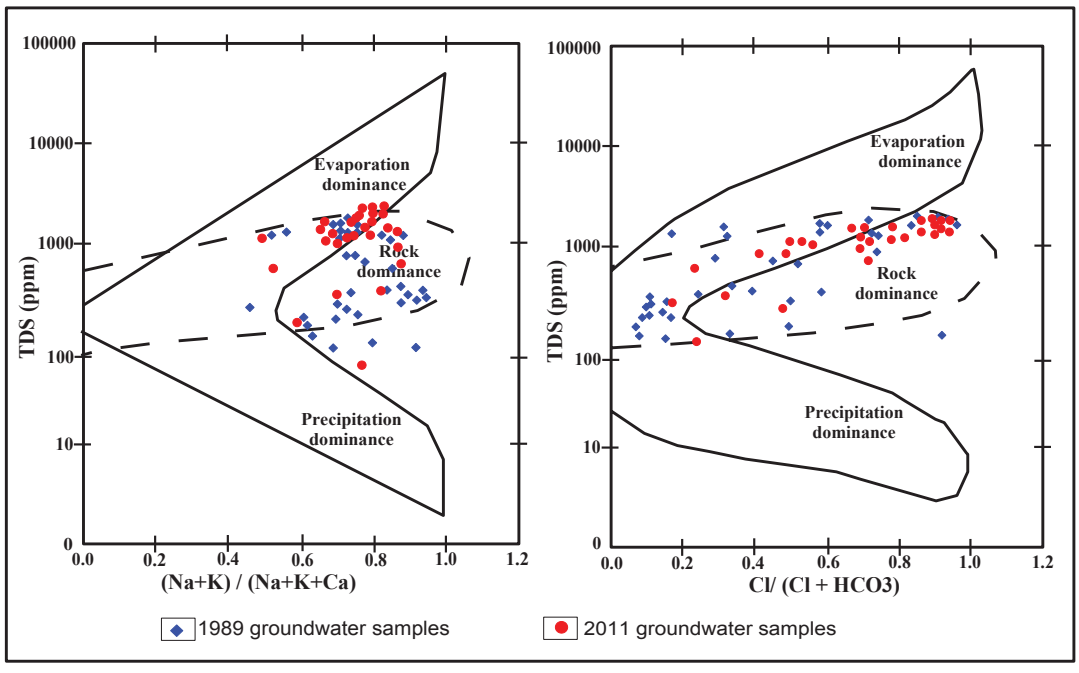

Fig. (4.21): Gibbs diagram of the studied water samples

4.3. Comparison between 1989 and 2011 groundwater samples

In this part we compare the hydrogeology and hydrochemical data from west Tahta area collected in 1989 and in 2011 (Fig. 4.1). This comparison depends on 36 groundwater samples collected by RIGW in 1989 (Tables 4.14 to 4.16) and 28 groundwater samples collected in 2011 (Tables 4.3 and 4.4). This comparison is useful for showing the changes in the groundwater during these 22 years, as well as the change in the water table, water level, TDS, total hardness, water type, ion dominance, and the quality of the groundwater for different purposes.

4.3.1. Water table and water level

The main direction of the groundwater flow in the study area is northeast, toward the River Nile (Fig.4.3 and 4.22). This direction did not change from 1989 to 2011 due to the influence of canals recharge. Figures 4.4 and 4.23 prove the change in the depth to the groundwater was affected by extensive use and the increase toward the west. In 1989 the depth to the groundwater ranged from 1m to 45m while in 2011it ranged from 9m to 56m.

Table (4.14) : Chemical analysis data and hydrochemical parameters of the surface water and groundwater samples collected in 1989

S.No.	W.No.	pH	E.C	TDS	Units	Cations				Total Cations	Anions			Total Anions	TH	SAR	Hydrochemical Coefficients(epm)			Ion Dominance	water type
						Ca^{++}	Mg^{++}	Na^{+}	K^{+}		HCO_3^-	Cl^-	SO_4^{--}				r(Na+K)/rCl	rCa/rMg	rSO4/rCl		
1	IRR1	7.40	300	192	ppm	23.8	11.76	21.85	27.69	3.83	194.59	16.685	9.6	3.86	107.821	1	3.53	1.21	0.43	Na > Ca > Mg HCO_3 > Cl > SO_4	$NaHCO_3$
					epm	1.19	0.98	0.95	0.71		3.19	0.47	0.20								
					epm%	31.07	25.59	24.80	18.54		82.64	12.18	5.18								
2	IRR2	7.60	680	435	ppm	45.8	26.64	50.83	6.63	6.89	304.39	50.055	19.68	6.81	223.986	1	1.69	1.03	0.29	Na > Ca > Mg HCO_3 > Cl > SO_4	$NaHCO_3$
					epm	2.29	2.22	2.21	0.17		4.99	1.41	0.41								
					epm%	33.24	32.22	32.08	2.47		73.27	20.70	6.02								
3	Nile	7.40	340	218	ppm	30.4	23.76	26.68	12.09	4.97	189.1	35.5	41.76	4.97	173.681	1	1.47	0.77	0.87	Mg > Ca> Na HCO_3 > Cl > SO_4	$Mg(HCO_3)_2$
					epm	1.52	1.98	1.16	0.31		3.10	1.00	0.87								
					epm%	30.58	39.84	23.34	6.24		62.37	20.12	17.51								
4	1	7.50	2470	1581	ppm	128.6	59.16	276	22.62	23.94	213.5	304.24	573.6	24.02	564.558	5	1.47	1.30	1.39	Na >Ca >Mg SO4 >Cl >HCO_3	Na_2SO_4
					epm	6.43	4.93	12.00	0.58		3.50	8.57	11.95								
					epm%	26.86	20.59	50.13	2.42		14.57	35.68	49.75								
5	2	9.00	707	452	ppm	7.8	9.84	109.94	3.9	6.09	304.39	33.725	7.68	6.10	59.9682	6	5.14	0.48	0.17	Na >Mg >Ca HCO_3>Cl >SO_4	$NaHCO_3$
					epm	0.39	0.82	4.78	0.1		4.99	0.95	0.16								
					epm%	6.40	13.46	78.49	1.64		81.80	15.57	2.62								
6	4	7.70	1380	883	ppm	64.8	14.76	220.8	4.68	14.19	274.5	116.09	296.64	13.95	222.543	6	2.97	2.63	1.89	Na > Ca > Mg SO_4 >HCO_3 >Cl	Na_2SO_4
					epm	3.24	1.23	9.6	0.12		4.5	3.27	6.18								
					epm%	22.83	8.67	67.65	0.85		32.26	23.44	44.30								
7	5	7.80	2360	1510	ppm	60	60	349.6	3.9	23.30	231.8	284	552.96	23.32	396.72	8	1.91	0.60	1.44	Na > Mg > Ca SO_4>Cl >HCO_3	Na_2SO_4
					epm	3.00	5.00	15.20	0.10		3.80	8.00	11.52								
					epm%	12.88	21.46	65.24	0.43		16.30	34.31	49.40								
8	6	8.20	2300	1472	ppm	110.6	24.6	455.17	7.8	27.57	237.9	337.25	687.36	27.72	377.397	10	2.10	2.70	1.51	Na > Ca > Mg SO_4 > Cl > HCO_3	Na_2SO_4
					epm	5.53	2.05	19.79	0.20		3.90	9.50	14.32								
					epm%	20.06	7.44	71.78	0.73		14.07	34.27	51.66								
9	8	7.50	2900	1856	ppm	140.6	55.2	396.29	7.8	29.06	152.5	810.11	181.92	29.11	578.226	7	0.76	1.53	0.17	Na > Ca >Mg Cl >SO_4 >HCO_3	NaCl
					epm	7.03	4.60	17.23	0.20		2.50	22.82	3.79								
					epm%	24.19	15.83	59.29	0.69		8.59	78.39	13.02								
10	10	7.30	2640	1690	ppm	140.6	26.64	396.29	3.9	26.58	225.7	648.59	222.72	26.61	460.702	8	0.95	3.17	0.25	Na > Ca> Mg Cl >SO_4 > HCO_3	NaCl
					epm	7.03	2.22	17.23	0.10		3.70	18.27	4.64								
					epm%	26.45	8.35	64.82	0.38		13.90	68.66	17.44								
11	11	7.10	800	512	ppm	54.8	13.8	106.03	11.7	8.80	274.5	50.055	138.72	8.80	193.623	3	3.48	2.38	2.05	Na > Ca> Mg HCO_3 >SO_4 > Cl	$NaHCO_3$
					epm	2.74	1.15	4.61	0.30		4.50	1.41	2.89								
					epm%	31.14	13.07	52.39	3.41		51.14	16.02	32.84								
12	12	8.60	880	563	ppm	16.6	3.24	300.15	21.84	14.71	303.17	273.35	46.08	13.63	54.7828	18	1.77	3.07	0.12	Na >Ca >Mg Cl > HCO_3 > SO_4	NaCl
					epm	0.83	0.27	13.05	0.56		4.97	7.70	0.96								
					epm%	5.64	1.84	88.72	3.81		36.46	56.49	7.04								
13	15	7.90	870	557	ppm	15.8	9.84	120.06	4.68	6.95	304.39	50.055	24.96	6.92	79.9442	6	3.79	0.96	0.37	Na >Mg >Ca HCO_3 >Cl >SO_4	$NaHCO_3$
					epm	0.79	0.82	5.22	0.12		4.99	1.41	0.52								
					epm%	11.37	11.80	75.11	1.73		72.11	20.38	7.51								

[Geben Sie Text ein]

Table (4.15) : Continued

S.No.	W.No.	pH	E.C	TDS	Units	Cations				Total Cations	Anions			Total Anions	TH	SAR	Hydrochemical Coefficients(epm)			Ion Dominance	water type
						Ca^{++}	Mg^{++}	Na^{+}	K^{+}		HCO_3^-	Cl^-	SO_4^{--}				r(Na+K)/rCl	rCa/rMg	rSO4/rCl		
14	17	7.40	1950	1248	ppm	150	70	148	15	20.15	626	275	105	20.20	662.6	2	0.88	1.29	0.28	Ca> Na> Mg HCO_3 > Cl >SO_4	$Ca(HCO_3)_2$
					epm	7.50	5.83	6.43	0.38		10.26	7.75	2.19								
					epm%	37.22	28.95	31.93	1.91		50.81	38.36	10.83								
15	19	7.60	718	460	ppm	74.8	14.76	69.92	4.68	8.13	383.69	33.725	39.84	8.07	247.513	2	3.33	3.04	0.87	Ca> Na> Mg HCO_3 > Cl >SO_4	$Ca(HCO_3)_2$
					epm	3.74	1.23	3.04	0.12		6.29	0.95	0.83								
					epm%	46.00	15.13	37.39	1.48		77.94	11.77	10.29								
16	22	8.30	1300	832	ppm	62.8	28.56	232.07	69.81	17.40	353.8	287.2	162.72	17.28	274.336	6	1.47	1.32	0.42	Na > Ca >Mg CL >HCO_3 > SO_4	NaCl
					epm	3.14	2.38	10.09	1.79		5.80	8.09	3.39								
					epm%	18.05	13.68	57.99	10.29		33.56	46.82	19.62								
17	23	7.60	639	409	ppm	45.8	28.56	64.86	2.73	7.56	396.5	33.725	7.68	7.61	231.887	2	3.04	0.96	0.17	Na >Mg > Ca HCO $_3$>CL > SO_4	$NaHCO_3$
					epm	2.29	2.38	2.82	0.07		6.50	0.95	0.16								
					epm%	30.29	31.48	37.30	0.93		85.41	12.48	2.10								
18	25	7.60	1000	640	ppm	15.8	12.72	198.03	5.85	10.61	457.5	50.055	83.52	10.65	91.7954	9	6.21	0.75	1.23	Na >Mg > Ca HCO_3 >SO_4 > CL	$NaHCO_3$
					epm	0.79	1.06	8.61	0.15		7.50	1.41	1.74								
					epm%	7.45	9.99	81.15	1.41		70.42	13.24	16.34								
19	33	6.90	1500	960	ppm	59.8	14.76	172.96	44.85	12.89	109.8	337.25	74.88	12.86	210.058	5	0.91	2.43	0.16	Na > Ca> Mg Cl > HCO_3 > SO_4	NaCl
					epm	2.99	1.23	7.52	1.15		1.80	9.50	1.56								
					epm%	23.20	9.54	58.34	8.92		14.00	73.87	12.13								
20	46	8.70	410	262	ppm	13.4	0.12	142.6	10.92	7.16	362.95	65.675	10.08	8.01	33.9536	11	3.50	67.00	0.11	Na > Ca >Mg HCO_3> Cl > SO_4	$NaHCO_3$
					epm	0.67	0.01	6.20	0.28		5.95	1.85	0.21								
					epm%	9.36	0.14	86.59	3.91		74.28	23.10	2.62								
21	50	8.00	320	205	ppm	33	17.64	45.77	19.5	5.61	165.92	83.425	25.92	5.61	154.99	2	1.06	1.12	0.23	Na> Ca> Mg HCO_3 > Cl > SO_4	$NaHCO_3$
					epm	1.65	1.47	1.99	0.50		2.72	2.35	0.54								
					epm%	29.41	26.20	35.47	8.91		48.48	41.89	9.63								
22	58	7.50	660	422	ppm	66.6	33.24	43.24	11.7	8.28	420.9	35.5	18.24	8.28	303.083	1	2.18	1.20	0.38	Mg >Ca > Na HCO_3> Cl > SO_4	$Mg(HCO_3)_2$
					epm	3.33	2.77	1.88	0.30		6.90	1.00	0.38								
					epm%	40.22	33.45	22.71	3.62		83.33	12.08	4.59								
23	65	7.30	2600	1664	ppm	88	44.4	174.8	5.85	15.85	347.7	280.45	120	16.10	402.442	4	0.98	1.19	0.32	Na> Ca> Mg Cl > HCO_3 > SO_4	NaCl
					epm	4.40	3.70	7.60	0.15		5.70	7.90	2.50								
					epm%	27.76	23.34	47.95	0.95		35.40	49.07	15.53								
24	70	7.20	3700	2368	ppm	273.4	153.96	681.49	5.85	56.28	159.82	1261.7	868.8	56.26	1316.23	8	0.84	1.07	0.51	Na > Ca >Mg Cl >SO_4 >HCO_3	NaCl
					epm	13.67	12.83	29.63	0.15		2.62	35.54	18.10								
					epm%	24.29	22.80	52.65	0.27		4.66	63.17	32.17								
25	71	8.00	4100	2624	ppm	305.2	63.12	966	7.8	62.72	57.95	977.32	1596	61.73	1021.82	13	1.53	2.90	1.21	Na > Ca > Mg SO_4 > Cl >HCO_3	Na_2SO_4
					epm	15.26	5.26	42.00	0.20		0.95	27.53	33.25								
					epm%	24.33	8.39	66.96	0.32		1.54	44.60	53.86								
26	72	7.60	3100	1984	ppm	178.6	44.4	630.43	4.68	40.16	203.74	936.14	502.56	40.18	628.67	11	1.04	2.41	0.40	Na >Ca > Mg Cl > SO_4 > HCO_3	NaCl
					epm	8.93	3.70	27.41	0.12		3.34	26.37	10.47								
					epm%	22.24	9.21	68.25	0.30		8.31	65.63	26.06								

Table (4.16) : Continued

S.No.	W.No.	pH	E.C	TDS	Units	Cations				Total Cations	Anions			Total Anions	TH	SAR	Hydrochemical Coefficients(epm)			Ion Dominance	water type
						Ca^{++}	Mg^{++}	Na^{+}	K^{+}		HCO_3^{-}	Cl^{-}	SO_4^{--}				r(Na+K)/rCl	rCa/rMg	rSO4/rCl		
27	78	7.76	930	595	ppm	19.2	17.64	157.55	3.12	9.36	142.74	182.83	87.84	9.32	120.531	6	1.35	0.65	0.36	Na > Mg> Ca Cl >HCO_3 > SO_4	NaCl
					epm	0.96	1.47	6.85	0.08		2.34	5.15	1.83								
					epm%	10.26	15.71	73.18	0.85		25.11	55.26	19.64								
28	82	7.70	430	275	ppm	58	32.76	57.5	37.05	9.08	411.75	71	15.84	9.08	279.633	1	1.73	1.06	0.17	Na > Ca > Mg HCO_3> Cl >SO_4	$NaHCO_3$
					epm	2.90	2.73	2.50	0.95		6.75	2.00	0.33								
					epm%	31.94	30.07	27.53	10.46		74.34	22.03	3.63								
29	84	7.40	800	512	ppm	34.4	22.56	115	42.9	9.70	466.65	60.35	16.8	9.70	178.731	4	3.59	0.91	0.21	Na >Mg > Ca HCO_3> Cl > SO_4	$NaHCO_3$
					epm	1.72	1.88	5.00	1.10		7.65	1.70	0.35								
					epm%	17.73	19.38	51.55	11.34		78.87	17.53	3.61								
30	85	7.70	430	275	ppm	57.6	32.4	57.27	36.27	9.00	412.97	71.71	16.32	9.13	277.153	1	1.69	1.07	0.17	Na > Ca> Mg HCO_3> Cl >SO_4	$NaHCO_3$
					epm	2.88	2.70	2.49	0.93		6.77	2.02	0.34								
					epm%	32.00	30.00	27.67	10.33		74.15	22.12	3.72								
31	87	7.70	460	294	ppm	193.4	109.92	759	12.09	52.14	131.15	1050.8	978.72	52.14	935.241	11	1.13	1.06	0.69	Na > Ca> Mg Cl > SO_4 > HCO_3	NaCl
					epm	9.67	9.16	33.00	0.31		2.15	29.60	20.39								
					epm%	18.55	17.57	63.29	0.59		4.12	56.77	39.11								
32	88	7.70	1000	640	ppm	52.6	15.48	133.4	10.14	9.98	286.7	157.98	39.84	9.98	195.042	4	1.36	2.04	0.19	Na > Ca > Mg HCO_3 > Cl >SO_4	$NaHCO_3$
					epm	2.63	1.29	5.80	0.26		4.70	4.45	0.83								
					epm%	26.35	12.93	58.12	2.61		47.09	44.59	8.32								
33	89	8.00	928	594	ppm	68.6	32.04	147.2	9.75	12.75	387.96	106.5	174.72	13.00	303.139	4	2.22	1.28	1.21	Na > Ca > Mg HCO_3> SO_4 > Cl	$NaHCO_3$
					epm	3.43	2.67	6.40	0.25		6.36	3.00	3.64								
					epm%	26.90	20.94	50.20	1.96		48.92	23.08	28.00								
34	91	8.30	1400	896	ppm	65.4	36.36	184	35.1	15.20	294.02	237.85	176.64	15.20	312.925	5	1.33	1.08	0.55	Na > Ca > Mg SO_4 > HCO_3 > Cl	Na_2SO_4
					epm	3.27	3.03	8.00	0.90		4.82	6.70	3.68								
					epm%	21.51	19.93	52.63	5.92		31.71	44.08	24.21								
35	92	7.80	1800	1152	ppm	85.6	42.12	230	11.31	18.08	462.99	237.85	181.92	18.08	387.067	5	1.54	1.22	0.57	Na > Ca > Mg HCO_3 > Cl > SO_4	$NaHCO_3$
					epm	4.28	3.51	10.00	0.29		7.59	6.70	3.79								
					epm%	23.67	19.41	55.31	1.60		41.98	37.06	20.96								
36	93	8.20	2100	1344	ppm	78.8	28.56	340.4	11.7	21.42	579.5	266.25	212.16	21.42	314.288	8	2.01	1.66	0.59	Na> Ca> Mg HCO_3 > Cl > SO_4	$NaHCO_3$
					epm	3.94	2.38	14.80	0.30		9.50	7.50	4.42								
					epm%	18.39	11.11	69.09	1.40		44.35	35.01	20.63								
37	96	7.96	920	589	ppm	15.6	15.48	162.15	3.12	9.20	237.9	154.43	67.68	9.66	102.653	7	1.64	0.60	0.32	Na> Mg> Ca Cl > HCO_3 > SO_4	NaCl
					epm	0.78	1.29	7.05	0.08		3.90	4.35	1.41								
					epm%	8.48	14.02	76.63	0.87		40.37	45.03	14.60								
38	97	7.29	2600	1664	ppm	185.4	18.72	188.6	3.9	19.13	158.6	355	297.6	18.80	539.977	4	0.83	5.94	0.62	Ca > Na > Mg Cl > SO_4 > HCO_3	$CaCl_2$
					epm	9.27	1.56	8.20	0.10		2.60	10.00	6.20								
					epm%	48.46	8.15	42.86	0.52		13.83	53.19	32.98								
39	98	7.27	4500	2880	ppm	206.4	38.16	581.9	7.8	39.00	112.85	1105.8	249.6	38.20	672.409	10	0.82	3.25	0.17	Na > Ca > Mg Cl > SO_4 > HCO_3	NaCl
					epm	10.32	3.18	25.30	0.20		1.85	31.15	5.20								
					epm%	26.46	8.15	64.87	0.51		4.84	81.54	13.61								

[Geben Sie Text ein]

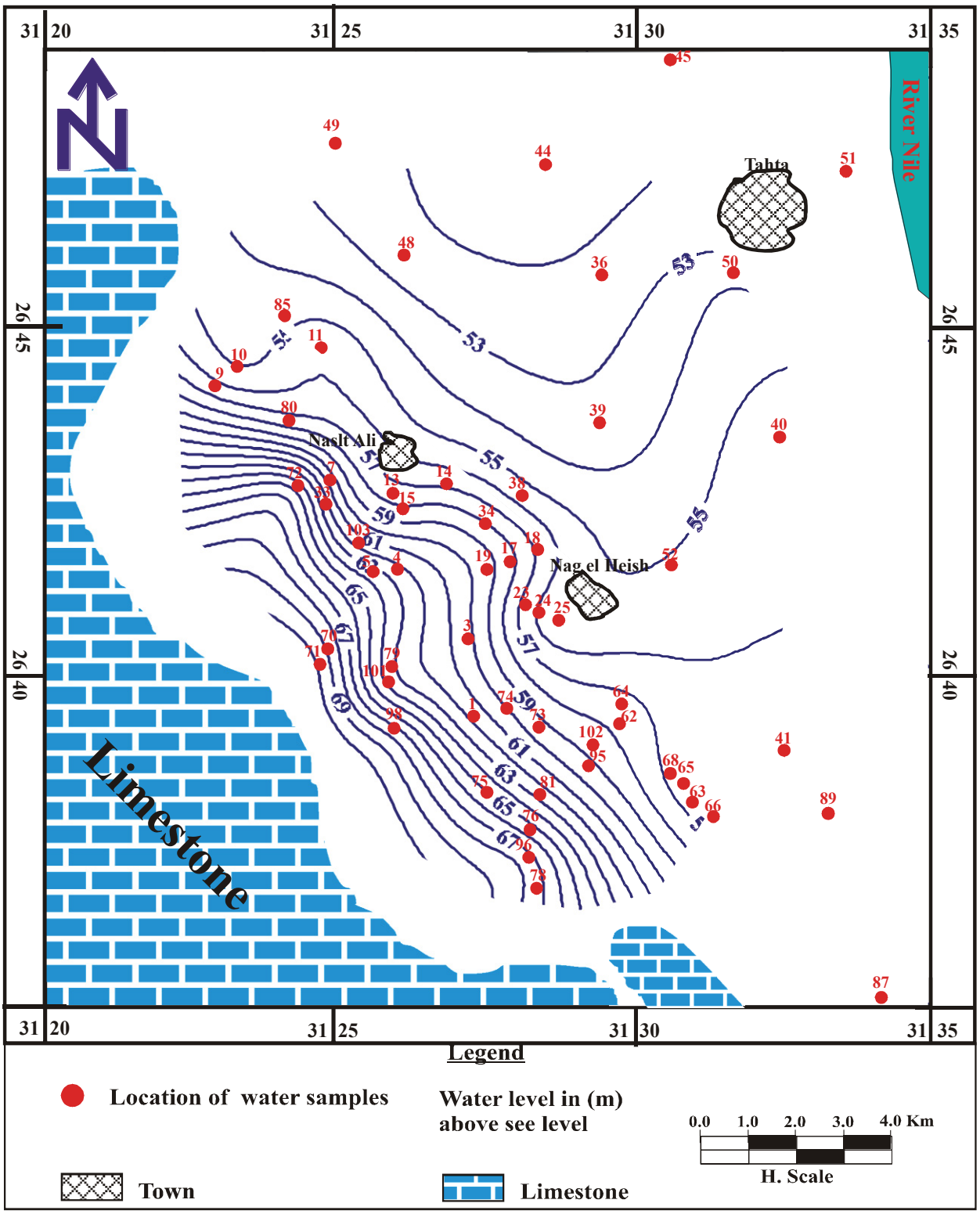

Fig. (4.22): Water level contour map 1989

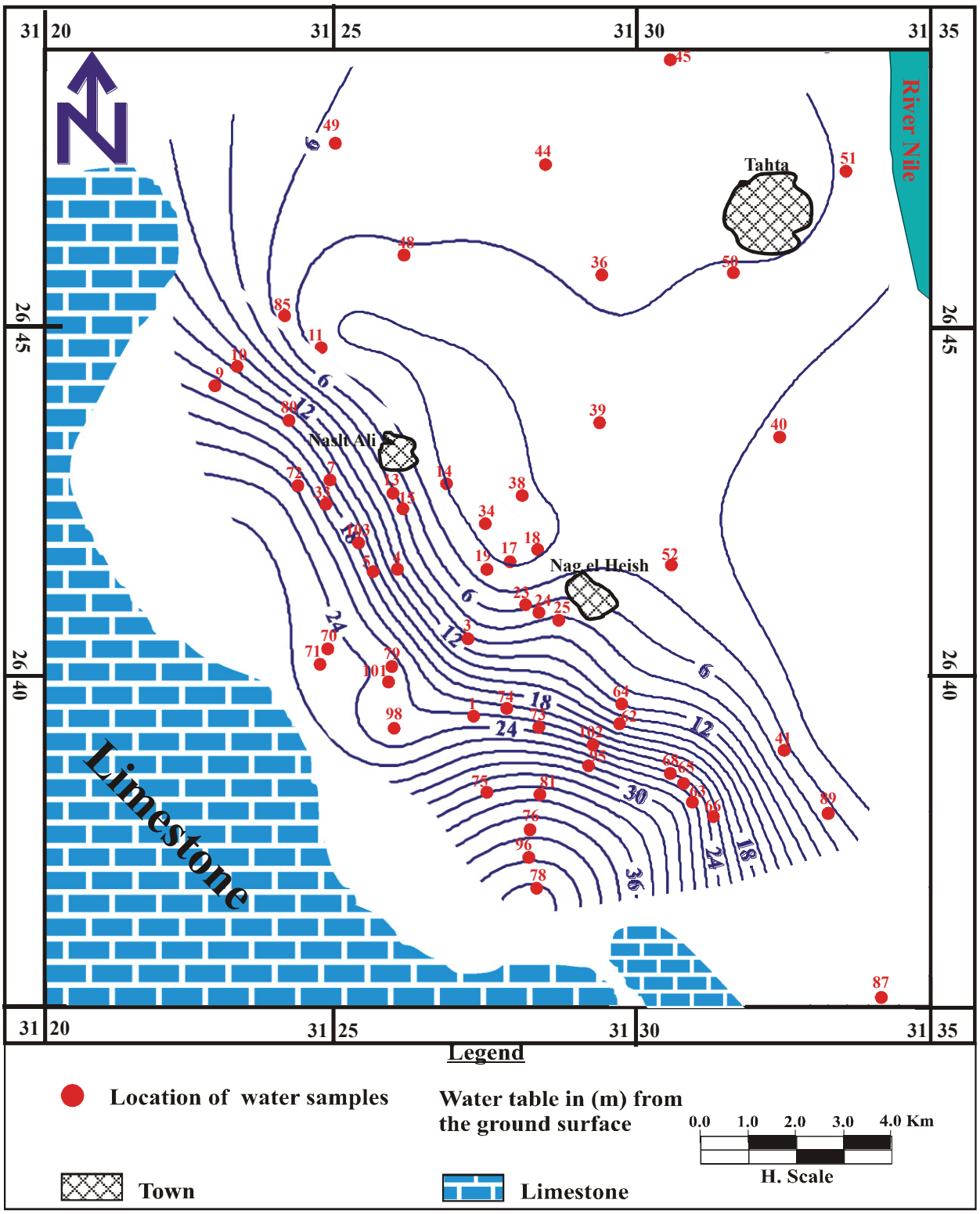

Fig. (4.23): Water table contour map 1989

4.3.2. Total dissolved solids (TDS)

According to Hem (1970), the salinity of the groundwater collected in 1989 varies between fresh and slightly saline water, ranging from 205 to 2880ppm, while the salinity of the samples collected in 2011 ranged between fresh and moderately saline. The increase of the salinity from 1989 to 2011 is attributed to leaching processes and dissolution of limestone affected by extensive water taking, as well as the effect of direct evaporation of the surface by the irrigation. The iso-salinity contour maps (Figures 4.7 and 4.24) show that the salinity increases from east to west, reflecting the impact of the leaching and dissolution of limestone bordering the study area in the west.

4.3.3. Total hardness (TH)

The classification of the groundwater collected in 1989 and 2011 based on hardness (Sawyer and McCarthy, 1967) has been analyzed and presented in the following table.

Table (4.17): Classification of groundwater based on hardness

TH as $CaCO_3$ (mg/L)	Water Classes	1989	2011
< 75	Soft	3 samples 8%	----
75 – 150	Moderately hard	4 samples 11%	3 samples 11%
150 – 300	Hard	11 samples 31%	4 samples 14%
> 300	Very hard	18 samples 50%	21 samples 75%

The dramatic increase in the total hardness in the samples collected in 2011 reflects the heavy influence of the limestone clearly seen in Figures 4.8 and 4.25.

4.3.4. Ion dominance and water type

The ion dominance and water types of the groundwater samples from 1989 and 2011 are plotted together in Tables 4.18 and 4.19. Concerning the ion dominance, sodium is dominant among the cations, while the dominant anions are greatly variable. $NaHCO_3$, NaCl, and Na_2SO_4 are

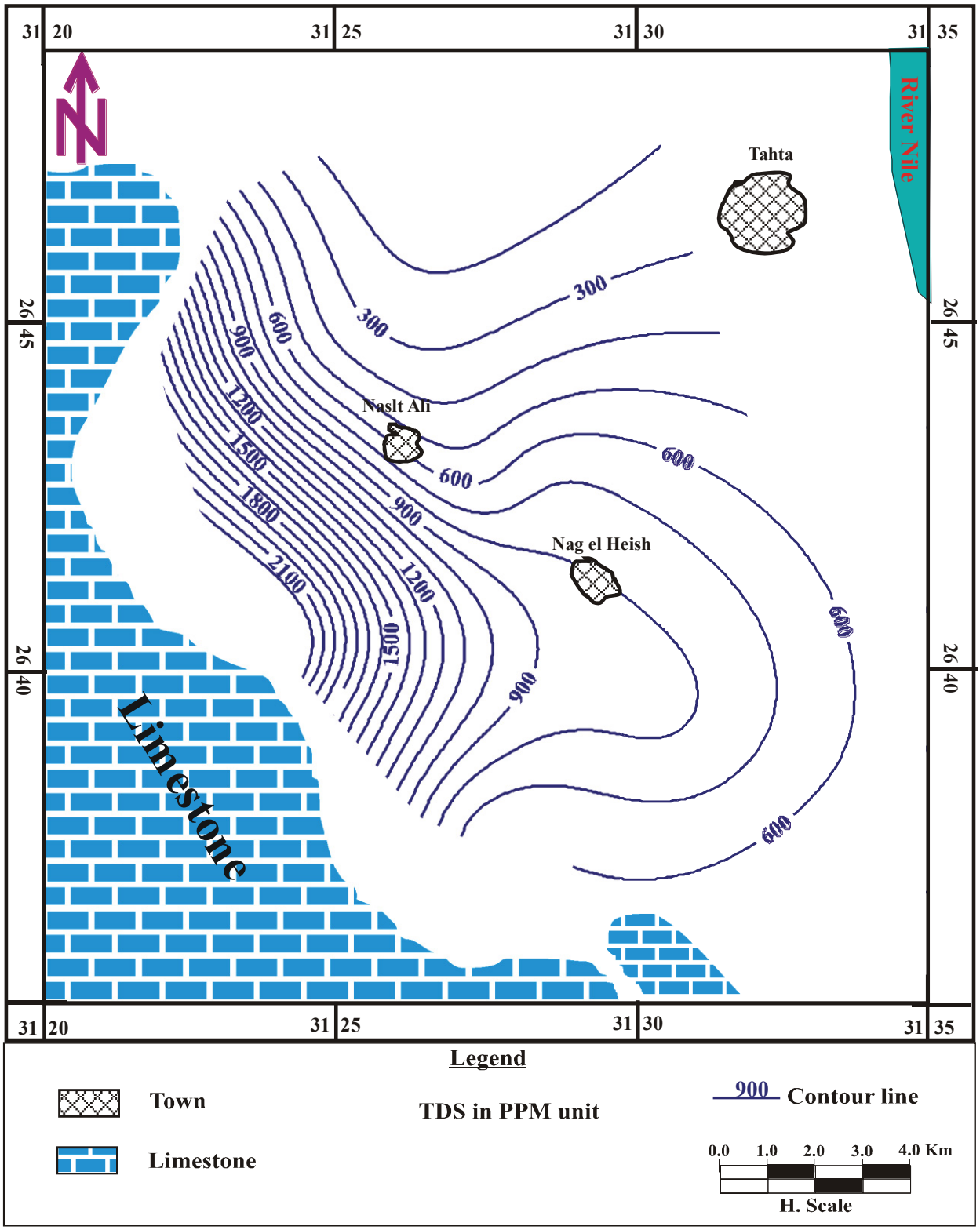

Fig. (4.24): Iso-salinity contour map 1989 (groundwater samples)

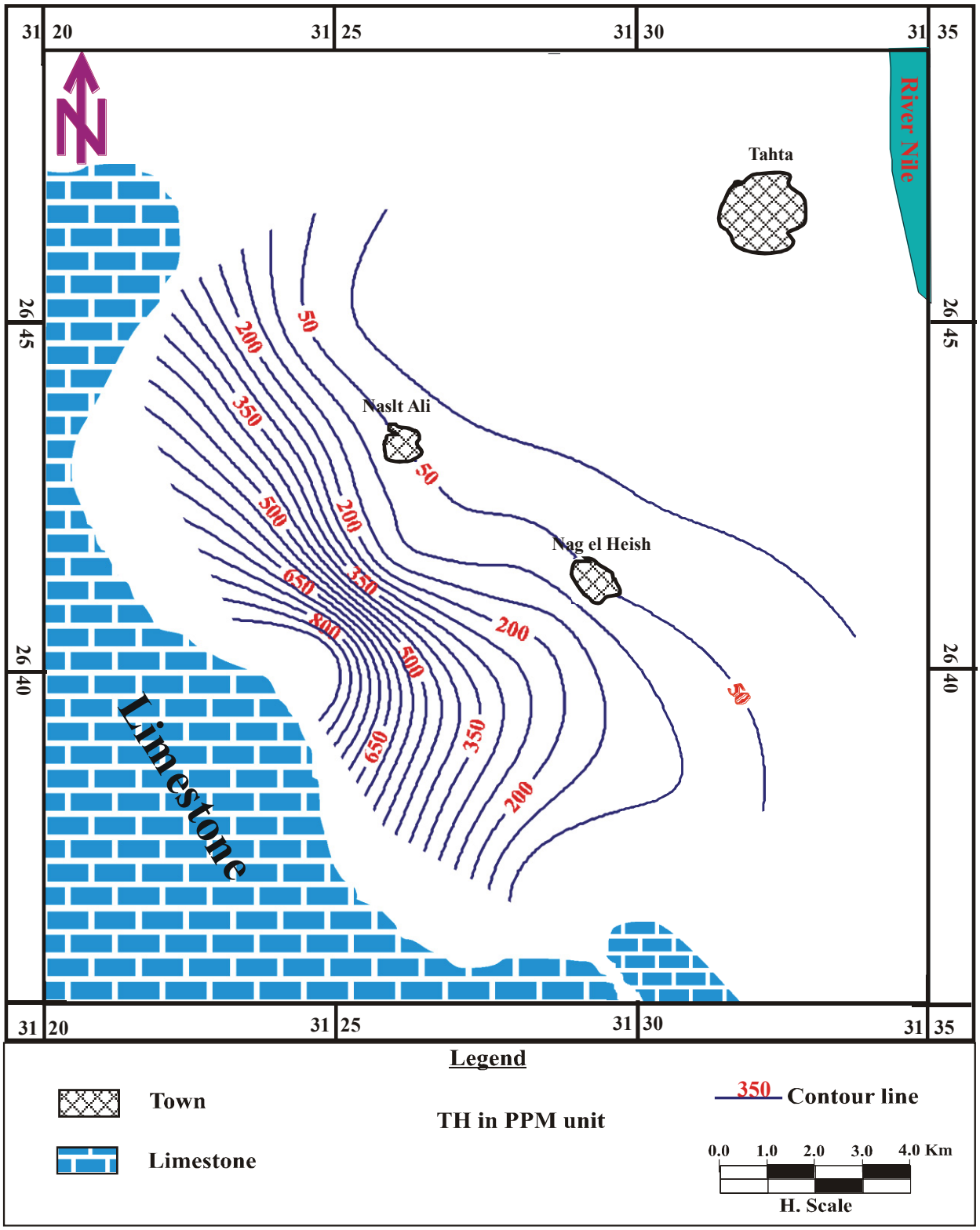

Fig. (4.25): Hardness contour map 1989 (groundwater samples)

dominant in the 1989 groundwater samples, whereas Na_2SO_4, NaCl, and $NaHCO_3$ are most common in the 2011 samples. Sodium bicarbonate indicates the recharge of the groundwater in the study area mainly by the Nile water seeping in from irrigation canals. The sodium chloride and sodium sulfate enrichment in the water samples from the western part of the study area proves the extensive use of fertilizers for improving the soil characteristics in the new reclamation project. The water quality is changing as well.

Table (4.18): Ion dominance of the study water samples

Ion dominance	1989	2011
HCO_3> Cl> SO_4/ Na> Ca (or Mg)> Mg (or Ca)	31%	7%
Cl> HCO_3> SO_4/ Na> Ca (or Mg)> Mg (or Ca)	17%	4%
Cl> SO_4> HCO_3/ Na> Ca (or Mg)> Mg (or Ca)	17%	21%
SO_4> Cl > HCO_3/ Na >Ca (or Mg)> Mg (or Ca)	11%	43%
HCO_3l> SO_4> Cl / Na> Ca (or Mg)> Mg (or Ca)	8%	4%
SO_4 > HCO_3> Cl / Na >Ca (or Mg)> Mg (or Ca)	5%	18%
HCO_3> Cl> SO_4/ Ca (or Mg) > Na> Mg (or Ca)	5%	--
Cl> SO_4> HCO_3/ Ca > Na (or Mg)> Mg (or Na)	3%	--
HCO_3> Cl> SO_4/ Ca (or Mg)> Mg (or Ca)> Na	3%	--
SO_4 > HCO_3> Cl / Ca (or Mg)> Na > Mg (or Ca)	--	3%

Table (4.19): Water types of the studied water samples

Water types	1989	2011
$NaHCO_3$	39%	11%
NaCl	33%	25%
Na_2SO_4	17%	61%
$Ca(HCO_3)_2$	5%	--
$Mg(HCO_3)_2$	3%	--
$CaCl_2$	3%	--
$CaSO_4$	--	3%

From the ion dominance and chemical water type, we found that the HCO_3> Cl> SO_4/ Na> Ca (or Mg)> Mg (or Ca) causes an abundance in ions in the groundwater collected in 1989 and in the sodium bicarbonate water type. Most of the groundwater samples collected in 2011

have SO_4> Cl > HCO_3/ Na >Ca (or Mg)> Mg (or Ca) and Na_2SO_4 water type. This suggests that the chemistry of the groundwater in the study area was affected during this time by extensive water being taken from the aquifer, as well as the extensive use of fertilizers.

4.3.5. Hypothetical salt combinations:

Collin's (1923) bar-graph method is used to represent the salt combinations of the water samples, shown in Figures 4.15, 4.16, and 4.26, and 4.27. The following table shows the possible salt combinations of the groundwater demonstrated by samples collected in 1989 and 2011.

Table (4.20): Salt combinations of the studied water samples

Salt combinations	1989	2011
$Ca(HCO_3)_2$, $Mg(HCO_3)_2$, $Na(HCO_3)_2$, Na_2SO_4, and NaCl	50%	26%
$Ca(HCO_3)_2$, $Mg(HCO_3)_2$, $MgSO_4$, Na_2SO_4, and NaCl	11%	15%
Ca(HCO3)2, CaSO4, MgSO4, Na2SO4, and NaCl	17%	53%
$Ca(HCO_3)_2$, $CaSO_4$, $MgSO_4$, $MgCl_2$, and NaCl	11%	--
$Ca(HCO_3)_2$, $CaSO_4$, $CaCl_2$, $MgCl_2$, and NaCl	8%	--
$Ca(HCO_3)_2$, $Mg(HCO_3)_2$, Na_2SO_4, and NaCl	3%	--
$Ca(HCO_3)_2$, $MgSO_4$, Na_2SO_4, and NaCl	--	6%

In conclusion, $Ca(HCO_3)_2$, $Mg(HCO_3)_2$, $Na(HCO_3)_2$, Na_2SO_4, and NaCl and $Ca(HCO_3)_2$, $Mg(HCO_3)_2$, $MgSO_4$, Na_2SO_4, and NaCl salt assemblages are common in the 1989 samples while $Ca(HCO_3)_2$, $CaSO_4$, $MgSO_4$, Na_2SO_4, and NaCl, and $Ca(HCO_3)_2$, $Mg(HCO_3)_2$, $Na(HCO_3)_2$, Na_2SO_4, and NaCl are the abundant salt assemblages in the 2011 samples.

4.3.6. Application of Piper trilinear diagram

By plotting the results of the chemical analysis of the water samples of 1989 and 2011 in the Piper diagram (Fig. 4.17), we can see that about 61% from1989 and 86% from 2011 water samples are of meteoric origin. About 25% from 1989 and 11% from 2011

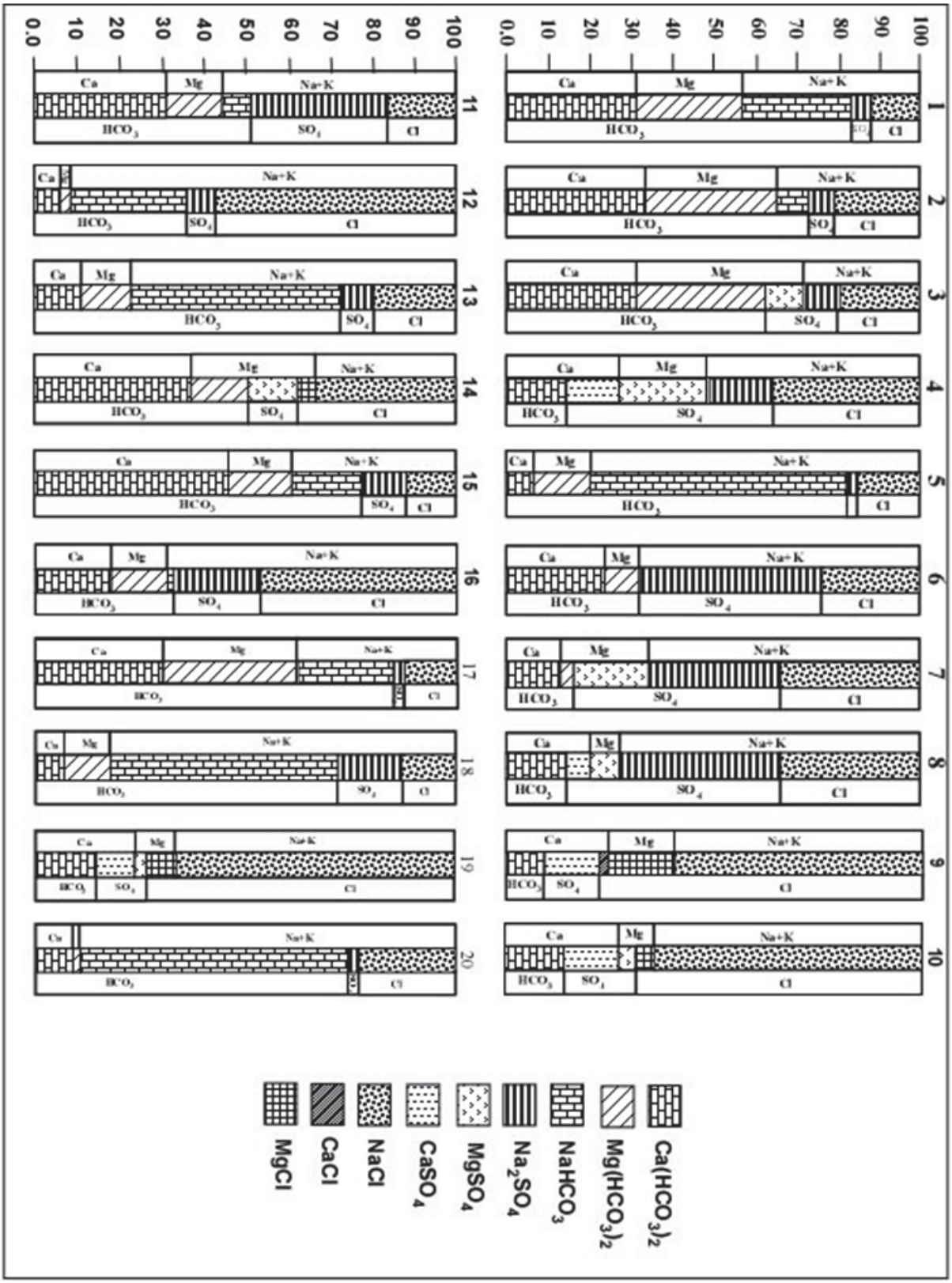

Fig. (4.26): Bar-graph method of the 1989 water samples

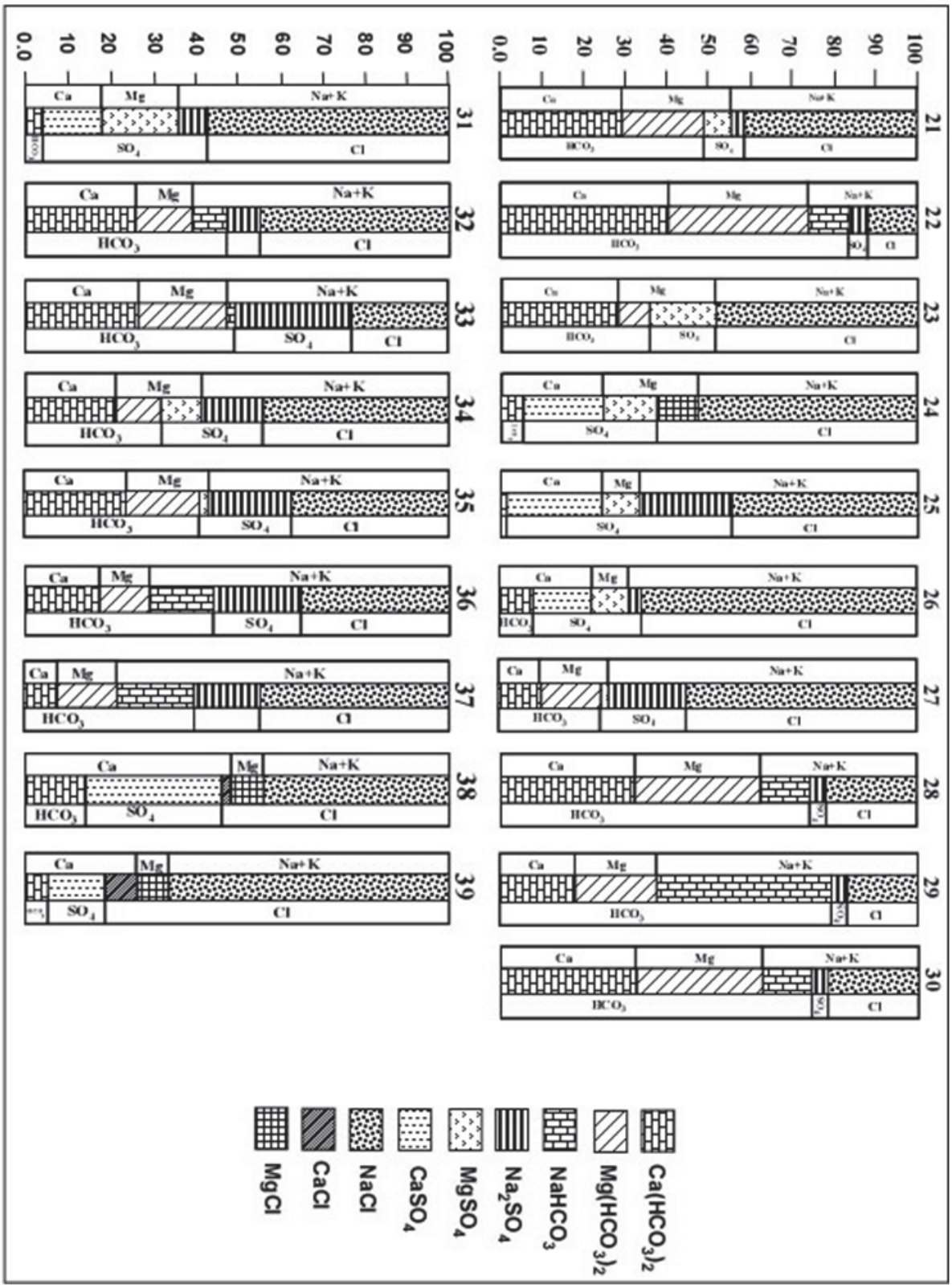

Fig. (4.27): Continue bar-graph method of the 1989 water samples

are mixed water, and the rest is of marine origin. The presence of water with higher salinity mixed with the meteoric origin water is probably due to the salt enrichment of evaporation in the soil for thje 1989 water samples and the presence of clay and shale deposits in the 2011 samples. The ionic exchange between the groundwater and the aquifer sediments is rich in clay lenses.

4.3.7. Application of the Grid system method

Figure 4.18 shows that the water samples collected in 1989 are mainly characterized by sodium bicarbonate and sodium chloride, sometimes sodium sulphate. The water samples collected from west Tahta in 2011 are mainly characterized by sodium sulphate and sodium chloride.

4.3.8. Evaluation of groundwater quality for drinking

By comparing the groundwater samples from the area under investigation from 1989 and 2011 to the guidelines for human drinking water (International Standards and the Egyptian Committee for Water, 2007), (Table 4.8), it is clear that most of the groundwater (64%) collected in 1989 is suitable for drinking due to low levels of salinity (>1200ppm) and also major ions within the permissible limits. The rest of samples (36%) are unsuitable due to their high total salinity and major ions concentrations higher than the permissible limits. On the other hand, the majority of the groundwater collected in 2011 (71%) is unsuitable for human drinking, because its salinity is higher than 1200ppm (up to 4453ppm) and major ions more than the permissible limits. The rest of the samples (29%) are suitable for drinking due to low of salinity (>1200) and also the major ions within the permissible limits.

4.3.9 Evaluation of groundwater quality for irrigation purposes

-According to the salinity index or total dissolved salts as computed by measured EC values: Based on Bauder et. al. (2007), the studied water samples have been classified and are given in Table 4.21. From this classification, we found that the 1989 groundwater samples are categorized under good quality to very doubtful quality for irrigation purposes, while half of the 2011 ground water samples are categorized under unsuitable, and the other half ranged between good quality and doubtful quality for irrigation purposes.

Table (4.21): Classification of water samples based on E.C

EC (µS/cm)	Water Salinity Range	1989	2011
< 250	excellent quality	--	--
251–750	good quality	28%	3%
751–2000	permissible quality	42%	32%
200–3000	Doubtful	30%	11%
>3000	Unsuitable	--	54%

-According SAR or sodicity index: The classification of groundwater samples from the study area based on SAR values, according to Bauder et. al. (2007), are presented in Table 4.22. This table shows that all the groundwater samples collected in 1989 and 2011 range from excellent to good for irrigation.

Table (4.22): Classification of water samples based on SAR values (Bauder et al, 2007) and sodium hazard classes based on USSL classification.

SAR values	Sodium hazard to water	Remark on quality	1989	2011
<10	Low	Excellent	81%	75%
10–18	Medium	Good	19%	25%
19 26	High	Doubtful / Fair poor	--	--
>26	Very high	Unsuitable	--	--

-According to the U.S. Laboratory Staff's diagram (Richards, 1954); (Fig. 4.19) 84% of the groundwater samples collected in 1989 are suitable and 17 are unsuitable for irrigation purposes, while about 54% of the groundwater samples collected in 2011 are suitable and 46% are bad or unsuitable for irrigation purposes due to their high salinity.

-Percent sodium; according to Eaton's (1950) classification Table 4.23. We found that about 48% of water samples from 1989 and 61% from 2011 are unsafe and 42% from the groundwater samples of 1989 and 39% from 2011 are safe.

Table (4.23): Sodium percent water class (Eaton 1950)

Sodium %	Water class	1989	2011
>60	Unsafe	48%	61%
<60	Safe	42%	39%

Also Wilcox (1948) classified groundwater for irrigation purposes by correlating percent sodium (i.e., sodium in irrigation waters) and electrical conductivity. A perusal of Wilcox's (1995) diagram (Fig. 4.20) shows that the groundwater samples collected from west Tahta in 1989 have the following percents: 36% are permissible to doubtful, 25% doubtful to unsuitable, 22% excellent to good, 6% good to permissible, and 11% unsuitable. The 2011 groundwater samples have the following percents: 54% unsuitable, 14% doubtful to unsuitable, 21% permissible to doubtful, 7% good to permissible, and 4 % excellent to good.

-According to residual sodium carbonate; in addition to the SAR and Na%

The groundwater samples collected in 1989 and 2011 were classified on the basis of RSC, and the results are presented in Table 4.24. This table shows that most of the groundwater samples collected in 1989 and 2011 are good for use in irrigation.

Table (4.24): Groundwater quality based on RSC (Richards, 1954)

RSC (epm)	Remark on quality	1989	2011
<1.25	Good	72%	96%
1.2 –2.5	Doubtful	8%	4%
>2.5	Unsuitable	20%	--

4.3.10. Mechanisms controlling groundwater chemistry

The chemical data from the 1989 and 2011 groundwater samples are plotted in the Gibbs diagram (Fig. 4.21). The majority of the groundwater samples suggest that the chemical weathering of rock-forming minerals influence the groundwater quality through the dissolution of the host rock.

Conclusion

The area under investigation (West Tahta) belongs to the Sohage Governorate in Upper Egypt. This area is characterized by long, hot summers, warm winters, and scarce rainfall, except for the occasional storms. Rain is generally rare and randomly distributed over the area. West Tahta represents one of the most important land reclamation projects on the western bank of the Nile Valley. The exploited amount of groundwater is actually very limited in this area. In the study area, a relatively thick sedimentary section occurs, ranging in age from Eocene to Quaternary age. One aquifer was detected in the study area, the by Pleistocene aquifer.

The main aim of the present study is the representation of the changes in the River Nile, as well as in the agricultural and urban development between 1987 and 2011. The identification of the groundwater aquifers and the delineation of the subsurface conditions on the basis of the interpretation of available geophysical data, and hydrochemical characteristics of the aquifers and the evaluation of the water quality for different purposes were carried out. Finally, the change in the groundwater quality between 1989 and 2011was recorded.

Geologically: The west Tahta area in Sohag Governorate, is bordered by the Eocene plateau in the west and the Nile River in the east, and is a part of the Nile Valley. The rock units in the study area and its surroundings are mainly of sedimentary origin, ranging in age from the Holocene to the Eocene period.

Holocene deposits; these deposits are accumulated under different environmental conditions and contain all varieties of unconsolidated sediments and are represented by Nile silt, wadi deposits, and fanglomerates.

Pleistocene deposits; these deposits are lie directly under the Holocene deposits overlying the Pliocene clay and Eocene limestone. They are composed of sand and gravel. Pleistocene deposits represent the main water bearing formation in the Nile Valley (the Quaternary aquifer).

Pliocene Deposits; Pliocene deposits consist of a lower marine and higher fluvial sequence. They are represented by dark colored clays inter-bedded with sandstone lenses. The Pliocene deposits lie under the Pleistocene deposits and act as a thick, impermeable bottom layer.

Eocene Deposits; These deposits on both the eastern and western sides build up the scarps and consist of carbonates intercalated by clays, shale, and sand. The exposed part of the formation decreases gradually toward the north due to gentle regional slope towards the north.

Geophysical Investigations: The geoelectrical resistivity soundings have successfully established the nature and configuration of the Pleistocene aquifer within the study area. Based on the analytical and interpretative results of the processed data, it has been concluded that the study area represents a geophysical four-layer case. The first layer (surface layer) has various resistivity values different from the west to the east due to the presence and influence of wadi deposits in the west and clay in the east. This layer is thin; the thickness varies from 1 to 5m.

The second layer shows resistivity values between 111 and 325ohm.m and a variation in thickness between 5 and 34m. This layer is composed of wet sand.

The third geoelectric layer is the main water-bearing formation in the study area. It consists of sand and gravel with resistivity values ranging from 28 to 99ohm.m. The thickness of this layer decreases towards west and ranges from 18 to 144m. The thickness of this layer in some areas is not defined due to the limitations of the instrument.

The fourth geoelectric layer represents the base of the water-bearing layer and is represented by Pliocene clay showing resistivity values ranging from 1.7 to 12.9ohm.m. The total thickness is not defined in some locations.

The thickness of the quaternary aquifer increases toward the east, while the resistivity increases toward the west due to the presence of wadi deposits clearly seen from the contour maps. The largest thickness of the groundwater formation can be seen in the different course of the River Nile in the pre-Pliocene age.

Remote Sensing study: The agriculture in the study area covered 34573.90ha in 1987, and reached 36359.80ha in 2009. The total increase in the agricultural area from 1987 to 2009 is about 1785.9ha with an average annual growth rate of 81.2ha/year. This increase in the agriculture area results from the extensive reclamation project, taking place in the study area.

The fundamental condition is the presence of groundwater in the Quaternary aquifer. The presence of suitable water was the precondition for the extensive urban project in this area, which has an increasing population. The total urban area in 1987 was 6034.37ha and 8265.58ha in 2009. The total increase is 2231.21ha with an average annual growth rate 101.45ha/year. River Nile is the main source of surface water in the study area, i.e. the source of the recharge of the Quaternary aquifer. By monitoring the change in the River Nile from 1987 to 2009, we found that the River Nile covered about 686.79ha in 1989 and 825.11ha in 2009, with a total change in this period of about 138.32ha and an average annual growth rate of 6.29ha/year.

Hydrogeologically: The data for the hydrogeological study came from 56 wells in case of 1989 and 28 wells in 2011. These wells are distributed throughout the study area and were the basis for the maps showing the hydrogeological conditions.

The study area is characterized by one aquifer system (Quaternary aquifer) in a hydrogeological sense. This aquifer is recharged mainly from surface water, especially from the irrigation canals, which play a main role in the configuration of the water table. The discharge of this aquifer takes place during evaporation. The main direction of the flow of the groundwater in the study area is towards the northeast, towards the River Nile. This direction did not change from 1989 to 2011 due to the influence of canal's recharge. The depth to the groundwater is affected by the extensive use of the groundwater, which is increasing towards the west. In 1989 the depth to the groundwater ranged from 1m to 45m while in 2011 from 9m to 56m.

Hydrogeochemically:

-The pH of the surface water varies from 7.1 to 7.6, and the pH of the groundwater varies from 6 to 7.7. This indicated a slightly acidic to slightly basic nature. All the water samples showed a pH within the permissible limit of 6.5 - 8.5.

- The electric conductivity of the surface water ranges from 230 to 2386µS/cm and that of the groundwater samples from 356 to 7550µS/cm. The surface water and about 46% of the studied water samples showed conductivity values below the permitted limit of 3000 µS/cm.

- The salinity of the surface water is lower than that of fresh water. The salinity of the groundwater collected in 1989 varies between fresh and slightly saline, ranging from 205 to 2880ppm, while the salinity of the samples collected in 2011 ranged between fresh and moderately saline water. The increase of salinity is attributed to leaching processes and the dissolution of limestone, as well as evaporation from the irrigation water. The iso-salinity contour map shows the increase of the salinity from east to west, reflecting the impact of the leaching effect of the limestone in the west.

- Based on the chemical ions, the dominant chemical water types of surface water samples are $NaHCO_3$, $Ca(HCO_3)_2$, and Na_2SO_4. $NaHCO_3$, NaCl, and Na_2SO_4 are dominant water types in the 1989 groundwater samples, while Na_2SO_4, NaCl, and $NaHCO_3$ are the dominating types in the 2011 samples.

- The Piper diagram (Fig. 4.17) shows that most of the water samples are present in sector 1 which reflect meteoric origin. That indicates that the main source of recharge comes from the surface water through the irrigation canals.

- The grid system method shows that the water samples collected in 1989 are mainly characterized by sodium bicarbonate and sodium chloride, sometimes sodium sulphate. The water samples collected from west Tahta in 2011 contain mainly sodium sulphate and sodium chloride.
- The majority of the surface water appears to be suitable for drinking. Most of the groundwater (64%) collected in 1989 is suitable for drinking and the rest of the samples (36%) are unsuitable. On the other hand, the majority of the groundwater collected in 2011 (71%) are unsuitable for human drinking because the salinity is higher than 1200 PPM.
- Most of the groundwater samples collected in 1989 are suitable for irrigation purposes, while about half of the groundwater samples collected in 2011 is suitable. The other half are unsuitable due to their high salinity.

- Gibbs diagram shows that the majority of the groundwater samples collected from the study area suggests that the chemical weathering of rock-forming minerals influence the groundwater quality through the dissolution of the host rock.

The combination between remote sensing techniques, geoelctrical studies, as well as hydrogeology and hydrogeochemical studies is very useful for understanding the changes in the study area. Detecting the changes in an area allows us to create scenarios for the future as well as to make decisions for the development of the area.

References

Abdalla, M. F. and Abdulaziz, M. A. (2011): Monitoring land-use change associated land reclamation using multitemporal landsat data and geoinformatics in Kom Ombo area, South Egypt. International journal of remote sensing (in press).

Abdel Moneim, A. A. (1988): Hydrogeology of the Nile basin in Sohag Province. M.Sc. Thesis, Geol., Dept., Fac. Sci., Assiut Univ., Egypt. 131 p.

Abdel Moneim, A. A. (1992): Numerical simulation and groundwater management of Sohag aquifer, the Nile Valley, Egypt. Ph.D. Thesis, Civil Eng. Dept. Strathclyde Univ., Glagov, Scotland, Great Britain.

Abdel Moneim, A. A. (1999-a): Groundwater studies in and around Abydous Temples, El-Balyana, Sohag, Egypt. Ann. Geol. Surv. Egypt. 22, pp. 357-368.

Abdel Moneim, A. A. (1999-b): Geoelectrical and hydrogeological investigations of the groundwater resources on the area to the west of the cultivated land at Sohag. Upper Egypt, Egyptian Journal of Geology, Vol. 43/ 2, pp. 253-268.

Abdulaziz, A.M., (2007): Applications of remote sensing, GIS, and groundwater flow modeling in evaluating groundwater resources; two case studies: East Nile Delta, Egypt and Gold Valley, California, USA. PhD dissertation, University of Texas at El Paso, El Paso, Texas, USA.

Abdulaziz, A., M.; Hurtado, J. M, and Al-Douri, R. (2009): Application of multitemporal landsat data to monitor land cover changes in the Eastern Nile Delta region, Egypt. International Journal of Remote Sensing, 30(11): 2977–2996.

Ahmed, A. A. (2007): Using lithologic modeling techniques for aquifer characterization and groundwater flow modeling of Sohag area, Egypt. Second International Conference on Geo-Resources in the Middle East and North Africa, Cairo, 24-28 February 2007.

Ahmed, S. M. (1980): Geological studies on the west and southwest of Sohag. M.Sc. Thesis, Geol. Dept., Fac. Sci., Sohag, Assiut Univ., Egypt.

Amer, A. F., Krintsov, M. L. and Hanna, F. L. (1970): The Egyptian carbonates rocks and the possibilities of their utilization. In: studies on some mineral deposits of Egypt. Geol. Surv. Egypt, p. 195-208.

Anderson, J. R., Hardy, E. E., Roach, J. T., & Witmer, R. E. (1976): A land use and land cover classification system for use with remote sensor data. Washington, DC: U.S. Geological Survey. No. Professional paper 964.

Anderson, W. L., (1979): Program MARQDCLAG, Marquard inversion of Dc Scheumberger sounding by lagged-convolution, U.S. Geolog. Survey, Open File Rep. V. 58, p. 79- 1432.

Attia, M. I. (1954): Deposits in the Nile Valley and Delta. Geol. Surv., Cairo, Egypt P. 356.

Attia, F. R., (1985): Management of water systems in Upper Egypt. Ph.D. Thesis, Faculty of Engineering, Cairo Univ., Egypt.

Atwa, S. M. M., (1979): Hydrogeology and Hydrogeochemistery of the North Western Coast of Egypt, Faculty of Science, Alex. Univ.

Awad, M. A., Nada, A. A., Hamza, M. S. and Froehlich, K. (1995): Chemical and Isotopic investigation of groundwater in Tahta region, Sohag, Egypt. Environmental Geochemistry and Health, 17 pp. 147-153.

Awad, A. O., (2008): Integration of remote sensing, geophysics and GIS to evaluate groundwater potentiality- a case study in Sohag Region, Egypt.

Ayman A. Ahmed, (2009): Using generic and pesticide DRASTIC GIS based models for vulnerability assessment of the Quaternary aquifer at Sohag, Egypt. Hydrogeology Journal 17 pp. 1203 – 1217.

Ayman A. Ahmed & Mohamed H. Ali (2009): Hydrochemical evolution and variation of groundwater and its environmental impact at Sohag, Egypt. Arab J Geosci. DOI 10.1007/s12517-009-0055-z

Ball, J. (1909): On the origin of the Nile Valley and Gulf of Suez. Cairo Sci. Jour., Vol. 3, pp. 250- 25.

Barber, W. and Carre, D. P. (1981): Water management capabilities of the alluvial aquifer system of the Nile Valley, Upper Egypt. Technical Report No. 11, Water Master Plane, Ministry of Irrigation, Cairo, Egypt. 145p.

Bauder, T. A., Waskom, R. M. And Davis, J. G., (2007): Irrigation water quality criteria. Extension fact sheet No. 0.506, Colorado State University. pp 1-5.

Bakr, N., Weindorf D. C., Bahnassy M. H., Marei S. M., and El-Badawi M. M. (2010): Monitoring land cover changes in a newly reclaimed area of Egypt using multi-temporal Landsat data. Applied Geography, 30 (2010), 592–605.

BIS (1998): Drinking water specific actions (revised 2003).Bureau of Indian Standards, IS: 10500.

Blomquist, W., Heikkila, T. and Schlager, E. (2001): Institutions and Conjunctive Water Management among Three Western States." Natural Resources Journal 41(3): 653-84.

Brikowski, T. H., and Faid, A. M. (2006): Pathline-calibrated groundwater flow models of Nile Valley aquifers, Esna, Upper Egypt. Journal of Hydrology, 324: 195–209.

Campbell, J. B. (2002): Introduction to remote sensing (3rd ed.). New York: The Guilford Press.

Central Agency for Population Mobilization and Statistics - Population Clock (2011): Msrintranet.capmas.gov.eg. Retrieved 2011- 03-03.

http://www.msrintranet.capmas.gov.eg/pls/fdl/tst12e?action=&lname

Chumakove, I. S. (1967): Pliocene and Pleistocene deposits of the Nile Valley in Nubia and Upper Egypt. (In Russian). Trans. Geol. Inst. Acad. USSR, V. 170, pp. 1-110.

Collins, W.D., (1923): Graphical representation of water analysis. Ind. Eng. Chem., Vol. 15.

Collins, J.B. and Woodcock, C.E. (1996): An assessment of several linear changes detection techniques for mapping forest mortality using multitemporal Landsat TM data. Remote Sensing of Environment, 56, pp. 66–77.

Congalton, R. G. (1991): A review of assessing the accuracy of classifications of remotely sensed data. Remote Sensing of Environment, 37, 35 – 46.

Congalton, R. G., & Green, K. (1999): Assessing the accuracy of remotely sensed data: Principles and practices. Boca Raton: Lewis Publishers.

DeFries, R.S., and Townshend, J.R.G. (1994): Global land cover: comparison of ground based data sets to classifications with AVHRR data, Wiley, Chichester.

Diab, M. Sh., El-Shayeb, M. H., Abdel Moneim, A. A., Said, M. M. and Zaki, S. R. (2002): Evaluation of water resources and land suitability for development in southern part of Sohag, Upper Egypt. Annals Geol. Surv. Egypt, V. XXV (2002), pp. 487-512.

Eaton, E. M., (1950): Significance of carbonate in irrigation water. Soil Science, 69, 12–133.

EHCW "Egyptian Higher Committee for Water (2007): Egyptian standards for drinking and domestic uses.

Elachi, C., and Van Zyl, J., (2006): Introduction to the physics and techniques of remote sensing. By C., John Wiley & Sons, Inc.

El-Haddad, A., Abdel Moneim A. A., and Omer A. A., (2003): Influence of the transverse channels on the geometrical and hydrochemical characteristics of the Quaternary aquifer in the peripheral areas of the Nile Basin, Sohag, Egypt. Bull. of the Third International Conference on the Geology of Africa. Assuit University 7-9 Dec. 2003.

El-Hinnawi, M., Abdallah A. A., and Issawi, B. (1978): Geology of Abou Bayan, Bolaq stretch, Western Desert, Egypt. Ann. Geology. Survey., Cairo, Egypt, v. 8, p. 19-50.

El-Sayed, H., (2010): Environmental investigation on Lake Maryut, west of Alexandria, Egypt: Geochemical, Geophysical and Remote Sensing study. MSc. Thesis. 2010

El-Sayed, S. A. and EL-Shater, A.A. (2010): Engineering aspects and associated problems of flood plain deposits in Sohag Governorate, Upper Egypt. Journal of American Science, 2010; 6 (12) pp. 1614-1623

FAOSTAT (2006): Statistical Year Books 2005–2006, Issue 2 (Rome: Food and Agriculture Organization of the United Nations).

Foster, S. (1998): Groundwater: Assessing vulnerability and promoting protection of a threatened resource. In Proceedings of the 8th Stockholm Water Symposium, 10– 13 August 1998, Sweden (Stockholm: International Water Institute), pp 79–90

Gibbs, R. J., (1970): Mechanism controlling world water chemistry. Science, 170, 1088–1090.

Gish, O. H., and Rooney, W. J., (1925): Measurement of resistivity of large masses of undisturbed earth, Terrestrial Magnetism and Atmospheric Electricity 30: 161-188.

Gomaa, A. A. A. A., (2006): Hydrogeologic and Geophysical assessment of the reclaimed areas in Sohag, Nile Valley, Egypt. Ph.D. Thesis, Geology dept. Faculty of Science, Ain Shams University, 272p.

Goudie, A. S., (1993): Land Transformation. In: The Challenge for Geography: A Changing World, A Changing Discipline, ed. R. J. Johnston, Cambridge: Blackwell. pp.117-137.

Green, K., Kempka, D. and Lackey, L., (1994): Using remote sensing to detect and monitor land-cover and land-use change. Photogrammetric Engineering and Remote Sensing, 60, pp. 331–337.

Gutman, G., (2004): Land Change Science. In: Monitoring and Understanding Trajectories of

Change on the Earth's Surface. Dordrecht: Kluwer Academic Publishers. pp.329-350.

Harris, P. M. and Ventura, S. J., (1995): The integration of geographic data with remotely Sensed imagery to improve classification in an urban area. Photogrammetric Engineering and Remote Sensing, V. 61(8), pp.993-998.

Hassan, M.Y., Isawi, B. and Zaghloul, E. A. (1978): Geology of the area east of Beni-Suef, Eastern Desert, Egypt. Annals of the Geo. Surv. of Egypt, Vol. VIII pp. 129- 162.

Hassan, A.M. (2005): Geochemical characteristics of the superficial Nile Basin sediments and their environmental Relevance, Sohag Area, Egypt. M. Sc. Thesis, Fac. of Sci. South Valley University (Sogah Branch).

Hathout, S., (2002): The use of GIS for monitoring and predicting urban growth in East and

West St. Paul, Winnipeg, Manitoba, Canada. Journal of Environmental Management. V. 66, pp.
229-238.

Hay, A. M. (1979): Sampling designs to test land use map accuracy. Photogrammetric Engineering and Remote Sensing, 42, pp. 671–677.

Hem, J. D., (1970): Study and interpretation of the chemical characteristics of natural water, Second Ed. U.S. Geol. Survey water supply paper 1473, 363 pp

Hem, J. D., (1985): Study and interpretation of the chemical characteristics of natural water (pp. 117–120, 264). USGS, Water Supply Paper no. 2254.

Hem, J. D., (1989): Study and interpretation of the chemical characteristics of natural water. U.S. Geol. Surv., water supply paper 2254, Third printing, 264p.

Herold, M., Goldstein, N. C. and Clarke, K. C., (2003): The spatiotemporal form of urban growth: measurement, analysis and modeling. Remote Sensing of Environment, V. 86, pp. 286-
302.

Hsu¨, K.J., Ryan, W.B.F., Cita, M.B., (1973): Late Miocene desiccation of the Mediterranean. Nature 242, 240–244.

Hudson, W., & Ramm, C., (1987): Correct formula of the Kappa coefficient of agreement. Photogrammetric Engineering and Remote Sensing, 53(4), 421–422.

IPI2Win, (2003): Resistivity Sounding Interpretation. Moscow State University 2003

IWMI (2001): The Strategic Plan for IWMI 2000–2005 (Colombo, Sri Lanka: International Water Management Institute).

Jensen, R. J. and Narumalani, S., (1992): Improved remote sensing and GIS reliability diagrams, image genealogy diagrams, and thematic map legends to enhance communication. International Archives of Photogrammetry and Remote Sensing. V.6, pp.125-132.

Jensen, R. J., (1995): Introductory Digital Image Processing, Prentice-Hall, Upper Saddle River, pp. 467-475.

Jensen, J. R., (2004): Digital change detection. In Introductory Digital Image Processing – A Remote Sensing Perspective, pp. 467–494 (Upper Saddle River, NJ: Pearson Prentice Hall).

Jensen, J. R., (2007): Remote Sensing of the Environment: An Earth Resource Perspective (2^{nd}
ed.). Upper Saddle River, NJ: Prentice-Hall.

Kaufman, R. K. and Seto, K. C., (2001): Change detection, accuracy, and bias in a sequential analysis of Landsat imagery in the Pearl River Delta, China: econometric techniques. Agriculture, Ecosystems and Environment, 85, pp. 95–105.

Koefoed, O. (1976): Recent development in the direct interpretation of resistivity sounding. Geophysic. Explor. Vol. 14, p. 243 – 250.

Korany, E. A., Omran, A. A., Abdel- Aal, A. A. (2006): Hydrogeochemical approach for the assessment of the recharge routes of groundwater in the Quaternary aquifer, Nile Valley of Sohag area, Egypt, Proc. of the 7th int. Conf. on Geochemistry, Alexandria, September (2006).

Kuntez, G., and Rocroi, M. (1970): Traitment outomatique des sondages Electriques. Geophys. Prosp. V. B., pp. 157-198.

Leica Geosystems, (2008): Leica geosystems geospatial imaging ERDAS IMAGINE 9.2. Norcross, USA: Leica Geosystems Geospatial Imaging.

Levin, N., (1999): Fundamentals of Remote Sensing. 1st Hydrographic Data Management course, IMO-International Maritime Academy, Trieste, Italy

Lillesand, T. M., & Kiefer, R. W., (1994): Remote sensing and image interpretation (4th ed.). New York: John Wiley & Sons (724 pp.).

Lu, D. Mausel, P. Brondízio, E. and Moran, E., (2004): Change Detection Techniques, International Journal of Remote Sensing, Vol. 25, No. 12, pp. 2365-2407.doi:10.1080/0143116031000139863

Mahran, T. M. and El-Haddad, A. (1992): Facies and depositional environments of Upper Pliocene- Pleistocene Nile sediments around Sohag area, Nile Valley, Egypt. Journal of Saharian studies, V. 1, No. 2, pp. 11-40.

Maillet, R., (1947): The fundamental equation of geoelectrical prospecting. Geophys., V. 12. p.529- 556.

Meteorological Authority of Egypt (MAE), (2000): Meteorological database, Cairo, Egypt.

Milne, A. K., (1988): Change detection analysis using Landsat imagery a review of methodology. In Proceedings of IGARSS, 88 symposium (pp. 541–544), Edinburgh, Scotland, 13–16 September.

Mousa, S., Attia, F. A., and Abu El-Fotouh, M. (1994): Geoelectrical and Hydrogeological study on the Quaternary aquifer in the Nile Valley between Asyut and Sohag governorates, Egypt. Geol. J. Egypt., vol. 38-2, pp. 1-20.

Ola, H. and Hay, G.J., (2003): A multi scale object-specific approach to digital change detection. International Journal of Applied Earth Observation and Geoinformation, 4, pp. 311–327.

Omer, A. A. M. (1996): Geological, mineralogical and geochemical studies on the Neogene and Quaternary Nile basin deposits, Qena- Assiut stretch, Egypt. Ph.D. Thesis, Geol. Dept., Fac. Sci., South Valley Univ.

Omer, A. A. M. and Abdel Moneim, A. A. (2001): Geochemical characteristics of the Pliocene and Pleistocene Nile basin deposits and their influence on the groundwater chemistry in Sohag area. Annals Geol. Surv. Egypt. V. XXIV, p. 567-584.

Omran, A.A., Korany, E. A., and Abdel-Rahman, A.A. (2006): An integrated approach to evaluate groundwater potentiality – A case study, Proc. Of the 3rd int. Conf. of Applied Geophysical, ESAP, 18-20 March 2006, National Research Center, Cairo, Journal of Applied Geophysics, Vol. 5, part1.

Omran, A. A., (2008): Integration of Remote Sensing, Geophysics and GIS to Evaluate Groundwater Potentiality – A Case Study In Sohag Region, Egypt, The 3rd International Conference on Water Resources and Arid Environments (2008) and the 1st Arab Water Forum

Orellana, Ernesto, and Mooney, ll. M., (1966): Master tables and curves for vertical electrical sounding over layered structures Madrid Interciecia 34 p., 66 tables

Pax-Lenney, M., Woodcock, C.E., Collin, J.C. and Hamdi, H., (1996): The status of agriculture in Egypt: the use of multitemporal NDVI features derived from Landsat TM. Remote Sensing of Environment, 56, pp. 8–20.

Piper, A. M., (1944): A graphic procedure in the geochemical interpretation and analysis of water samples U.S. Geol. Survey. Water Supply paper 1454.

Ragunath, H.M., (1987): Groundwater (p. 563). New Delhi: Wiley Eastern.

Richards, L. A. (US Salinity Laboratory) (1954): Diagnosis and improvement of saline and alkaline soils (p. 60). US Department of Agriculture hand book.

RIGW, (1989): Hydrogeological map of Egypt, Tahta area 1st ede.

RIGW, IWACO, (1989): Groundwater development for irrigation and drainage in the Nile Valley: Groundwater development in the area of West Tahta. Technical Note 70.124-89-05 (internal report).

Rasool, S. I., (1987): Potential of Remote Sensing for the Study of Global Change: COSPAR Report to the International Council of Scientific Unions (ICSU), Advances in Space Research,
V. 7(1), Oxford: Pergamon Press.

Rosenfield, G., & Fitzpatrick-Lins, K., (1986): A coefficient of agreement as a measure of thematic classification accuracy. Photogrammetric Engineering and Remote Sensing, 52(2), 223–227.

Sabins, F. F., (1997): Remote Sensing, Principles and Interpretation. Freeman New York, 494 p.

Said R., (1960): Planktonic Foraminifera from the Thebes Formation, Luxor. Micropaleontology V. 6 pp.277-286

Said, R. (1962): Planktonic Foraminifera from Thebes Formation. Luxor, Egypt. Micro paleontology. Vol. 16, p. 277-286.

Said, R. (1971): Explanatory notes to accompany the geological map of Egypt 1:2,000,000. Geol. Surv. Egypt. Paper 56, 123p.

Said, R. (1975): The geology evaluation of the River Nile. In: problems in prehistory of Northern Africa and the Levant Wendorf, F. & Marks, A. F. (eds). Southern Methodist University press. Dallas, Taxas, pp. 1-44.

Said, R., (1981): The Geologic Evaluation of the River Nile Springer- verlage; New York, Inc. p. 151.

Said, R., (1990): The geology of Egypt. Balkema Publ., Rotterdam Netherlands, 734 p.

Saleh, A.,Al-Ruwaih, F.,&Shehata,M. (1999): Hydrogeochemical processes operating within the main aquifersof Kuwait. Journal of Arid Environments, 42, 195–209.

Sawyer, G. N., & McCarthy, D. L., (1967): Chemistry of sanitary engineers (2nd ed., p. 518). New York: McGraw Hill.

Scepan, J., Menz, G., and Hansen, M. C., (1999): The DIS Cover validation image interpretation process. Photogrammetric Engineering and Remote Sensing, 65(9), 1075–1081.

Serra, P., Pons, X. and Sauri, D., (2008): Land-cover and land-use change in a Mediterranean landscape: a spatial analysis of driving forces integrating biophysical and human factors. Applied Geography, V. 28, pp.189-209.

Shalaby, A. and Tateishi, R., (2007): Remote sensing and GIS for mapping and monitoring land cover and land-use changes in the Northwestern coastal zone of Egypt. Applied Geography, 27 (2007) 28–41

Singh, A. (1989): Digital change detection techniques using remote sensed data. International journal of remote sensing 10, pp. 989-1003

Story, M., & Congalton, R. G., (1986): Accuracy assessment: a user's perspective. Photogrammetric Engineering and Remote Sensing, 52(3), 397–399.

Thomlinson, J. R., Bolstad, P. V., & Cohen, W. B., (1999): Coordinating methodologies for scaling landcover classifications from site-specific to global: steps toward validating global map products. Remote Sensing of Environment, 70(1), 16–28. Page 22 of 36

Todd, D. K., (1959): Groundwater hydrology (p. 535). New York: Wiley.

Todd, D. K., (1980): Groundwater hydrology (2nd ed., p. 315). New York: Wiley.

Todd, D. K., and Mays, L. W. (2005): Groundwater Hydrogeology. John Wiley & Sons, New **York. Uma, K. O., Egboka, B. C. E., and Onuoha, K. M. (1989).** New Statistical Grain-Size Method for Evaluating the Hydraulic Conductivity of Sandy Aquifers. Journal of Hydrogeology, Amesterdam, 108, 367- 386. 16.

Townshend, J.R.G., (1992): Improved Global Data for Land Applications: A Proposal for a New High Resolution Data Set. Report No. 20. International Geosphere-Biosphere Program, Stockholm.

Turner, R. M., (1990): Long-Term Vegetation Change at a Fully Protected Sonoran Desert Site. Ecology. V. 71 (2), pp.464-477.

Ustin, S., (2004): Manual of Remote Sensing: Remote Sensing for Natural Resource Management and Environmental Monitoring. Chichester: John Wiley and Sons.

Velpen, V. D. B. A., (1988): Resist, a computer program for the interpretation of resistivity sounding curves. An ITC. M. Sc. Research project. ITC. Delft, The Netherlands.

Vogelmann, J.E., Helder, D., Morfitt, R., Choate, M.J., Merchant, J.W. and Bulley, H., (2001): Effect of Landsat 5 Thematic Mapper and Landsat 7 Enhanced Thematic Mapper Plus radiometric and geometric calibrations and corrections on landscape characterization. Remote Sensing of Environment, 78, pp. 55–70.

Wiemker, R. Speck, A., Kulbach, D., Spitzer, H., and Bienlein, J., (1997): Unsupervised robust change detection on multispectral imagery using spectral and spatial features. Third International Airborne Remote Sensing Conference and Exhibition, 7-10 July 1997, Copenhagen, Denmark, V. 1, pp. 640-647.

Weismiller, R. A., Kristof, S. J., Scholz D. K., Anuta, P. E., and Momen, S. A., (1977): Change detection in coastal zone environment. Photogrammetric Engineering and Remote Sensing. V.43(12), pp.1533-1539.

Wilcox, L. V., (1948): The quality water for irrigation use. US Department Agricultural Bulletin, 1962, 40.

Wilcox, L. V., (1995): Classification and use of irrigation waters (p. 19). Washington: US Department of Agriculture.

Wolter, P.T., Mladenoff, D.J., Host, G.E. and Crow, T.R., (1995): Improved forest classification in the Northern Lake States using multitemporal Landsat imagery. Photogrammetric Engineering and Remote Sensing, 61, pp. 1129–1143.

World Health Organization (1984): International Standards for Drinking water". 3rd Edition, Vol.1, Geneva, Switzerland.

World Health Organization (WHO) (2004): Guidelines for drinking water quality. Final task group meeting. WHO press/ World Health Organization, Geneva.

Yeh, V. and X. Li, (1999): Economic Development and Agri- Cultural Land Loss in the Pearl River Delta, China, Habitat International, Vol. 23, No. 3, , pp. 373-390. doi:10.1016/S0197-3975(99)00013-2

Youssef, A. M., Abdel Moneim, A. A. and Abu El-Maged, S. A., (2005): Flood hazard assessment and its associated problems using geographic information systems, Sohage Governorate, Egypt. In the 4th International Conference on the Geology of Africa, Nov. 2005, Assiut, Egypt, Vol. 1, pp. 1-17.

Yuan, D., Elvidge, C. D., & Lunetta, R. S. (1998). Survey of multispectral methods for land cover change analysis. Remote sensing change detection: Environmental monitoring methods and applications (pp. 21 – 39). Michigan' Ann Arbor Press.

Yuan, F., Sawaya, K.E., Loeffelholz, B.C. and Bauer, M.E., (2005): Land cover classification and change analysis of the Twin Cities (Minnesota) Metropolitan Area by multitemporal Landsat remote sensing. Remote Sensing of Environment, 98, pp. 317– 328.

Zaki, S. R. (2001): Hydrogeological studies and application of Geographic information system for evaluation of water resources and land use projects in the southern part of Sohag Governorate. M.Sc. Thesis, Geology Dep. Faculty of Science, Monufiya University.

Zhang, B. P., Yao, Y. H., Cheng, W. M., Zhou, C. H., Lu, Z. and Chen, X. D., (2002): Human-induced changes to biodiversity and alpine pastureland in the Bayanbulak Region of the East Tianshan Mountains. Mountain Research and Development. 22, pp. 1-7.

Zohdy, A. A. R., (1973): A computer program for the automatic interpretation of schlumberger sounding curves over horizontally stratified media. Nat. Tech. Inform. Serv., Pb-232-703, 27.

Zohdy, A. A. R., (1974): A computer program for the calculation of Schlumberger sounding curves by convolution. U.S. Geological survey, rept. U.S.G.S. - GD-74-010,p. 232-256.

Zohdy, A. A. R., (1975): Automatic interpretation of Schlumberger sounding curves using modified Dar Zarrouk functions. U.S Geol. Surv., Bull. 13- E, 39p.

Zohdy, A. A. R., and Bisdorf, R. J., (1989): Programs for the automatic processing and interpretation of Schlumberger sounding curves in Quick Basic. U.S. Geological Survey Open File Report 89-137-2, 64 p.